Jerry Ray Dias

Molecular Orbital Calculations Using Chemical Graph Theory

With 30 Figures

Professor Dr. Jerry Ray Dias
Department of Chemistry
University of Missouri
Kansas City, MO 64110-2499
USA

*This book is dedicated
to the deserving women of my family–
my mother, Margurette Ruth (Bass),
my wife, Barbara Jean (Turner),
my daughter, Jennifer Jean,
and my granddaughter, Regina Ann.*

Preface

Professor John D. Roberts published a highly readable book on *Molecular Orbital Calculations* directed toward chemists in 1962. That timely book is the model for this book. The audience this book is directed toward are senior undergraduate and beginning graduate students as well as practicing bench chemists who have a desire to develop conceptual tools for understanding chemical phenomena. Although, ab initio and more advanced semi-empirical MO methods are regarded as being more reliable than HMO in an absolute sense, there is good evidence that HMO provides reliable relative answers particularly when comparing related molecular species. Thus, HMO can be used to rationalize electronic structure in π-systems, aromaticity, and the shape of simple molecular orbitals. Experimentalists still use HMO to gain insight into subtle electronic interactions for interpretation of UV and photoelectron spectra. Herein, it will be shown that one can use graph theory to streamline their HMO computational efforts and to arrive at answers quickly without the aid of a group theory or a computer program of which the experimentalist has no understanding. The merging of mathematical graph theory with chemical theory is the formalization of what most chemists do in a more or less intuitive mode. Chemists currently use graphical images to embody chemical information in compact form which can be transformed into algebraical sets. Chemical graph theory provides simple descriptive interpretations of complicated quantum mechanical calculations and is, thereby, in-itself-by-itself an important discipline of study. A frequent criticism levied against investigators developing rapid manual computational methods is "what can be simpler than computing it on a personal computer?" In this age of computers, one can rapidly compute kinetic, quantum mechanical, thermodynamic, and other parameters almost without any effort, understanding, or arithmetic skills. With a word processor containing dictionary software, one does not even have to know how to spell! Clearly this criticism is absurd. Developing and using facile manual computational methods leads to a deeper insight and understanding of the variables and underlying principles associated with the systems under investigation. Simpler computational methods are always used as the first step in deciding whether one needs to invest in higher computational methods to solve a problem.

J. R. Dias

Contents

List of Tables

Chapter 1
Small Conjugated Polyenes

1.1 Introduction

The current molecular model uses the localized bond, hybridization, and resonance (electron delocalization) concepts as the basis for chemical thinking [1]. These concepts are descriptive translations of molecular quantum mechanics. According to this model, bonds are formed by pairs of electrons shared between pairs of nuclei and are said to be localized; a bond is regarded as the net force of attraction between two nuclei having an intervening electron pair. Observed directional properties of localized bonds are explained by the hybridization of atomic orbitals on a single atom. Electron delocalization occurs in cyclic conjugated molecules and reaction transition states. Collective properties of molecules depend on all the electrons taken together. Thermodynamic quantities, geometries, and dipole moments are examples of collective properties and can be treated in terms of localized bonds.

Collective phenomena are properties associated with a molecule in a single state usually described by a singlet ground state. One-electron properties involve electronic transitions between two states of a system where the initial state is usually the singlet ground state. If a molecule can be described by singlet ground state with doubly occupied MOs, then the Hartree-Fock (H-F) procedure will always allow the orbitals for that state to be transformed into a valid localized orbital equivalent description. For excited states associated with one-electron properties, some of the orbitals must have a unique form leading to non-localizable orbitals observed in spectroscopy; this latter is a characteristic of the final state of the transition and does not imply anything about the initial ground state. Localized (hybrid) orbitals in a ground state molecule arise in the H-F procedure purely as a computational convenience and have no equivalent form in excited state molecules. Thus, methane has two principal PES peaks separated by 10 eV where the lower energy peak is three times more intense and is broadened by the Jahn-Teller splitting expected of a threefold degenerate state which results from the unique singly occupied orbital left in the ion that is not hybridized [2].

In the application of molecular orbital theory to molecules, we shall make the following assumptions: 1) The consequence of inner core electrons will be disregarded. 2) Only the valence electrons which are usually the $p\pi$ electrons will be treated. 3) The linear combination of atomic orbitals (LCAO) approximation will be used to obtain the appropriate molecular orbitals.

4) Electrons may be assigned to definite orbitals. 5) An electron in a particular orbital may be assigned a definite energy. 6) Only two nonidentical electrons may occupy a given orbital. 7) The forces involved in chemical bonding are electrostatic in nature.

In the following sections, the essence of Hückel molecular orbital (HMO) theory will be reviewed and translated into graph theoretical terminology. Noncomputer methods for facile determination of the characteristic polynomials, eigenvalues (energy levels), and eigenvectors (wave functions) of small molecular graphs (graphs representing molecules) will be developed. For the completely uninitiated reader, the notes on "Molecular Orbital Calculations" by John D. Roberts published in 1962 is recommended for supplementary reading [3]. Only knowledge of algebra will be required of the reader, and the polynomial roots needed can be easily obtained by iteration on a hand calculator/programmable computer or by a simplified version of a BASIC program for finding polynomial roots (Appendix A). In subsequent chapters, it will be shown how to decompose large molecular graphs into smaller fragments. Using the methods of this chapter on these fragments will lead to the HMO parameters for the larger molecular graphs.

In order to derive various quantities (bond order, charge density, energy, etc.) in a molecule from HMO, we need to know its electronic configuration. To assign the appropriate HMO electronic configuration of a conjugated polyene, it is assumed that each orbital (energy level) can only be populated by a maximum of two electrons of opposite spin in accordance with the Pauli exclusion principle, the orbitals are successively filled from the lowest unoccupied energy level (most positive eigenvalue) in accordance to the aufbau principle, and for degenerate energy levels spin pairing of the electrons only occurs when all the degenerate levels are half filled per Hund's rule. The highest occupied MO (filled energy level of smallest eigenvalue) and the adjacent lowest unoccupied MO are called HOMO and LUMO, respectively. These are analogous to the valence shell in atoms and are called *frontier orbitals*. Oxidation or ionization removes electrons from the HOMO and reduction places electrons into the LUMO.

In the HMO method, only one–two (1–2) and cyclic interactions of conjugated polyenes are considered. Thus, it is assumed that only nearest neighbor and circuit conduits are available for easy electron flow to manifest itself. Because of this, the idea of connectivity of an atom in a molecular system takes on even greater importance in our description of it. Greater connectivity of an atomic center in a molecule means that it engages in more 1–2 interactions which are presumed to be more energetically favorable. This is clearly in agreement with our chemical intuition. As it will be shown, the degree of a carbon vertex is an important graphical invariant for connectivity. Constitutional (structural) isomers have different connectivities and stereoisomers have the same connectivity but different spatial orientations. Enantiomers have the same energy content whereas conformational isomers and diastereomers do not. Since only 1–2 interactions are considered in the HMO method, the different energy contents

of conformational isomers and diastereomers can not be determined by HMO theory.

Two different approach philosophies exist among chemists. One group strives to develop ab initio quantum mechanical methods for computing all chemical properties of molecules from first principles. This approach is computationally intensive. The other group takes a semiempirical/molecular modelling approach. Our approach is the latter. Within this approach, we restrict ourselves to methods that are fundamentally simple, capable of being quantitative, and pedagogically favorable. We seek to develop descriptive and conceptual tools for understanding and predicting chemical properties without resorting to computationally intensive methodologies. Our strategy is to develop methods which allow one to understand the properties of small molecules, and then learn how to decompose large molecules into small substructures that are computationally amenable to the methods developed for the small molecules. A key feature of this strategy is the identification of elementary substructures that we call bonds, excised internal structures, functional groups, irreducible subgraphs (Chapter 2), Sachs graphs, and Ulam subgraphs which serve as embodiments of the essential information needed for computing the parameters of interest. These substructures provide us with mental images that are carriers of information which is critically dependent upon molecular connectivity. This connectivity transmits the major sources of local interactions. Discrete mathematics, the study of infinite systems, uses vectors, matrices, set theory, graph theory, combinatorics, and relations which are the tools of our approach. Any chemical properties associated by these mathematical characteristics will hold for all structurally related objects. Since imagery is important to the mental processing of chemical information, our computational methodology focuses on identifying and studying the properties of elementary substructures that can be assembled into molecular graphs. In this first chapter, we will utilize bonds, Sachs graphs, and Ulam subgraphs in the determination of eigenvalues and eigenvectors of molecular graphs. In Chapter 2, it will become apparent that for every molecular graph fragmentation there is a corresponding factorization of its characteristic polynomial.

1.2 Hückel Molecular Orbital Calculations

1.2.1 The Wave Equation

The energy (E) of a molecular system can be partitioned into kinetic (K) and potential (P) energy terms per $E = K + P$. For wave motion, $H\psi = E\psi$, where H is the Hamiltonian energy operator and ψ is the molecular wave function. The molecular orbital method assumes that the properties of a molecule might be calculated by considering the nuclei as being jointly surrounded by molecular orbitals in analogy to atomic orbitals that surround a single nucleus. The atomic

$$X = \frac{\varepsilon - \alpha}{\beta}$$

$$P(CH_3; X) = X = 0$$

$\psi = \phi$

AMO

$$\psi_2 = \frac{1}{\sqrt{2}}\phi_1 - \frac{1}{\sqrt{2}}\phi_2$$

AO

basis orbitals

$\pi^* \quad \alpha - \beta$

$\phi_1 \quad \phi_2 \quad \alpha$

$\pi \quad \alpha + \beta$

BMO

$$\psi_1 = \frac{1}{\sqrt{2}}\phi_1 + \frac{1}{\sqrt{2}}\phi_2$$
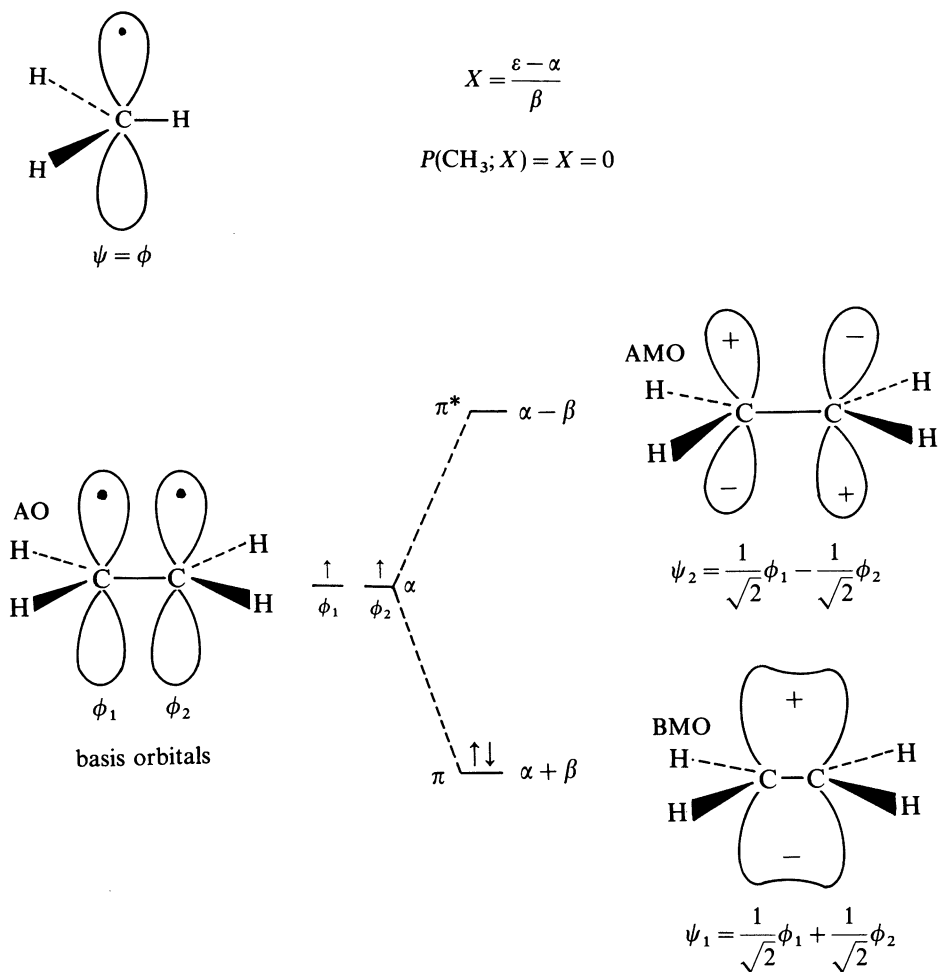
Secular   Characteristic
Determinant   Polynomial

$$\begin{vmatrix} X & -1 \\ -1 & X \end{vmatrix} = 0 = P(C_2H_4; X) = X^2 - 1$$

ethene   molecular graph   adjacency matrix
structure $L_2 = K_2$

$$A = \begin{pmatrix} 0 & 1 \\ 1 & 0 \end{pmatrix} \begin{matrix} 1 \\ 2 \end{matrix}$$
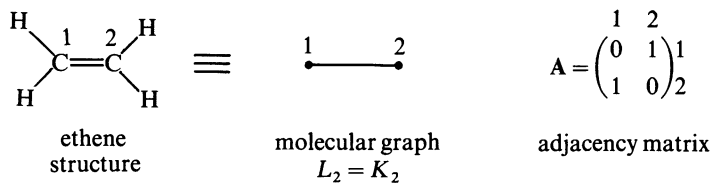
Fig. 1.1. HMO solutions for methyl radical and ethene

Determining eigenvalues

$$P(C_2H_4; X) = \left| X\mathbf{I} - \mathbf{A} \right| = \left| X\begin{pmatrix} 1 & 0 \\ 0 & 1 \end{pmatrix} - \begin{pmatrix} 0 & 1 \\ 1 & 0 \end{pmatrix} \right| = \left| \begin{pmatrix} X & 0 \\ 0 & X \end{pmatrix} - \begin{pmatrix} 0 & 1 \\ 1 & 0 \end{pmatrix} \right|$$

$$= \begin{vmatrix} X & -1 \\ -1 & X \end{vmatrix} = X^2 - 1 = (X+1)(X-1) = 0$$

Determining eigenvectors

$$\mathbf{A}\Psi = X\Psi = \begin{pmatrix} 0 & 1 \\ 1 & 0 \end{pmatrix}\begin{pmatrix} C_1 \\ C_2 \end{pmatrix} = X\begin{pmatrix} C_1 \\ C_2 \end{pmatrix} = \begin{pmatrix} C_2 \\ C_1 \end{pmatrix} = \begin{pmatrix} XC_1 \\ XC_2 \end{pmatrix} \quad \text{therefore} \quad \begin{matrix} C_2 = XC_1 \\ C_1 = XC_2 \end{matrix}$$

For $X = 1$, $C_1 = C_2 = 1$ and for $X = -1$, $C_1 = -C_2$ or $C_1 = 1$ and $C_2 = -1$

normalization constant $= N = (C_1^2 + C_2^2)^{-1/2} = (1^2 + 1^2)^{-1/2} = 1/\sqrt{2}$

Wave functions

$X = 1$, $\Psi_1 = (1/\sqrt{2})(\phi_1 + \phi_2)$

$X = -1$, $\Psi_2 = (1/\sqrt{2})(\phi_1 - \phi_2)$

Fig. 1.1. (*Continued*)

orbitals are described by atomic wave functions ϕ and molecular orbitals are described by molecular wave functions ψ. Figure 1.1 shows the wave equations and corresponding $p\pi$ orbitals for methyl radical and ethene.

1.2.2 The LCAO Method

The LCAO method assumes that molecular orbitals (ψ) can be obtained as linear combinations of atomic orbitals (ϕ). Each molecular orbital (MO) will have a specific energy value and wave function. For conjugated polyenes, electrons in $p\pi$ bonds are treated separately from the electrons in σ bonds which are regarded as being localized in deep energy wells and are subject to additivity principles. In the simple molecular orbital treatment, 1,3-butadiene is treated as a system of delocalized $p\pi$ electrons on a framework of localized σ electrons. Application of the LCAO method to the $p\pi$ electrons of ethene (Figure 1.1) gives $\psi = c_1\phi_1 + c_2\phi_2$. The number of MOs obtained will always be equal to the number of AOs used to construct them. Using the variation method which minimizes energy with respect to the coefficients (c_i) in the wave functions, one obtains the *secular determinant*. The roots of the secular determinant corresponds to the allowed energy values for the relevant molecule.

Secular determinants possess diagonal symmetry and depend on the values of the overlap, $S_{ij} = \langle \phi_i | \phi_j \rangle$, and Coulomb, $H_{ij} = \langle \phi_i | H | \phi_j \rangle$, integrals. For $i = j$, $S_{ii} = 1$ and $H_{ii} = \alpha_i$. Within the Huckel MO approximation, if $i \neq j$, then

$S_{ij} = 0$ and $H_{ij} = \beta_{ij}$ when atom i is adjacent to atom j, otherwise $H_{ij} = 0$. For conjugated polyenes, it is assumed that α_i and β_{ij} can be replaced by the average quantities of α and β, respectively.

The parameters α and β have dimension of energy with negative values. For conjugated polyenes, α is a function of the ionization energy of the carbon p-orbital electron and β is a function of the bond dissociation energy of the C—C $p\pi$ bond. Their average values are determined for a particular series of molecules by empirical fitting of the experimental values of a representative subset. The order of magnitude expected for α is about $-8\,eV$ and for β about $-2\,eV$.

The three fundamental types of information given for a molecule by the LCAO method are bond orders, electron densities, and molecular orbital energies. Only the latter requires specific values, for α and β. However, if one is only interested in relative electronic stability of closely related molecules, then absolute values for α and β are still not necessary. Because of this, we will generally take $\alpha = 0$ and $\beta = 1$.

The LCAO method only requires one to know how to set up and solve secular determinants. While this is not very difficult in-itself, noncomputer solution of large determinants become exceedingly time consuming and error prone. Thus, our goal in the following sections is to provide one with the methodologies to circumvent solving large secular determinants. We will do this by translating molecules into molecular graphs and formulating the LCAO method into graph theoretical terminology and mathematics. By this approach, one will be able to streamline their computations and learn to extract the desired information about molecules with a facility that allows them to conceptualize chemical information with ease.

1.3 Graph Theoretical Terminology

1.3.1 Molecular Graph Notation

Throughout this work the carbon and hydrogen atoms and the $p\pi$ bonds in all molecular graphs (graphs representing molecules) will be omitted and only the C—C σ-bond skeleton will be shown. The various types of (carbon) vertices referred to herein are methylene $=C\underset{\diagdown H}{\overset{\diagup H}{}}$ shown as a primary (degree-one) graph vertex, methine $=C\underset{\diagdown}{\overset{\diagup H}{}}$ shown as a secondary (degree-two) graph, vertex, and carbon $=C\underset{\diagdown}{\overset{\diagup}{}}$ shown as a tertiary (degree-three) graph vertex. As examples, methyl radical will be represented by a point and ethene by a line.

Alternant hydrocarbon polyenes (bipartite molecular graphs) have no odd size rings and can be maximally labelled with nonadjacent stars. Odd carbon hydrocarbons will always be radical species when electronically neutral. The radical nature of odd carbon polyenes will be implied.

1.3.2 1-Factor Subgraphs and Kékulé Structures

A factor of a molecular graph G is a spanning subgraph (spans all the carbon vertices) that is not totally disconnected. When G has a 1-factor, then N (the number of carbon atom vertices) must be even and the 1-factor lines are point disjoint. The number of distinct 1-factor subgraphs of G is equal to the number of Kékulé structures (**K**). A graph is 2-factorable if it has spanning subgraphs that are regular of degree-2. Examples of a 1-factor and the only 2-factor subgraph of naphthalene is presented by the following.
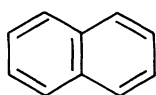
naphthalene σ-bond molecular graph

2-factor subgraph   1-factor subgraph
C_{10} five K_2 components

1.3.3 Common Molecular Graphs

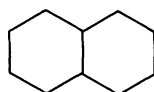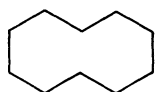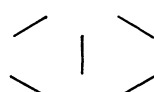Common molecular graphs (G) include linear polyenes (L_n) and monocyclic conjugated hydrocarbons (C_n) of $n = N_c = N$ carbon vertices. For example, methyl radical and ethene would be designated by L_1 and L_2, respectively, and benzene would be designated by C_6. The *complete graph* K_n on n vertices has all its vertices connected by an edge (representing a σ-bond in molecular graphs) to every other vertex. The smallest complete graphs have the following equalities: $K_1 = L_1$, $K_2 = L_2$, $K_3 = C_3$, and K_4 = tetrahedron. A 1-factor subgraph has K_2 components and 2-factor subgraphs are made up of C_n components. Sachs graphs are made up of K_2 and C_n components [4]. Additional terms used in this monograph can be found in Table 1.1.

1.4 Determining Characteristic Polynomials

1.4.1 Characteristic Polynomials

Expansion of the Hückel molecular orbital (HMO) secular determinant for a molecular graph gives the characteristic polynomial $P(G; X) = \det|X\mathbf{I} - \mathbf{A}|$ of the corresponding conjugated system where $\mathbf{I}$ is the identity matrix, $X = (\varepsilon - \alpha)/\beta$, and $\mathbf{A}$ is the adjacency matrix [5]. The matrix $\mathbf{A}$ is an $n \times n$ matrix whose (i,j) entry is 1 if vertices v_i and v_j are adjacent in G and 0 otherwise.

Table 1.1. Glossary of terms

a_4	–	fourth coefficient in the characteristic polynomial
a_6	–	sixth coefficient in the characteristic polynomial
α (α_c)	–	HMO Coulomb integral (of carbon)
α_3	–	number of branches on a trigonal ring
α_4	–	number of branches on a tetragonal ring
β	–	HMO exchange integral
C_n	–	cycle or circuit of size n
C_{rj}	–	eigenvector coefficient for atom r and the jth eigenvalue
d_i	–	number of vertices of degree i
$e(i,j)$	–	number of edges with a vertex of degree i at one end and a vertex of degree j at the other end
$e_{\underline{k}}$	–	an edge of weight $\underline{k}$
ε	–	energy level or HMO eigenvalue
E_π	–	total pπ energy
G	–	a molecular or isoconjugate graph
G_x	–	a molecular graph with a single weighted vertex
$G_{\underline{k}}$	–	a molecular graph with a single weighted edge
h	–	the weight of a heteroatom vertex $[h = (\alpha_x - \alpha_c)/\beta]$
$\underline{k}$	–	the weight of an edge $[\underline{k} = \beta_{cx}/\beta_{cc}]$
L_n	–	linear polyconjugated system of size n
N (N_c)	–	number of (carbon atom) vertices
$P(G;X)$	–	characteristic polynomial of a molecular graph
q	–	number of C—C σ-bond edges
r_n	–	number of rings (cycles) of n vertices
r'_3	–	number of combinatorial pairs of trigonal rings
v	–	vertex
X	–	$(\varepsilon - \alpha)/\beta$ = graph eigenvalue
$Z_{\underline{k}}$	–	cycles containing edge of weight $\underline{k}$

alternant hydrocarbons (bipartite graphs) have no odd size rings

      a) odd carbon (vertex) – OAH
      b) even carbon (vertex) – EAH

characteristic polynomials are monic polynomials with only real roots that correspond to the eigenvalues of some molecular graph

energy level – eigenvalue

frontier orbitals are the highest occupied and lowest unoccupied molecular orbitals and associated energy levels

graphical invariants are properties of graphs that remain unchanged regardless of the orientation of the molecular graph or how it is numbered

isoconjugate molecular graph is a molecular graph of a hydrocarbon reference frame corresponding to a heteroatomic (edge/vertex weighted) molecular graph with the same number of conjugated atoms

molecular graph is a C—C σ-bond skeleton of a conjugated polyene molecule

molecular orbital is an energy level and associated wave function of a molecule

Sachs graphs are subgraphs composed of disjoint K_2 and C_n components

similarity is the degree of overlap between two or more structures (molecular graphs)

subspectral – two or more molecular graphs with a common subset of eigenvalues

Ulam subgraphs are graphs generated by deleting vertices from other graphs

Wave function coefficient set – eigenvector

The characteristic polynomial of an N carbon atom system has the following form

$$P(G; X) = \sum_{n=0}^{N} a_n X^{N-n} = 0$$

where a_n are coefficients that can be obtained without having to solve the HMO secular determinant. The roots of the characteristic polynomial give the eigenvalues (energy levels) of the corresponding molecular graph. A major thrust of this monograph is the development of facile procedures for solving the above characteristic polynomial for obtaining energy, bond order, and electron density parameters for most molecular graphs of chemical interest. Most of these procedures will owe their origin to the elegant method involving enumeration of all Sachs graphs which is totally general [5].

1.4.2 Sachs graphs

The determination of the coefficients a_n of the characteristic polynomial $P(G; X)$ by the Sachs graph theoretical method is a formalized variant of the procedure first presented by Coulson [6]. This method is summarized by the following formula

$$a_n = \sum_{s \in S_n} (-1)^{c(s)} 2^{r(s)}$$

where $0 \le n \le N$, s is a Sachs graph, S_n is a set of all Sachs graphs with exactly n vertices, $c(s)$ is the total number of K_2 and C_m components, and $r(s)$ is the total number of rings (cycles) in s. All combinations of lK_2 and kC_m such that $2l + km = n$ are enumerated. By definition $a_0 = 1$. Since only K_2 and C_m components are allowed, $S_1 = \phi$ (the empty set) giving $a_1 = 0$. The set S_2 of all Sachs graphs on two vertices leads to the value of $a_2 = -q$ which is equal to the negative number of graph edges (σ-bonds). Only C_m components or C_n ($n =$ odd) components together with K_2 components are allowed for $m =$ odd. Consider the cyclopentadienyl (C_5) system. The set of Sachs graphs of S_3 is zero since there are no trigonal rings in the cyclopentadienyl molecule. For S_4 the following enumerates all Sachs graphs on four vertices

$$S_4 = \left\{ \text{〈graphs〉} \right\}$$

which give $a_4 = 5(-1)^2 2^0 = 5$. For S_5, there is only a single C_5 component giving $a_5 = (-1)2 = -2$. Thus, the characteristic polynomial for the cyclopentadienyl molecule is $P(C_5H_5; X) = X^5 - 5X^3 + 5X - 2$.

For larger molecular graphs the manual enumeration of all Sachs graphs, represents a labor-intensive, error-prone process. We will circumvent this through the use of a combination of algebraic, combinatoric, and discrete

Table 1.2. Equations for the calculation of characteristic polynomials of molecular graphs

Eq. no.	Equation
(1)	$a_4 = (1/2)(q^2 - 9q + 6N_c) - 2r_4 - d_1 - d_4 - 3d_5 - 6d_6 - \ldots$
(2)	$a_6 = -(1/6)(q^3 - 27q^2 + 116q) - N_c(3q - 16) - 2r_6 - e(3,3) + (q - 6)e(2,1)$
	$\quad + (q - 5)e(3,1) + 2\Sigma(q - 4 - \alpha_4)r_4 + r_3 + 4r_3'$
(3)	$P(G; X) = X^N - qX^{N-2} - 2r_3X^{N-3} + a_4X^{N-4} - [2r_5 - 2(q - 3 - \alpha_3)r_3]X^{N-5}$
	$\quad + a_6X^{N-6} + \ldots$
(4)	$P(G_x; X) = XP(G_x - v_x; X) - hP(G_x - v_x; X) - \underline{k}^2[XP(G_x - v_x; X) - P(G; X)]$
	for edge/vertex weighted graphs
(5)	$P(G_{\underline{k}}; X) = P(G_{\underline{k}} - e_{\underline{k}}; X) - \underline{k}^2P(G_{\underline{k}} - (e_{\underline{k}}); X) - 2\underline{k}\Sigma P(G_{\underline{k}} - Z_{\underline{k}}; X)$
	for edge weighted graphs
(6)	$P(G_o; X) = P(G; X) + P(G_o - v_o; X)$
	for right mirror-plane fragment
(7)	$P(G_{e1}; X) = P(G_{e1} - e_\omega; X) - P(G_{e1} - (e_\omega); X) + \Sigma P(G_{e1} - Z_\omega; X)$
	for the identical fragments of vertex-centric 3-fold graphs
(8)	$P(G_{e2}; X) = P(G_{e2} - e_\omega; X) - P(G_{e2} - (e_\omega); X) - \Sigma P(G_{e2} - Z_\omega; X)$
	for the identical fragments of ring-centric 3-fold graphs
(9)	$P(L_n; X) = XP(L_{n-1}; X) - P(L_{n-2}; X)$, where $P(L_o; X) = 1$ and $P(L_1; X) = X$
(10)	$C_{rj}^2 = [P(G - v_r; X_j)/P'(G; X_j)]$
	for atom r and eigenvalue j

When it is obvious from the context C_n will be used for $P(C_n; X)$ and L_n will be used for $P(L_n; X)$.

mathematics. General equations for the a_4 and a_6 (Table 1.2) have been derived by the author [7]. Using these equations along with embedding [8], mirror plane fragmentation [9], and other graph theoretical decomposition schemes [10, 11], we will show how to arrive at the characteristic polynomials for most molecular graphs of chemical interest.

Table 1.3. The set of Sachs graphs used for calculating the coefficients of the characteristic polynomials of molecular graphs

Coefficient	Set of Sachs Graphs
a_0	$S_0 = \{\phi\}$
a_2	$S_2 = \{K_2\}$
a_3	$S_3 = \{C_3\}$
a_4	$S_4 = \{2K_2, C_4\}$
a_5	$S_5 = \{C_5, K_2 \cup C_3\}$
a_6	$S_6 = \{3K_2, K_2 \cup C_4, C_3 \cup C_3, C_6\}$
a_7	$S_7 = \{C_7, C_4 \cup C_3, K_2 \cup C_5, 2K_2 \cup C_3\}$
a_8	$S_8 = \{4K_2, K_2 \cup C_6, K_2 \cup C_3 \cup C_3, 2K_2 \cup C_4, C_4 \cup C_4, C_5 \cup C_3, C_8\}$
$\ldots$	$\ldots$

Table 1.3 summarizes all the Sachs graphs, needed for computing the coefficients up to a_8. For a given molecular graph of size N_c, one determines all the various combinations of subgraphs containing mutually disjoint K_2 and C_n components on a given number of vertices ranging from 1 to N_c. This method obviously considers only 1–2 interactions by K_2 and cyclic interactions by C_n. This arises quite naturally from the symmetric property of the adjacency matrix where only nearest neighbors are inputted. Alternant hydrocarbons (AHs) have no odd size rings and, therefore, all the odd coefficients of the characteristic polynomials are zero. A single C_{4n} component makes a negative contribution to the even coefficients of AHs. In general, the number of combinations of Sachs graphs for the odd coefficients of nonAHs are smaller than for even ones. Also, the number of Sachs graphs associated with the tail coefficient of nonAHs are frequently sufficiently small that one will usually have no difficulty in their determination.

1.4.3 The Fourth and Sixth Coefficients

Using combinatoric and discrete mathematics the author previously derived general expressions for a_4 and a_6 [7]. From the Sachs graph formulation, a_4 will consist of all combinations of two disjoint K_2 subgraphs and one C_4 subgraph. For conjugated hydrocarbons

$$a_4 = (1/2)(q^2 - 9q + 6N_c) - 2r_4 - d_1 - \ldots \tag{1}$$

where q is the number of σ-bonds (edges), N_c is the number of carbon vertices, r_4 is the number tetragonal rings, and d_1 is the number of vertices of degree-1 (methylene groups) in the molecular graph. The sixth coefficient for conjugated hydrocarbons is given by all disjoint combinations of three K_2, one K_2 and one C_4, one C_6, and two C_3 subgraphs. Thus,

$$\begin{aligned} a_6 = &-(1/6)(q^3 - 27q^2 + 116q) - N_c(3q - 16) - 2r_6 - e(3,3) \\ &+ (q-6)\,e(2,1) + (q-5)\,e(3,1) + 2\Sigma(q - 4 - \alpha_4)\,r_4 + r_3 + 4r_3' \end{aligned} \tag{2}$$

where $e(i,j)$ is the number of edges between vertices of degree-i on one end and degree-j at the other end, α_4 is the number of branches on a tetragonal ring, and r_3' is the number of combinatorial pairs of trigonal rings. With these relationships for a_4 and a_6, the characteristic polynomial for any molecular graph having six carbon vertices or less is specifically given by Eq. (3) in Table 1.2.

Consider benzene with the C_6 molecular graph. From Eq. (3), we obtain $P(C_6; X) = X^6 - 6X^4 + a_4 X^2 + a_6$ since benzene has no odd size rings. Solving Eq. (1) and Eq. (2) with $q = 6$, $N_c = 6$, $r_6 = 1$, and all other parameters zero gives $P(C_6H_6; X) = X^6 - 6X^4 + 9X^2 - 4$. Benzene is an even alternant hydrocarbon (EAH). Alternant hydrocarbons (AHs) have no odd size rings and consequently all odd coefficients $a_3, a_5, a_7, \ldots$ are zero. The odd coefficients in the characteristic polynomials will be only required for nonalternant hydrocarbons (nonAHs) and will usually have smaller values than the even ones. It is useful to distinguish between even and odd carbon alternant and nonalternant

hydrocarbons. Both even and odd carbon alternant hydrocarbons (EAHs and OAHs) have characteristic polynomials with only even coefficients of alternating signs. OAHs will always have at least one zero eigenvalue (i.e., a NBMO).

1.4.4 Odd Coefficients

Per the Sachs graph formalism, odd coefficients only occur for molecular graphs having at least one odd size ring, i.e., nonAHs. Since odd coefficients are smaller than even ones, it is usually quite easy to count the Sachs graphs for smaller molecular graphs. For larger molecular graphs, one can use Eq. (1) for a_4 and Eq. (2) for a_6 on appropriate subgraphs produced by deleting the odd size rings. For example, if the sole odd size ring in a molecular graph is C_m, then the a_{m+2}, a_{m+4}, and a_{m+6} coefficients to the relevant characteristic polynomial can be obtained by determining the a_2, a_4, and a_6 coefficients for the subgraph obtained upon deleting C_m from the molecular graph. Consider cyclopropabenzene [12]. From Eq. (1) to Eq. (3) in Table 1.2, we obtain

$$P(C_7H_5; X) = X^7 - 8X^5 - 2X^4 + 17X^3 + 6X^2 - 10X + a_7$$
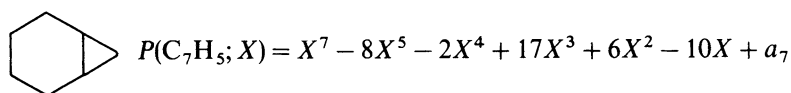
without enumerating Sachs graphs since Eq. (3) is totally general for molecular graphs up to $N_c = 6$. The set of Sachs graphs on seven vertices is

$$S_7 = \left\{ \bigcirc, \diagup\diagdown, \triangleright \right\}$$
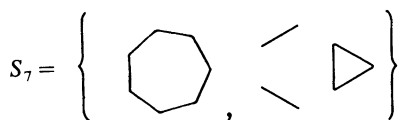
which gives $a_7 = (-1)2 + (-1)^3 2 = -4$. We now obtain a_5 for cyclopropabenzene by two different methods. The set of Sachs graphs on five vertices is
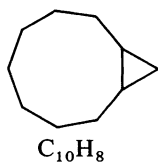
$$S_5 = \left\{ \diagup \triangleright, |\triangleright, \diagdown\triangleright \right\}$$
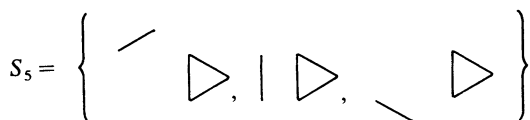
which gives $a_5 = 3(-1)^2 2 = 6$. Alternatively, by deleting C_3 from cyclopropabenzene we obtain

$$\text{G} \qquad\qquad L_4 \qquad\qquad C_3$$
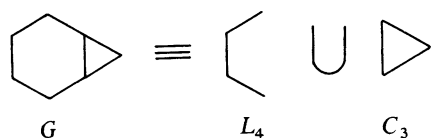
For L_4, $a_2 = -q = -3$ and $a_4 = 1$. Thus, $a_5(C_7H_5) = a_2(L_4) \cdot a_3(C_3) = -3(-2) = 6$. Similarly, the second term to a_7 above is given by $a_4(L_4) \cdot a_3(C_3) = 1(-2) = -2$.

A more complicated example is provided by planar bicyclo[7.1.0]de-capentaene [13] as follows.

$$P(C_{10}H_8; X) = X^{10} - 11X^8 - 2X^7 + 41X^6 + a_5X^5$$
$$- 60X^4 + a_7X^3 + a_8X^2 + a_9X + a_{10}$$

$C_{10}H_8$

Deletion of C_3 from $C_{10}H_8$ gives L_7 for which $a_2 = -6$, $a_4 = 10$, and $a_6 = -4$. Thus, $a_5(C_{10}H_8) = a_2(L_7) \cdot a_3(C_3) = -6(-2) = 12$, $a_7(C_{10}H_8) = a_4(L_7) \cdot a_3(C_3) = 10(-2) = -20$, and $a_9(C_{10}H_8) = a_6(L_7) \cdot a_3(C_3) + a_9(C_9) = (-4)(-2) + (-2) = 6$. The very last coefficient a_{10} can be easily computed by determining all the Sachs graphs on ten vertices giving $a_{10} = (-1)2 + 2(-1)^5 = -4$. Determination of $a_8(C_{10}H_8)$ can be accomplished by deleting the six distinct K_2 subgraphs and determining a_6 for the six different remaining subgraphs. This gives $a_8 = 29$.

1.4.5 The Tail Coefficient

The absolute value of the last coefficient a_N of the characteristic polynomial of an even AH devoid of 4n rings (n = integer) is equal to the square of the number of Kekule structures of the corresponding molecular graph, i.e., $|a_N(\text{EAH})| = \mathbf{K}^2$. For example, benzene has $\mathbf{K} = 2$ and $|a_6| = 4$. Similarly, the sum of the squares of the unnormalized integral coefficients to the NBMO (eigenvector coefficients for $\varepsilon = 0$) of an OAH gives the tail coefficient (a_{N-1}) to the corresponding characteristic polynomial. For nonAH, one will have to enumerate all the Sachs graphs on N vertices as it was done above for bicyclo[7.1.0]decapentaene.

In summary, all molecular graphs of size $N_c \leq 8$ and no symmetry can have their HMO parameters easily determined by the methods outlined in this section. In the next section, it will be shown that some molecular graphs can have additional eigenvalues determined by a method called embedding. Obtaining additional eigenvalues by embedding will permit us to cross-check our computed characteristic polynomials for small molecular graphs and to frequently obtain characteristic polynomials for even larger ones.

1.5 Determining Select Eigenvalues by Embedding

1.5.1 Introduction

In a series of papers, Hall provided the basis for recognition of the presence of select eigenvalues in AHs by inspection of their molecular topology [13]. Whenever a smaller molecular graph can be embedded onto a larger one, then the eigenvalues of the smaller graph will be found among the eigenvalues of the larger one. In many respects, this is like the functional group concept used

**Table 1.4.** Common embedding fragments and their corresponding eigenvalues and eigenvectors

Fragment Graph	Organic Equivalent	Eigenvalues	Eigenvectors
L_1	methyl	0	(1)
L_2	ethene	± 1	$(\sqrt{2}/2, \pm\sqrt{2}/2)$
L_3	allyl	$\pm\sqrt{2}$	$(\frac{1}{2}, \pm\sqrt{2}/2, \frac{1}{2})$
L_4	butadiene	$\pm\frac{1}{2}(\sqrt{5}+1)$	$(0.3718, \pm 0.6015, 0.6015, \pm 0.3718)$
		$\pm\frac{1}{2}(\sqrt{5}-1)$	$(0.6015, \pm 0.3718, -0.3718, \mp 0.6015)$
L_5	pentadienyl	$\pm\sqrt{3}$	$(\sqrt{3}/6, \pm\frac{1}{2}, \sqrt{3}/3, \pm\frac{1}{2}, \sqrt{3}/6)$
		± 1	$(\frac{1}{2}, \pm\frac{1}{2}, 0, \mp\frac{1}{2}, -\frac{1}{2})$
C_6	benzene	± 2	$(1/\sqrt{6}, \pm 1/\sqrt{6}, 1/\sqrt{6}, \pm 1/\sqrt{6}, 1/\sqrt{6}, \pm 1/\sqrt{6})$
		± 1	$(0, \pm\frac{1}{2}, \frac{1}{2}, 0, -\frac{1}{2}, \mp\frac{1}{2})$
		± 1	$(1/\sqrt{3}, \pm 1/2\sqrt{3}, -1/2\sqrt{3}, \mp 1/\sqrt{3}, -1/2\sqrt{3}, \pm 1/2\sqrt{3})$

As a general rule, X and ε will be used interchangably for eigenvalue.

in organic chemistry. The rules for embedding derive directly from the eigen-vector equations themselves. Node positions between two embedded fragments are vertices with zero eigenvector coefficients for the relevant set of eigenvalues. The sum of the coefficients of the carbon vertices attached to each node vertex must equal to zero. Hall's rules were translated into descriptive form and, as it will become evident in the next chapter, are an extension of the mirror plane fragmentation process [13–14].

1.5.2 Descriptive Embedding Rules

To embed a fragment onto an AH molecule, the following rules must be followed: 1) All atoms connected directly to the fragments must be nodes; 2) on the other side of each these nodes will be a repetition of the fragment with the opposite sign; and 3) other branches at these nodes will also be nodes since at all nodes the sum of nearest neighbor fragments must be null in regard to their signs. Table 1.4 presents the eigenvalues and eigenvectors for the six smallest molecular graphs that are most commonly embedded in larger molecular graphs. Embedded fragments will be shown in bold and usually the intervening node positions will be labelled with open circles. With rare exceptions, the embedding of fragments other than methyl, ethene, and benzene must be done so as to always have corresponding fragment positions align through each node position. Thus, the following two examples illustrate an improper embedding versus a proper one.

$$X^8 - 8X^6 + 18X^4 - 12X^2 + 1$$
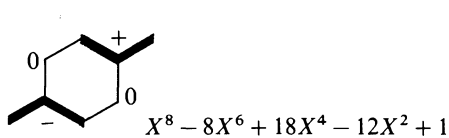
Improper embedding of
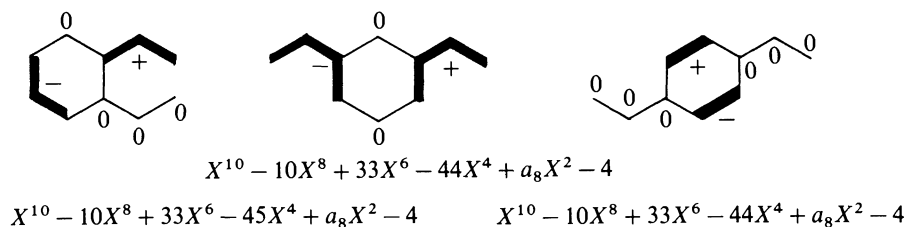allyl on p-quinodimethane

$$X^8 - 8X^6 + 18X^4 - 12X^2$$
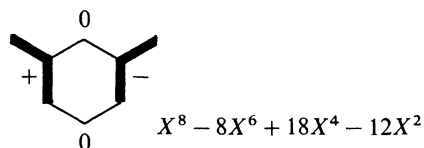
Proper embedding of allyl
on m-quinodimethane

Rules for Embedding Smaller Subgraphs onto Larger graphs

1. All vertices connected directly to the subgraph fragment must be nodes*.
2. On the other side of each of these nodes will be a repetition of the fragment with the opposite sign.
3. Other branches at these nodes will also be nodes.
   *Nodes have zero-value coefficients in the corresponding wave functions (eigenvectors).

Consider the three isomers of diethenylbenzene (divinylbenzene). 1,2-Diethenyl-benzene can be embedded by allyl, 1,3-diethenylbenzene can be embedded by butadiene, and 1,4-diethenylbenzene can be embedded by ethene as shown by the following. Note that only one of two possible allyl embeddings is shown for 1,2-diethenylbenzene. All the coefficients for the characteristic polynomials of the diethenylbenzene isomers but a_8 were determined by the inspection methods described by Eq. (1) to Eq. (3) and the relationship for the tail coefficient. To obtain a_8, one simply inserts one of the eigenvalues determined by embedding (Table 1.3) into the characteristic polynomials above and solve for the unknown a_8. For example, inserting $X = \sqrt{2}$, $(\frac{1}{2})(\sqrt{5} - 1)$, and 1.0 into the characteristic polynomials for 1,2-, 1,3-, and 1,4-diethenylbenzene give $a_8 = 24$, 23, and 24, respectively.

$$X^{10} - 10X^8 + 33X^6 - 44X^4 + a_8X^2 - 4$$

$$X^{10} - 10X^8 + 33X^6 - 45X^4 + a_8X^2 - 4 \qquad X^{10} - 10X^8 + 33X^6 - 44X^4 + a_8X^2 - 4$$

Additional examples of ethene embedding are provided by pentadienyl (Table 1.3), benzene, and p-quinodimethane. Thus, these molecules possess eigenvalues of ± 1 among their eigenvalue sets. Both allyl and pendadienyl can be embedded by methyl and all these molecules possess the eigenvalue of zero.

The molecular graph of an AH can be maximally starred such that no two starred (or nonstarred) positions are directly linked [15]. The number of zero eigenvalues in such a molecular graph is given by the difference between the number of starred positions (N_*) and nonstarred positions (N_0), provided it

has no $4n$ $(n = 1, 2, 3, \ldots)$ rings [16]. For example, allyl can be starred in positions 1 and 3 with position 2 being nonstarred giving $N_* - N_0 = 2 - 1 = 1$ zero eigenvalue. Similarly, pentadienyl has $N_* - N_0 = 3 - 2 = 1$ zero eigenvalue. m-Quinodimethane can be starred as shown below giving $N_* - N_0 = 5 - 3 = 2$ zero eigenvalues. Alternatively, the valence bond structure shows that m-quino-dimethane is a diradical. In general, AHs with a minimum of n unpaired electron sites for any combination of electron pairing will have n NBMOs (i.e., zero eigen-values) and $N_* - N_0 = n$. The presence of zero eigenvalues in molecular graphs possessing $4n$ rings can be determined by methyl embedding. 1,3-Dimethylenyl-cyclobutadiene can be embedded by methyl radical and ethene giving eigenvalues of $0, \pm 1$.

$$X^8 - 8X^6 + 18X^4 - 12X^2$$

$$X^6 - 6X^4 + 5X^2$$
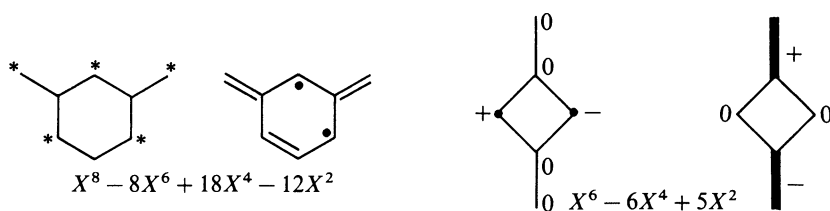
1.5.3 The Pairing Theorem

Alternant hydrocarbon (AH) molecular graphs have no odd size rings which lead to corresponding characteristic polynomials without odd (subscript) coefficients. In addition, AHs have plus and minus pairs of eigenvalues (energy levels), i.e., every positive bonding energy level (BMO) has a corresponding negative antibonding energy level (AMO) with the same absolute numerical value [17]. OAHs also have an unpaired zero eigenvalue. Table 1.3 gives the paired eigenvalues of representative AH molecular graphs. If one maximally stars an AH so that no two starred positions are adjacent, then in going from the BMO energy level to the corresponding AMO energy level the signs of eigen-vector (wave function) coefficients belonging to the starred positions remain unchanged whereas the signs to the nonstarred positions change. For example, consider ethene in Fig. 1.1. If one stars the left carbon and leaves the right one unstarred, then in going from the BMO to the AMO, the MO wave function (ψ) coefficient for the left atomic orbital ϕ_1 ramains unchanged ($\sqrt{2}/2$) and for the right atomic orbital ϕ_2 changes from positive ($\sqrt{2}/2$) to negative ($-\sqrt{2}/2$). The pairing theorem requires that both the eigenvalues with their associated eigenvectors are paired in AHs. HOMO and LUMO are paired MOs in EAHs.

A consequence of the pairing theorem is that alternant subgraphs can only be embedded in alternant molecular graphs or alternant subsections contained in nonalternant molecular graphs. Table 1.3 presents a list of the smallest alternant molecular graphs that are found frequently embedded in larger ones. Embedding nonalternant subgraphs on larger nonalternant molecular graphs will be only occasionally encountered. A further consequence of the pairing

theorem is that a necessary but not sufficient requirement for allyl or benzene embedding is that the number of Kékulé structures (**K**) of a test structure has to be divisible by two or a_{N-1} by two for OAH. Similarly, pentadienyl or naphthalene embedding can only be accomplished on structures with **K** values divisible by three or a_{N-1} by three for OAH. Ethene and butadiene embedding only require the **K** value of a test structure to be divisible by one. This is probably why ethene and butadiene embedding appear to be the most commonplace.

1.5.4 Relationships Between the Zero Roots and Coefficients of a Polynomial

In general, a polynomial can be written as follows

$$f(X) = a_0 X^n + a_1 X^{n-1} + a_2 X^{n-2} + \ldots + a_n$$
$$= a_0(X - r_1)(X - r_2)\ldots(X - r_n).$$

where $r_i, i = 1, 2, \ldots, n$, are the roots, repeated as necessary. For monic polynomials:

$$a_0 = 1$$

$$a_1 = -r_1 - r_2 - \ldots - r_n = -\sum_{i=1}^{n} r_i$$

$$a_2 = r_1 r_2 + r_1 r_3 + \ldots + r_1 r_n + \ldots + r_{n-1} r_n = \sum_{i<j}^{n} r_i r_j$$

$$a_n = (-1)^n r_1 r_2 \ldots r_n.$$

These general polynomial properties can be employed to obtain all the eigenvalues of certain embeddable polyenes. Styrene can be embedded by allyl and ethene and, therefore, has eigenvalues of $\varepsilon = \pm\sqrt{2}$ and ± 1.0. To obtain the remaining four eigenvalues of styrene, one can use the general relations between the roots ($X = \varepsilon$) and the coefficients of the characteristic polynomial. Specifically,

$$a_2 = -q = \sum_{i<j} \varepsilon_i \varepsilon_j \text{ and } |a_n| = \mathbf{K}^2 = \varepsilon_1 \varepsilon_2 \varepsilon_3 \ldots \varepsilon_n.$$

For styrene, $q = 8$ and $\mathbf{K} = 2$, and using the above relationships give

$$-8 = -2 - 1 - \varepsilon_a^2 - \varepsilon_b^2 \text{ and } 4 = 2 \cdot 1 \cdot \varepsilon_a^2 \cdot \varepsilon_b^2,$$

respectively. These reduce to the following respective equations.

$$\varepsilon_a^2 + \varepsilon_b^2 = 5 \text{ and } \varepsilon_a^2 = \frac{2}{\varepsilon_b^2}$$

Substitution of the later into the former gives the following biquadratic equation $\varepsilon^4 - 5\varepsilon^2 + 2 = 0$. Solution of this biquadratic gives the remaining four eigenvalues of ± 0.66215 and ± 2.13578 for styrene. The same approach can be used

for obtaining the four remaining eigenvalues of naphthalene (embeddable by ethene and 1,3-butadiene) and anthracene (embeddable by allyl in two distinct ways and by benzene).

1.6 Eigenvectors

1.6.1 Introduction

In this section we will show how to use the same inspection methods and equations (Table 1.2) to determine the eigenvectors (wave function coefficients) belonging to each eigenvalue (jth energy level) of the characteristic polynomial. Two principal methods will be presented [18–19]. The first method [18] involves deleting all mutually exclusive paths from vertex 1 to vertex r in a molecular graph to give a set of remaining subgraphs. The sum of the characteristic polynomials of these subgraphs gives the eigenvector polynomial for the C_{rj} coefficient corresponding to the vertex r of the parent molecular graph. The second method [19] involves deleting each vertex r of a molecular graph. The characteristic polynomial of the subgraph obtained by deleting vertex r divided by the derivative of the characteristic polynomial of the molecular graph when evaluated for each eigenvalue will give the corresponding normalized C_{rj} coefficient.

1.6.2 Path Deleting Procedure for Determining Eigenvectors

This graph theoretical procedure for directly writing down the eigenvectors of a molecular graph is based on the observation that a cofactor of the diagonal term a_{ii} is, within a multiplicative factor, equal to the characteristic polynomial produced from $|X\mathbf{I} - \mathbf{A}|$ by eliminating row i and column i. The corresponding graph is the subgraph which results from eliminating vertex i with its incident edges. The cofactor a_{ii} is, within the same signed multiplicative factor, equal to a linear combination of terms each containing the product of edge weights directed from vertex i to vertex j multiplied by the characteristic polynomial produced from $|X\mathbf{I} - \mathbf{A}|$ by eliminating rows and columns labeled by i and j along with any intervening indices. The corresponding graph is the subgraph which results from eliminating all edges directed from vertex i to vertex j. Each term in the expansion is then equivalent to tracing a path from vertex i to vertex j, taking the product of the edge weights traversed, and multiplying the product by the characteristic polynomial of the subgraph obtained by eliminating all vertices and incident edges along the traced path. For example, consider allyl and its secular determinant as follows:

$$P(\text{allyl}; X) = \begin{vmatrix} X & -1 & 0 \\ -1 & X & -1 \\ 0 & -1 & X \end{vmatrix} = X^3 - 2X = 0.$$

Deleting vertex 1 gives ethene and corresponds to the scoring out the first row and first column of the above determinant, namely

$$C_1 \equiv \begin{vmatrix} X & -1 \\ -1 & X \end{vmatrix} = X^2 - 1.$$

Similarly, deleting the path containing vertex 1 and vertex 2 leaves a methyl radical and corresponds to scoring out the first row and second column to the allyl secular determinant and multiplying the resulting cofactor by -1 gives

$$C_2 \equiv - \begin{vmatrix} -1 & -1 \\ 0 & X \end{vmatrix} = X.$$

Finally, deleting the path 1–2–3 leaves the null graph which corresponds to scoring out the first row and third column of the allyl secular determinant to give

$$C_3 \equiv \begin{vmatrix} -1 & X \\ 0 & -1 \end{vmatrix} = 1.$$

These are just the unnormalized eigenvector polynomials of allyl which give the specific eigenvectors by substituting in the corresponding eigenvalues. Thus, the respective unnormalized wave functions ($\psi = C_1\phi_1 + C_2\phi_2 + C_3\phi_3$) for the allyl eigenvalues of $X = \varepsilon = \sqrt{2}$, 0, and $-\sqrt{2}$ are

$$\psi_1 = \phi_1 + \sqrt{2}\,\phi_2 + \phi_3$$
$$\psi_2 = -\phi_1 + \phi_3$$
$$\psi_3 = \phi_1 - \sqrt{2}\,\phi_2 + \phi_3.$$

To obtain normalized eigenvectors, we can use either of the following two equations for each eigenvalue:

$$N = [C_1^2 + C_2^2 + C_3^2 + \ldots]^{-1/2}$$

or

$$N = [P(G - v_1; X) \cdot P'(G; X)]^{-1/2} = [C_1 \cdot P'(G; X)]^{-1/2}$$

The second equation is the product of the characteristic polynomial of the subgraph obtained by deleting vertex 1 from a precursor molecular graph and the derivative of the characteristic polynomial of the molecular graph. Multiplying each corresponding coefficient by the normalizing factor N gives the desired normalized eigenvectors. In the case of allyl, the first equation for $X = \varepsilon = \sqrt{2}$ gives

$$N = [1 + 2 + 1]^{-1/2} = \tfrac{1}{2}.$$

Alternatively, using the second equation for

$$P(G - v_1; X) = C_1 = X^2 - 1$$
$$P'(G; X) = 3X^2 - 2$$

gives

$$N = [1 \cdot (3 \cdot 2 - 2)]^{-1/2} = \tfrac{1}{2}.$$

As another example, consider the following styrene molecular graph:
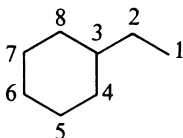
Using equations previously given (Table 1.2), the characteristic polynomial of styrene is easily deduced by inspection to be $X^8 - 8X^6 + 19X^4 - 16X^2 + 4$. Note that styrene can be embedded by ethene and allyl giving eigenvalues of $\varepsilon = \pm 1$ and $\pm \sqrt{2}$; the other four eigenvalues can be obtained easily by iteration with a hand calculator or by any programmable calculator/computer. The eigenvector polynomials for styrene as numbered above are

$$C_1 = P(\text{benzyl}) = X^7 - 7X^5 + 13X^3 - 7X$$
$$C_2 = P(\text{benzene}) = X^6 - 6X^4 + 9X^2 - 4$$
$$C_3 = L_5 = X^5 - 4X^3 + 3X$$
$$C_4 = C_8 = L_4 + L_0 = X^4 - 3X^2 + 2$$
$$C_5 = C_7 = L_3 + L_1 = X^3 - X$$
$$C_6 = 2L_2 = 2X^2 - 2.$$

When it is obvious from the context, L_n will be used for $P(L_n)$. Solutions of these eigenvector polynomials for $\varepsilon = \pm \sqrt{2}$ gives $C_1 = \mp \sqrt{2}$, $C_2 = -2$, $C_3 = \mp \sqrt{2}$, $C_4 = C_8 = 0$, $C_5 = C_7 = \pm \sqrt{2}$, and $C_6 = 2$. Dividing each of these coefficients by 4 gives the corresponding normalized vectors. In this example, all $C_i = 0$ for $\varepsilon = \pm 1$, although styrene is not degenerate in these eigenvalues. Nevertheless, the corresponding eigenvectors in this case are easily deduced from its ethene embedding. Ideally, one should select an initial vertex for eigenvalue evaluation which does not have a zero coefficient for any of the eigenvalues. Sometimes this is unavoidable and more than one vertex would have to be used to generate the complete eigenvector set. If styrene is renumbered as follows,
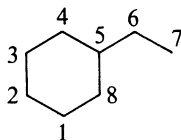
then the eigenvector polynomials become

$$C_1 = X^7 - 6X^5 + 9X^3 - 3X$$
$$C_2 = X^6 - 5X^4 + 6X^2 - 2$$

$$C_3 = X^5 - 3X^3 + X$$
$$C_4 = 2X^4 - 5X^2 + 2$$
$$C_5 = X^5 - 2X^3 + X$$
$$C_6 = X^4 - X^2$$
$$C_7 = X^3 - X$$
$$C_8 = X^6 - 5X^4 + 7X^2 - 2$$

which for $\varepsilon = \pm 1$ give $C_1 = \pm 1$, $C_2 = C_5 = C_6 = C_7 = 0$, $C_3 = \mp 1$, $C_4 = -1$, and $C_8 = 1$.

The graph theoretical procedure for determining an unnormalized eigenvector set for a molecular graph having degenerate eigenvalues will now be illustrated. The eigenvector coefficient C_1 for vertex 1 in a molecular graph is found by deleting vertex 1 and evaluating the characteristic polynomial of the resulting subgraph. Then C_2 is determined from a path of length one from vertex 1 to vertex 2 by evaluating the characteristic polynomial of the subgraph obtained by deletion of these two vertices. If there are several self-avoiding paths from vertex 1 to vertex i, then C_i is determined by the linear combination all the characteristic polynomials associated with the subgraphs resulting from deletion of all the inclusive vertices belonging to a set i of self-avoiding paths. The eigenvector coefficients for nondegenerate eigenvalues are obtained by substitution of the corresponding eigenvalue roots. The coefficients are all zero for degenerate eigenvalues as they are roots of the eigenvector polynomials. For an n-tuple degeneracy, take $n - 1$ derivatives of the eigenvector polynomials. This gives only one eigenvector solution where the remaining degenerate eigenvectors are frequently obtained through the use of symmetry. To illustrate, consider benzene with eigenvalues of $\varepsilon = \pm 1$, ± 1, and ± 2 and numbered counterclockwise as follows.

$$P(C_6H_6; X) = X^6 - 6X^4 + 9X^2 - 4$$
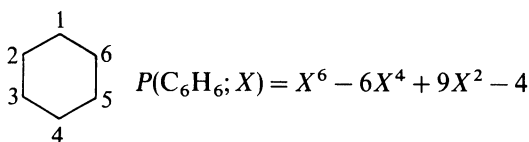
The eigenvector coefficient C_1 is found by deleting vertex 1 leaving the pentadienyl subgraph: $C_1 = L_5$. Since there are two self-avoiding paths from vertex 1 to vertex 2, namely 1–2 and 1–6–5–4–3–2, then $C_2 = L_4 + L_0$. Similarly, $C_3 = C_5 = L_3 + L_1$, $C_4 = 2L_2$, and $C_6 = C_2 = L_4 + L_0$. Note that here we represent $P(L_n)$ by L_n.

For eigenvalues of $\varepsilon = \pm 2$, we obtain

$$C_1 = L_5 = X^5 - 4X^3 + 3X$$
$$C_1(2) = 6 \text{ and } C_1(-2) = -6$$
$$C_2 = C_6 = L_4 + L_0 = X^4 - 3X^2 + 2$$
$$C_2(2) = C_6(2) = 6 \text{ and } C_2(-2) = C_6(-2) = 6$$

$$C_3 = C_5 = L_3 + L_1 = X^3 - X$$
$$C_3(2) = C_5(2) = 6 \text{ and } C_3(-2) = C_6(-2) = -6$$
$$C_4 = 2L_2 = 2(X^2 - 1)$$
$$C_4(2) = 6 \text{ and } C_4(-2) = 6$$

Since $C_1 = C_2 = C_3 = C_4 = 0$ for the degenerate eigenvalues of $\varepsilon = \pm 1$, the first derivative of the above eigenvector polynomials must be used. Thus,

$$C_1 = 5X^4 - 12X^2 + 3$$
$$C_1(1) = -4 \text{ and } C_1(-1) = -4$$
$$C_2 = C_6 = 4X^3 - 6X$$
$$C_2(1) = C_6(1) = -2 \text{ and } C_2(-1) = (-1) = 2$$
$$C_3 = C_5 = 3X^2 - 1$$
$$C_3(1) = C_5(1) = 2 \text{ and } C_3(-1) = C_5(-1) = 2$$
$$C_4 = 4X$$
$$C_4(1) = 4 \text{ and } C_4(-1) = -4.$$

From the mirror plane through vertices 1 and 4 and the antisymmetric relationship, the following is obtained for the second eigenvalue of $\varepsilon = \pm 1$:

$$C_1 = C_4 = 0$$
$$C_2 = -C_6$$
$$C_3 = -C_5$$

1.6.3 Vertex Deleting Procedure for Determining Eigenvectors

This procedure leads directly to normalized eigenvectors and is based on Ulam's subgraphs. An Ulam subgraph of graph G is obtained by deleting a vertex v with all incident edges from G. The derivative $P'(G; X)$ is equal to the sum of the characteristic polynomials of all the Ulam subgraphs [20]. It has been shown [19] that the normalized eigenvector coefficient of the rth vertex corresponding to the jth eigenvalue is given by

$$C_{rj}^2 = P(G - v_r; X_j)/P'(G; X_j).$$

Thus, the collection of Ulam subgraphs provides a graph theoretical route for obtaining eigenvectors. One shortcoming of this procedure is that the sign of C_{rj} must be determined by other means. For AH, one knows that these eigenvector coefficients are all positive for the most positive eigenvalue and one can use the pairing theorem to obtain the signs for these coefficients for the AMOs from the BMOs. Consider allyl as numbered previously. Using this method gives

$$C_{1j}^2 = C_{3j}^2 = L_2/P'(G; X) = (X^2 - 1)/(3X^2 - 2)$$

and

$$C_{2j}^2 = L_1^2/P'(G; X) = X^2/(3X^2 - 2).$$

For X evaluated at $\varepsilon = \sqrt{2}, 0, -\sqrt{2}$,
we obtain

$$C_1^2(\sqrt{2}) = C_3^2(\sqrt{2}) = 1/4 \text{ or } C_1 = C_3 = \tfrac{1}{2}$$

and

$$C_2^2(\sqrt{2}) = \tfrac{1}{2} \text{ or } C_2 = \sqrt{2}/2;$$
$$C_1^2(0) = C_3^2(0) = \tfrac{1}{2} \text{ or } C_1 = 1/\sqrt{2},\ C_3 = -1/\sqrt{2}$$

and

$$C_2^2(0) = 0 \text{ or } C_2 = 0;$$
$$C_1^2(-\sqrt{2}) = C_3^2(-\sqrt{2}) = 1/4 \text{ or } C_1 = C_3 = \tfrac{1}{2}$$

and

$$C_2^2(-\sqrt{2}) = \tfrac{1}{2} \text{ or } C_2 = -1/\sqrt{2}.$$

As another example, consider the following molecules:

$$P(G; X) = X^8 - 9X^6 - 2X^5 + 24X^4 + 8X^3 - 19X^2 - 4X + 5$$

$$P'(G; X) = 8X^7 - 54X^5 - 10X^4 + 96X^3 + 24X^2 - 38X - 4$$
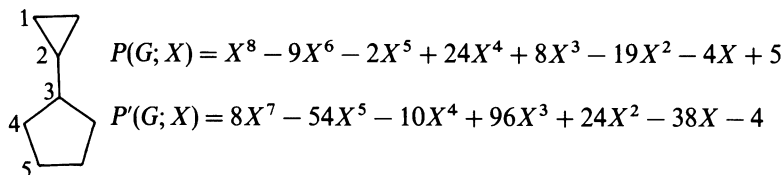
Using the equations in Table 1.2, one obtains all the coefficients to the above characteristic polynomials, except a_7 and a_8. From the set of Sachs graphs on seven vertices $S_7 = \{C_5 \cup K_2, C_3 \cup 2K_2\}$, we obtain

$$a_7 = a_5(C_5)\cdot a_2(C_3) + a_3(C_3)\cdot a_4(C_5)$$
$$= (-2)(-3) + (-2)(5) = -4$$

where a_2 and a_4 are given by equations in Table 1.2. From the set of Sachs graphs on eight vertices $S_8 = \{4K_2, C_3 \cup C_5\}$, one obtains

$$a_8 = (-1)^4 2^0 + (-1)^2 2^2 = 5.$$

The eigenvector polynomials per the vertex deletion procedure are

$$C_{1j}^2 = (X^7 - 7X^5 + 13X^3 - 2X^2 - 6X + 2)/P'(G; X)$$
$$C_{2j}^2 = (X^2 - 1)(X^5 - 5X^3 + 5X - 2)/P'(G; X)$$
$$C_{3j}^2 = (X^3 - 3X - 2)(X^4 - 3X^2 + 1)/P'(G; X)$$
$$C_{4j}^2 = (X^7 - 7X^5 - 2X^4 + 13X^3 + 6X^2 - 5X - 2)/P'(G; X)$$
$$C_{5j}^2 = (X^7 - 7X^5 - 2X^4 + 12X^3 + 6X^2 - 4X - 2)/P'(G; X).$$

It is not necessary to know the signs of the above coefficients, if we wish to use them for computing electron density (Q) or charge density $(1 - Q)$. The electron

density on atom r is given by

$$Q_r = \sum_{j=1}^{OCC} u_j C_{rj}^2$$

where u_j is the number of electrons in the jth energy level. The occupied energy levels are 2.3590, 1.8158, 0.6765, and 0.6180 with two electrons in each. The first eigenvector polynomial above gives a charge density of $+0.28$ ($Q = 0.72$) for atom 1, and the last eigenvector polynomial gives a charge density of -0.17 ($Q = 1.17$) for atom 5. Thus, the molecule above is principally a zwitterion with $+0.84$ positive charge on the cyclopropenyl ring and -0.84 negative charge on the cyclopentadienyl ring, i.e., the neutral species below makes a 16% contribution to the overall hybrid structure.

calicene
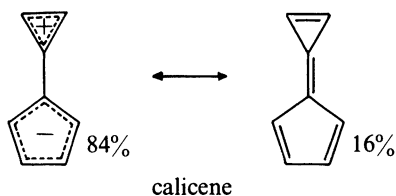
For this zwitterionic molecule all the eigenvector coefficients have positive values for the 2.3590 energy level; for the 0.6180, -1.0, and -1.6180 energy levels the corresponding signs of the eigenvector coefficients can be obtained from Table 1.4. This is because these eigenvalues result from a type of semi-embedding of ethene in the cyclopropenyl ring and butadiene in the cyclopentadienyl ring.

It is worthwhile to note that all the examples that we have dealt with thus far were implicitly assumed to be totally coplanar. If the last zwitterionic molecule assumed a perpendicular orientation of the cyclopropenyl and cyclopentadienyl rings, then its zwitterionic character should approach 100%. However, in going from a coplanar to perpendicular arrangement of its rings its total electronic pπ energy (E_π) would decrease from 10.94 to 10.47β.

A key concept which forms the basis of Dewar's perturbation molecular orbital (PMO) method is that the nonstarred positions of OAHs have zero eigenvector coefficients (zero nodes) for the unpaired zero eigenvalue and that the eigenvector coefficients to each nonstarred position must sum to zero. For OAHs this unpaired zero eigenvalue (energy level) is the frontier molecular orbital. Embedded fragment subgraphs (Table 1.4) are separated by zero nodes (zero eigenvector coefficients) and require opposite signs in order to have the eigenvector coefficients attached to each node sum to zero.

1.6.4 Determination of Bond Order

To determine the bond order P_{rs}^π between adjacent carbon atoms r and s, one needs the signs of the eigenvector coefficients. This is because the antibonding contributions for the relevant eigenvalues must be subtracted from the bonding

contributions. This is done automatically in the following bond order equation for pπ bonds

$$\dot{P}^{\pi}_{rs} = \sum_{j=0}^{OCC} u_j C_{rj} C_{sj}$$

where u_j is the number of electrons in the jth energy level. Thus, the path deleting procedure for determining eigenvectors becomes the preferred method when one needs to obtain bond orders. For the allyl radical, one obtains $P^{\pi}_{12} = P^{\pi}_{23} = 2 \cdot (\frac{1}{2}) \cdot (\sqrt{2}/2) + 1 \cdot (\frac{1}{2}) \cdot 0 = \sqrt{2}/2$ which is the same for the allyl carbocation and carbanion.

Consider the following zwitterionic molecule again, renumbered to avoid starting at the zero coefficients:

calicene
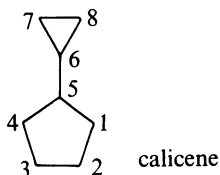
The unnormalized eigenvector polynomials per the path deleting procedure are

$$C_{1j} = X^7 - 7X^5 - 2X^4 + 13X^3 + 6X^2 - 5X - 2$$
$$C_{2j} = X^6 - 6X^4 - X^3 + 8X^2 + X - 3$$
$$C_{3j} = X^5 + X^4 - 5X^3 - 5X^2 + 2X + 2$$
$$C_{4j} = X^5 + X^4 - 4X^3 - 6X^2 + X + 3$$
$$C_{5j} = X^6 - 5X^4 - X^3 + 6X^2 + X - 2$$
$$C_{6j} = X^5 - 3X^3 + X^2 + 2X - 1$$
$$C_{7j} = X^4 + X^3 - 2X^2 - X + 1$$
$$C_{8j} = X^4 + X^3 - 2X^2 - X + 1.$$

The occupied energy levels for this zwitterionic molecule are 2.3590, 1.8158, 0.6765, and 0.6180 with two electrons in each. For the 5–6 bond, one obtains a bond order of 0.44 which can be compared to the bond order of 0.45 for the 2–3 bond of butadiene. The average bond order for the cyclopropenyl and cyclopentadienyl ring in this zwitterion is 0.63 which can be compared with the bond orders of 0.67 for the cyclopropenyl cation and 0.64 for the cyclopentadienyl anion.

To obtain bond lengths (BL) in angstroms (10^{-8} cm) from computed bond orders P^{π}_{rs} for AHs, one can use the equation of BL = 1.506 $-$ 0.169 P^{π}_{rs}.

1.6.5 Example Applications

To illustrate the application of HMO determination of electron density and bond order of real molecules consider the following compounds. By applying

I

II

III

IV $\dfrac{0.76}{}$ +0.38
fulvene

 V

VI $\dfrac{0.71}{}$ +0.46
benzo[b]fulvene

$X^6 - 6X^4 + 8X^2 - 2X - 1$ benzo[a]fulvene \0.80
+0.22

$$X^{10} - 11X^8 + 40X^6 - 2X^5 - 57X^4 + 6X^3 + 28X^2 - 4X - 1$$
$$X^{10} - 11X^8 + 40X^6 - 2X^5 - 58X^4 + 6X^3 + 31X^2 - 4X - 4$$
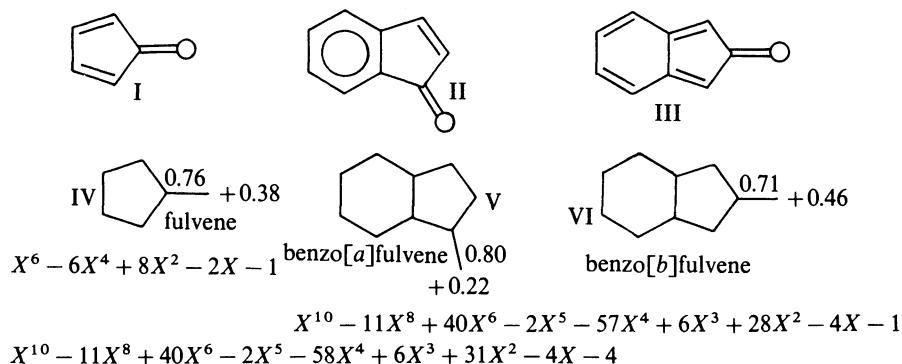
the principle of parallel correspondence, I to III are replaced by their isoconjugates IV to VI, respectively. The compound with the higher computed bond order in its isoconjugate will have the higher anticipated carbonyl frequency, and the compound with the higher electron density will have the higher anticipated basic carbonyl oxygen. To obtain the value of a_8 for benzo[b]fulvene (V), one can use the indicated semi-embedding of ethene for the eigenvalue of 1.0. Alternatively, if $G - e$ is the graph G with edge e deleted and $G - (e)$ is G with edge e and its associated vertices deleted, then $a_8(G) = a_8(G - e) - a_6(G - (e))$ is a useful relationship if e is not on a trigonal, tetragonal, hexagonal, or octagonal ring. Thus, $a_8(\text{indenyl}) = a_8(\text{2-vinylbenzyl}) - a_6(\text{benzyl}) = a_8(\text{1-allyl-benzene}) - a_6(L_7) = 15$ and $a_8(\text{benzo[b]fulvene}) = a_8(\text{indenyl}) - a_6(o\text{-quinodimethane}) = 28$. Thus, II is expected to have the higher carbonyl frequency and basicity.

1.7 References

1. Dewar MJS (1984) J Am Chem Soc 106; 669
2. Rabalais JW, Debies TP, Berosky JL, Huang J, Ellison FO (1974) J Chem Phy 61: 516
3. Roberts JD (1962) Molecular orbital calculations. Benjamin, NY
4. Sachs H (1963) Publ Math 11: 119; Cvetkovic' DM, Doob M, Sachs H (1980) Spectra of graphs-Theory and applications. Academic Press, NY
5. Trinajstic' N (1983) Chemical graph theory. CRC, Boca Raton, FL
6. Coulson CA (1950) Proc Cambridge Philos Soc 46: 202
7. Dias JR (1990) J Math Chem 4: 127; (1987) J Chem Educ 64: 213; (1985) Theor Chim Acta 68: 107
8. Hall GG (1957) Trans Faraday Soc 53: 573
9. McClelland BJ (1974) J Chem Soc, Faraday Tran II 70: 1453
10. D'Amato SS (1979) Theor Chim Acta 53: 319; (1979) Molec Phys 37: 1363; Davidson RA (1981) Theor Chim Acta 58: 193
11. Dias JR (1988) J Molec Struct (Theochem) 165: 125; (1989) Theor Chim Acta 76: 153; (1989) J Molec Struct (Theochem) 185: 57
12. Halton B, Randall CJ, Gainsford GJ, Stang PJ (1986) J Am Chem Soc 108: 5049
13. Dias JR (1985) Nouv J Chim 9: 125
14. Hall GG (1977) Molec Physics 33: 551; (1981) Bull Inst Math Appl 17: 70; Dias JR (1987) J Molec Struct (Theochem) 149: 213; (1987) Match 22: 257
15. Dewar MJS (1969) The molecular orbital theory of organic chemistry. McGraw-Hill, New York
16. Klein DJ, Nelin C, Alexander S, Matsen F (1982) J Chem Phy 77: 3101; Dias JR (1986) J Molec Struct (Theochem) 137: 9
17. Mallion RB, Rouvray DH (1990) J Math Chem 5: 1

18. Kassman AJ (1985) Theor Chim Acta 67: 2555
19. Mukherjee AK, Datta KK (1989) Proc Indian Acad Sci 101: 499
20. Randic' M (1982) J Comput Chem 3: 421

1.8 Problems

1   Give the total eigenvalue/eigenvector solution for cyclopentadienyl anion. Show that the charge density $(1 - Q)$ at every carbon atom is -0.2 and that the bond order between every pair of adjacent carbon atoms is 0.647. Note that one of the degenerate 0.61803 energy levels has eigenvectors listed in Table 1.3.

2   In (1987) J Chem Educ 64: 213, show that structure **17** has the missing term of $-19X^2$ by determining its characteristic polynomial.

3   In (1987) J Chem Educ 64: 213, show that structures **1, 2, 5, 6, 7, 9**, and **13** can be embedded by ethene. Similarly, show that structures **2, 4, 10**, and **15** can be embedded by allyl. What isomer of **8** can be embedded by butadiene?

4   In (1985) Nouv J Chim 9: 125, verify the characteristic polynomials for naphthalene, azulene, bicyclo[6.2.0]decapentaene, and bicyclo[7.1.0]-decapentaene. Show that naphthalene can be embedded by ethene and butadiene. Use the general properties of monic polynomials and solve the biquadratic equation thus obtained for the remaining eigenvalues of napththalene.

5   Compute the charge density on the cyclopentadienyl ring for the following molecules and compare these values versus the given average ^{13}C NMR chemical shifts [(1991) Tetrahedron Lett 29: 3499].

102.1   129.6   120.7   124.3
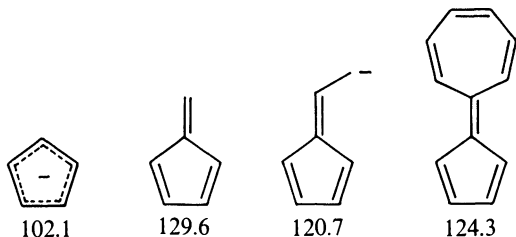
6   Corroborate the eigenvalue embedding given below.

$0, \pm 1$ $\pm 1, \pm 1, \pm 2$ $\pm\frac{1}{2}(\sqrt{5} \pm 1)$
$\pm\sqrt{2}$
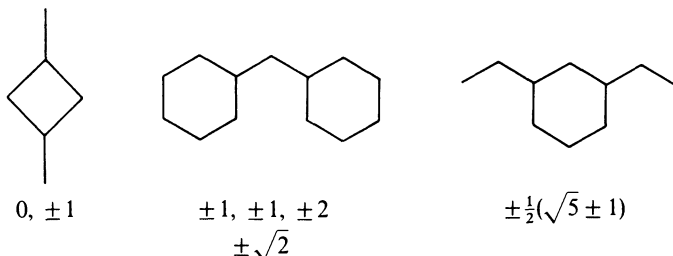
7 Substantiate the charge densities given below [(1991) Tetrahedron Lett 32: 4659].

+0.46

−0.19
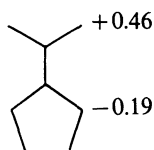
8 Show that the following molecular graphs are isospectral, i.e., have the same characteristic polynomials [(1975) Tetrahedron 31: 99].
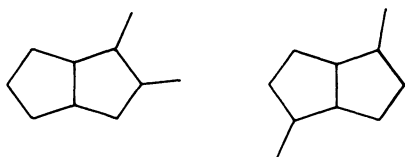
9 Discuss the probability of the following reaction occurring. Determine whether the opening of the cyclopropylidene ring is conrotatory or disrotatory.
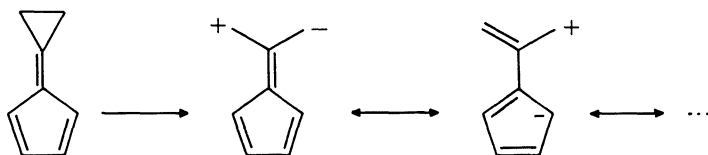
10 Dowd [(1986) J Am Chem Soc 108: 7416] has experimentally shown that the following is a ground-state triplet contrary to the ab initio prediction [(1987) J Am Chem Soc 109: 930]. Will the energy barrier for formation of the cyclobutane ring be higher for the triplet or singlet ground-state?

11 In the following reaction, a soft electrophile like an aldehyde adds to the exocyclic position where the HOMO has a large coefficient; whereas, harder electrophiles (i.e., proton or alkyl halides) preferentially add to the cyclo-pentadienyl ring where the negative charge is concentrated (90% according to a Hückel calculation). Verify the above HMO parameters and explain the reaction results [(1991) Tetrahedron Lett 32: 5247].
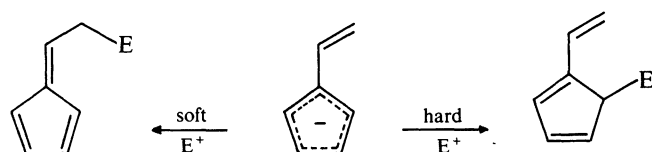
Chapter 2
Decomposition of Molecules with *n*-Fold Symmetry

2.1 Introduction

In Chapter 1 we developed graph theoretical methods for the facile solution of HMO parameters of conjugated polyenes with eight or less carbon vertices without having to expand their secular determinants. Also, it was shown that knowledge of some eigenvalues through other means, such as embedding, permitted us to solve even larger molecular polyenes for their HMO parameters. In this chapter, we will show how to decompose or fragment larger symmetrical molecular graphs into smaller subgraphs. The eigenvalues of these subgraphs then can be obtained by the methods discussed in Chapter 1. The collection of eigenvalues for these subgraphs will be eigenvalues of the precursor molecular graph. Mirror plane fragmentation of molecules having at least one mirror plane of symmetry (e.g., C_{2v} and D_{2h}) is the most general decomposition method.

2.2 Decomposition of Molecules with 2-Fold Symmetry

2.2.1 Mirror Plane Fragmentation

Molecules possessing a plane of symmetry can be decomposed into fragments having smaller corresponding secular determinants [1]. McClelland has described the following rules for the decomposition of a molecule with a plane of symmetry into smaller fragments [2]:

1) The symmetry plane divides a molecular graph into two fragment graphs—a right-hand fragment and a left-hand fragment.
2) Vertices on the plane of symmetry are included in the left fragment.
3) The weight of the edge between a vertex lying on the plane of symmetry and a vertex not on the plane but in the left fragment is $\sqrt{2}$.
4) If the symmetry plane bisects an edge originally connecting the left and right fragments, the vertex in the left fragment is weighted $+1$ (Coulomb integral = $\alpha - \beta$) and the vertext in the right fragment is weighted -1.
5) The eigenvalues of the original graph equal the eigenvalues of the fragment graphs.

For example, consider the σ-bond graph of ethene. Its mirror plane fragmentation gives the following where application of rule 4 results in $X = (\varepsilon - \alpha)/\beta = 1$

for the left fragment ($\oplus$) and $X = (\varepsilon - \alpha)/\beta = -1$ for the right fragment ($\bigcirc$).

mirror
plane

mirror
plane

decomposition

$\oplus$ $\bigcirc$

$X - 1 = 0$ $X + 1 = 0$

ethene
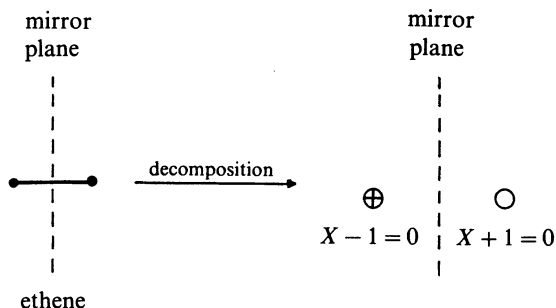
Mirror plane decomposition of allyl and application of rule 3 gives the following.

mirror
plane

mirror
plane

decomposition

$\sqrt{2}$

$X = 0$

$$\begin{vmatrix} X & -\sqrt{2} \\ -\sqrt{2} & X \end{vmatrix}$$

allyl

$= X^2 - 2 = 0$
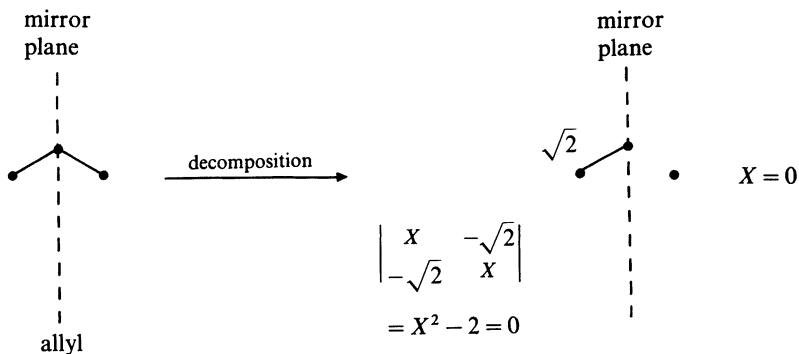
Mirror plane fragmentation of cyclopentadienyl is overall illustrative of these rules as shown by the following.

mirror
plane

mirror
plane

decomposition

left
fragment

$\oplus$ $\bigcirc$ right
fragment

$\sqrt{2}$

cyclopentadienyl

$$\begin{vmatrix} (X-1) & -1 & 0 \\ -1 & X & -\sqrt{2} \\ 0 & -\sqrt{2} & X \end{vmatrix}$$

$= X^3 - X^2 - 3X + 2$

$$\begin{vmatrix} (X+1) & -1 \\ -1 & X \end{vmatrix}$$

$= X^2 + X - 1$
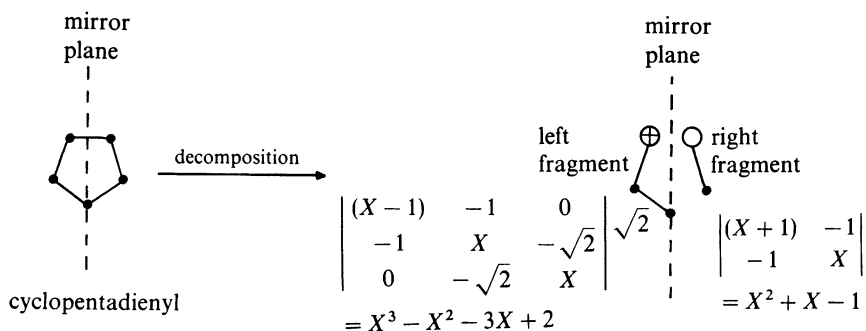
From these examples it should be evident that the eigenvalues of the right fragment are invariant in regard to the identity of the atoms or polyene substituents on the mirror plane vertices. Thus, the characteristic polynomial and eigenvalues of many chemically relevant mirror plane fragments are listed in Table 2.1. Mirror plane fragmentation of alternant hydrocarbons having a mirror plane passing exclusively through vertices is equivalent to embedding

**Table 2.1. Common mirror plane fragments and their eigenvalues**
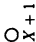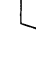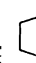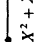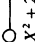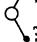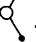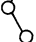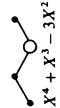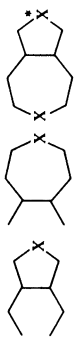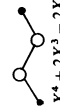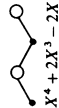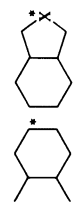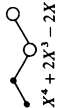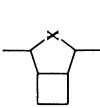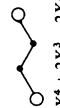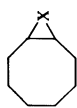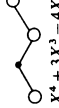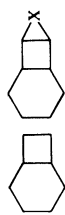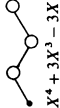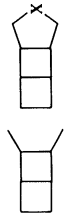
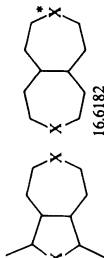| Mirror Fragment	Representative Polyene Family	Eigenvalues, β
$X+1$	2.000 5.1231	-1
X^2+X-1	6.4721	$\frac{1}{2}(\sqrt{5}-1),\ -\frac{1}{2}(\sqrt{5}+1)$
X^2+2X	5.8416 6.3402	$0,\ -2$
X^3+X^2-2X-1	7.9800 8.3184 8.0978	$1.2470,\ -0.4450,\ -1.8019$
X^3+X^2-2X	10.4556	$1,\ 0,\ -2$
X^3+2X^2-X-1	8.9061	$0.8019,\ -0.5550,\ -2.2469$
X^3+2X^2-X-2	9.2426	$1,\ -1,\ -2$
X^3+3X^2+X-1	9.2571 12.9952 11.5175	$(\sqrt{2}-1),\ -1,\ -(\sqrt{2}+1)$
$X^4+X^3-3X^2-2X+1$	11.3626	$1.5321,\ 0.3473,\ -1,\ -1.8794$

Table 2.1. (*Continued*)

Mirror Fragment	Representative Polyene Family	Eigenvalues, β
$X^4 + X^3 - 3X^2 - X + 1$	11.3756 11.0015 13.3635	1.3557, 0.4773, −0.7376, −2.0953
$X^4 + 2X^3 - 2X^2 - 2X + 1$	9.6569 13.4156	1, $(\sqrt{2}-1)$, −1, $-(\sqrt{2}+1)$
$X^4 + 2X^3 - 2X^2 - 3X + 1$	9.9540 12.1707	1.1935, 0.2950, −1.2950, −2.1935
$X^4 + 2X^3 - 2X^2 - 3X$		$\frac{1}{2}(\sqrt{13}-1)$, 0, −1, $\frac{1}{2}(\sqrt{13}+1)$
$X^4 + 2X^3 - 2X^2 - 4X$		$\sqrt{2}$, 0, $-\sqrt{2}$, −2
$X^4 + 3X^3 - 4X - 1$	10.3812	1.0953, −0.2624, −1.4773, −2.3557
$X^4 + 3X^3 - 3X$		0.8794, 0, −1.3473, −2.5321
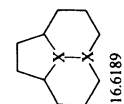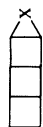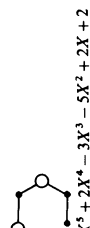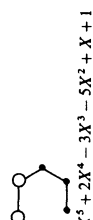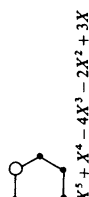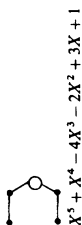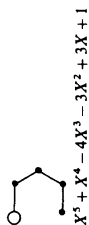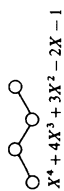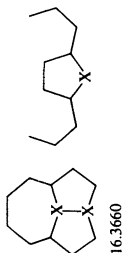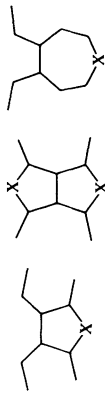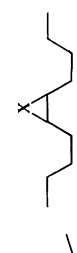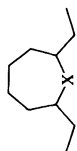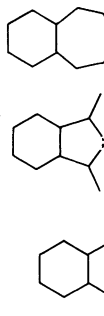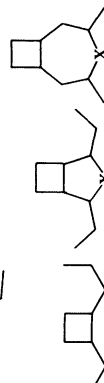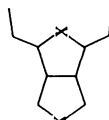
$\frac{1}{2}(\sqrt{5}-1)$, $-\frac{1}{2}(3-\sqrt{5})$, $-\frac{1}{2}(\sqrt{5}+1)$, $-\frac{1}{2}(3+\sqrt{5})$

1.6825, 0.83083, −0.28463, −1.3097, −1.9190
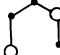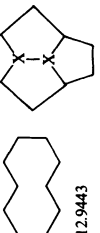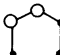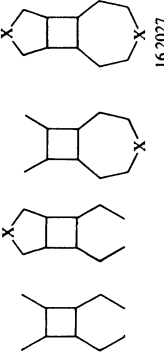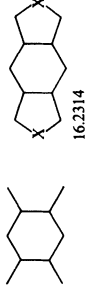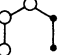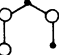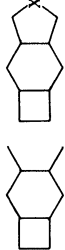
1.4812, 1, −0.31111, −1, −2.1701

1.5764, 0.74747, 0, −1.1971, −2.1268

1.5563, 0.50626, −0.41083, −1.3342, −2.31805

$\sqrt{2}$, 0.80194, −0.55496, $-\sqrt{2}$, −2.2470

16.3660

16.6189

16.6182

14.2518

12.8646

$X^4 + 4X^3 + 3X^2 - 2X - 1$

$X^5 + X^4 - 4X^3 - 3X^2 + 3X + 1$

$X^5 + X^4 - 4X^3 - 2X^2 + 3X + 1$

$X^5 + X^4 - 4X^3 - 2X^2 + 3X$

$X^5 + 2X^4 - 3X^3 - 5X^2 + X + 1$

$X^5 + 2X^4 - 3X^3 - 5X^2 + 2X + 2$

Table 2.1. (Continued)

Mirror Fragment	Representative Polyene Family	Eigenvalues, β
$X^5 + 2X^4 - 3X^3 - 5X^2 + 2X + 1$	12.9443	$1.48119, \frac{1}{2}(\sqrt{5}-1), -0.31105, -\frac{1}{2}(\sqrt{5}+1), -2.1701$
$X^5 + 2X^4 - 3X^3 - 6X^2 + X + 2$	16.1937	$\frac{1}{2}(\sqrt{5}+1), \frac{1}{2}(\sqrt{5}-1), -\frac{1}{2}(\sqrt{5}-1), -\frac{1}{2}(\sqrt{5}+1), -2$
$X^5 + 2X^4 - 3X^3 - 4X^2 + 2X + 1$	16.2027	$1.3354, 0.71453, -0.33933, -1.2607, -2.44983$
$X^2 + 2X^4 - 3X^3 - 4X^2 + 3X$	16.2314	$1.3028, \frac{1}{2}(\sqrt{5}-1), 0, -\frac{1}{2}(\sqrt{5}+1), -2.30278$
$X^5 + 3X^4 - X^3 - 6X^2 - X + 1$		$1.31801, 0.33419, -0.58962, -1.50629, -2.55629$
$X^5 + 3X^4 - X^3 - 6X^2 + 1$		$1.24698, \sqrt{2}-1, -0.44504, -1.8019, \sqrt{2}+1$

$1.44983, 0.26073, -0.66067, -1.71447, -2.33535$

$1.1701, \frac{1}{2}(\sqrt{5}-1), -0.68889, -\frac{1}{2}(\sqrt{5}+1), -2.48119$

$1, \frac{1}{2}(\sqrt{5}-1), -0.38197, -\frac{1}{2}(\sqrt{5}+1), -\frac{1}{2}(\sqrt{5}+3)$

$\frac{1}{2}(\sqrt{13}-1), \frac{1}{2}(\sqrt{5}-1), -1, -\frac{1}{2}(\sqrt{5}+1), -\frac{1}{2}(\sqrt{13}+1)$

$0.91899, 0.30972, -0.71537, -1.83083, -2.68251$

$1.12676, 0.19713, -1, -1.74747, -2.57636$

$1.17009, 0, -0.68889, -2, -2.48119$

$(\sqrt{3}-1), 0, -1, -2, -(\sqrt{3}+1)$

15.0253

13.6832

$X^5 + 3X^4 - X^3 - 7X^2 - 2X + 1$

$X^5 + 3X^4 - X^3 - 6X^2 + 2$

$X^5 + 3X^4 - X^3 - 5X^2 + X + 1$

$X^5 + 3X^4 - X^3 - 7X^2 - X + 3$

$X^5 + 4X^4 + 2X^3 - 5X^2 - 2X + 1$

$X^5 + 4X^4 + 2X^3 - 6X^2 - 4X + 1$

$X^5 + 4X^4 + 2X^3 - 6X^2 - 4X$

$X^5 + 5X^4 + 6X^3 - 2X^2 - 4X$
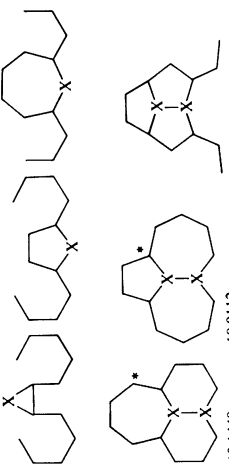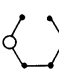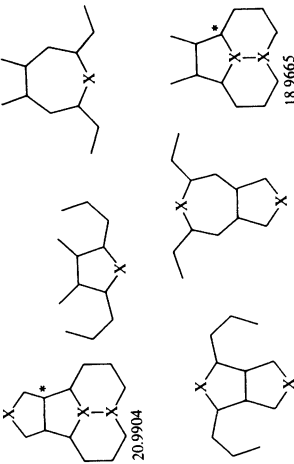
Table 2.1. (*Continued*)

Mirror Fragment	Representative Polyene Family	Eigenvalues, β
$X^6 + X^5 - 5X^4 - 4X^3 + 6X^2 + 3X - 1$	18.9112 19.1448	1.7709, 1.1361, 0.24107, -0.70921, -1.49702, -1.94188
	21.0450 20.7951	
$X^6 + X^5 - 5X^4 - 3X^3 + 6X^2 + X - 1$	18.9665 20.9904	1.70504, 1, 0.38348, -0.48980, -1.45989, -2.13883

$\frac{1}{2}(\sqrt{5}+1)$, 1.1935, 0.29496, $-\frac{1}{2}(\sqrt{5}-1)$, -1.2950, -2.1936

1.69523, 0.90163, 0, -0.729304, -1.5450, -2.32261

1.59615, 1, 0.18264, -1, -1.51572, -2.26308

1.551835, 1.11854, 0, -0.774909, -1.6713, -2.22418

1.64899, 0.87543, 0.221993, -0.81581, -1.77184, -2.15878

19.1243

$X^6 + X^5 - 5X^4 - 3X^3 + 6X^2 + 2X - 1$

$X^6 + 2X^5 - 4X^4 - 7X^3 + 3X^2 + 4X$

$X^6 + 2X^5 - 4X^4 - 7X^3 + 4X^2 + 5X - 1$

$X^6 + 2X^5 - 4X^4 - 7X^3 + 4X^2 + 5X$

$X^6 + 2X^5 - 4X^4 - 7X^3 + 4X^2 + 4X - 1$
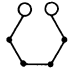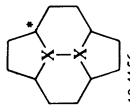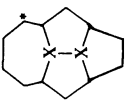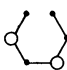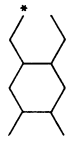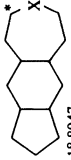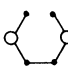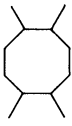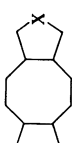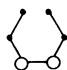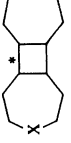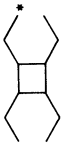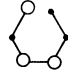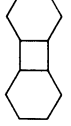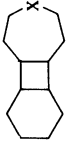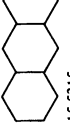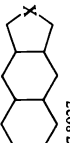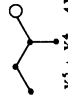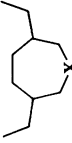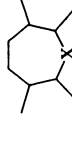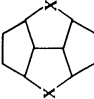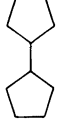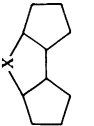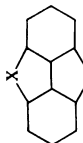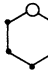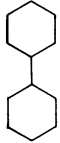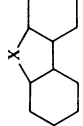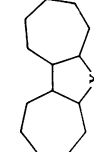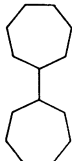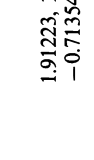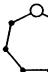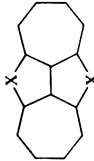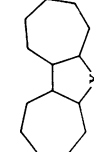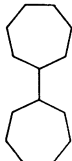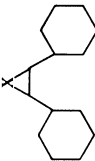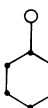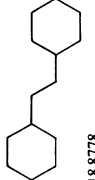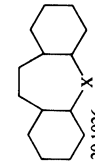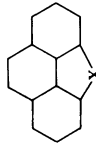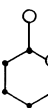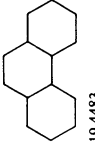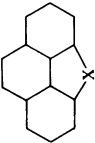
Table 2.1. (*Continued*)

Mirror Fragment	Representative Polyene Family	Eigenvalues, β
$X^6 + 2X^5 - 4X^4 - 8X^3 + 3X^2 + 6X$	19.4156 19.1279	$\sqrt{3}, 1, 0, -1, -\sqrt{3}, -2$
$X^6 + 2X^5 - 4X^4 - 6X^3 + 5X^2 + 3X - 1$	18.8947	1.44983, 1, 0.26073, -0.66067, -1.71453, -2.33536
$X^6 + 2X^5 - 4X^4 - 6X^3 + 5X^2 + 2X - 1$		1.53209, 0.8019, 0.3473, -0.5550, -1.87939, -2.2469
$X^6 + 2X^5 - 4X^4 - 6X^3 + 4X^2 + 4X$	18.5328	$\sqrt{2}, 1.1701, 0, -0.68889, -\sqrt{2}, -2.4812$
$X^6 + 3X^5 - 2X^4 - 9X^3 + 6X + 1$	17.2126	1.36234, 1, -0.174215, -1, -1.67964, -2.50848
$X^6 + 3X^5 - 2X^4 - 9X^3 + X^2 + 6X - 1$	15.5315 17.8027	1.37002, 0.84349, 0.16937, -1.16937, -1.84349, -2.37002
$X^5 + X^4 - 4X^3 - 3X^2 + 2X + 1$		1.76403, 0.69381, -0.39634, -1, -2.061508

$1.55628, 0.5063, -0.410375, -1.33416, -2.31801$

$1.89888, 0.86251, 0.328018, -0.65558, -1.3870, -2.04671$

$1.801938, 0.801938, 0.445042, -0.55496, -1.24697, -2.2470$

$1.860806, 1, 0.254102, -1, -1, -2.11492$

$1.71738, 0.771103, 0.233963, -1, -1.37486, -2.34756$

$\frac{1}{2}(\sqrt{5}+1), \frac{1}{2}(\sqrt{5}-1), (\sqrt{2}-1), -\frac{1}{2}(\sqrt{5}-1), -\frac{1}{2}(\sqrt{5}+1), -(\sqrt{2}+1)$

$X^5 + 2X^4 - 3X^3 - 5X^2 + X + 1$

$X^6 + X^5 - 5X^4 - 4X^3 + 5X^2 + 2X - 1$

$X^6 + X^5 - 5X^4 - 3X^3 + 5X^2 + X - 1$

$X^6 + X^5 - 5X^4 - 4X^3 + 5X^2 + 3X - 1$

$X^6 + 2X^5 - 4X^4 - 7X^3 + 3X^2 + 4X - 1$
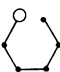
$X^6 + 2X^5 - 4X^4 - 6X^3 + 4X^2 + 2X - 1$

Table 2.1. *(Continued)*

Mirror Fragment	Representative Polyene Family	Eigenvalues, β
$X^5 + X^4 - 5X^3 - 3X^2 + 5X - 1$	16.1937, 12.7993, 14.8963	$1.86081, \frac{1}{2}(\sqrt{5}-1), 0.254102, -\frac{1}{2}(\sqrt{5}+1), -2.11491$
$X^6 + X^5 - 6X^4 - 4X^3 + 9X^2 + 3X - 4$	16.3834, 17.9059, 19.4098	$1.89122, 1, 0.704624, -1, -1.31743, -2.27841$
$X^7 + X^6 - 7X^5 - 5X^4 + 14X^3 + 6X^2 - 7X - 3$	22.0297, 19.7348, 18.0047	$1.91223, 1.24698, 1, -0.44504, -0.71354, -1.80194, -2.19869$
$X^7 + X^6 - 7X^5 - 6X^4 + 13X^3 + 9X^2 - 7X - 4$	18.8778, 20.1026, 19.7727	$2.06408, 1.15538, 1, -0.50428, -1, -1.50467, -2.21051$
$X^7 + 2X^6 - 6X^5 - 11X^4 + 9X^3 + 15X^2 - 4X - 5$	19.4483, 20.9623	$1.95063, 1.14238, 0.76905, -0.60523, -1.3058, -1.5163, -2.43476$

by the mirror plane fragment. This leads us to the concept of *local symmetry* (or hidden symmetry). Since within the HMO approximation only 1–2 interactions are taken into consideration, the absence or presence of symmetry associated with substituents attached to vertices lying on the mirror plane in the above examples has no consequence on the characteristic polynomial or eigenvalues of the right fragment, and the molecular graph as a whole does not need to possess symmetry but only needs to have local symmetry. This concept of local symmetry is the reason why embedding is possible on alternant hydrocarbons or on the alternant fragment of a nonalternant hydrocarbon that can be constructed by attaching bridging polyene substituents to node positions of the alternant fragment.

Specializing Eq. (4) in Table 1.2 by setting $h = -1$ and $\underline{k} = 1$ leads to Eq. (6) where G_0 is a graph with a weighted vertex v_0, G is its isoconjugate graph, and $G_0 - v_0$ is the graph where the weighted vertex has been deleted. Thus the polynomial of the right fragment resulting from mirror plane decomposition of cyclopentadienyl obtained in the example of the prior paragraph can be corroborated as follows:

$$P(\circ\!\!-\!\!\bullet) = P(\bullet\!\!-\!\!\bullet) + P(\bullet)$$
$$= (X^2 - 1) + (X) = X^2 + X - 1$$

To illustrate further, consider the mirror fragment of cyclobutadiene formed by bisecting two parallel bonds. Application of Eq. (6) gives

$$P(\circ\!\!-\!\!\circ) = P(\circ\!\!-\!\!\bullet) + P(\circ)$$
$$= (X^2 + X - 1) + (X + 1) = X^2 + 2X.$$

In general, if L_n represents the characteristics polynomial of a linear polyene on n carbon vertices, then

$$L[\circ\!\!-\!\!(-\!\!\bullet\!\!-)_{n-2}\!\!-\!\!\bullet] = L_n + L_{n-1}$$

and

$$L[\circ\!\!-\!\!(-\!\!\bullet\!\!-)_{n-2}\!\!-\!\!\circ] = (X + 2)L_{n-1}$$

Several generalizations about the characteristic polynomial of right mirror fragments are possible. The coefficient of the highest power X term is always plus one. The coefficient of the second highest X term is always equal to the positive number of weighted vertices (N_0). For a set of isomers the values for the coefficients to the third highest power of X are equal. When $N. > N_0$, this coefficient is given by $-(N. + r)$. The negative of the product of the eigenvalues of the mirror fragment gives the value to the coefficient of the lowest power of X.

To determine left-hand fragments with $\oplus (X - 1)$ weighted vertices (without $\sqrt{2}$ weighted edges), identify the corresponding right-hand fragment which only differs in its weighted vertices of $\circ (X + 1)$. To obtain the characteristic polynomial for the left-hand fragment change the sign for every other coefficient

in the corresponding characteristic polynomial of the right-hand fragment in Table 2.1 starting with the second term; in this case the eigenvalues of the characteristic polynomial of the left-hand fragment will have the same magnitudes but opposite signs as those for the characteristic polynomial of the corresponding right-hand fragment.

   Computation of the eigenvectors of the mirror plane fragments can be accomplished as was done in Chapter 1. The eigenvector coefficients of the vertices in these fragments not on the mirror plane must be multiplied by $1/\sqrt{2}$ to obtain the eigenvector coefficients belonging to the precursor molecular graph. Consider the vertex deleting procedure for obtaining the eigenvectors of the left-hand and right-hand mirror plane fragments of cyclopentadienyl. Let us number cyclopentadienyl clockwise starting with 1 at the bottom vertex on the mirror plane.

mirror	left fragment	right fragment
	$X^3 - X^2 - 3X + 2$	$X^2 + X - 1$
	2.0, 0.61803, -1.61803	0.61803, -1.61803
	$P'_L = 3X^2 - 2X - 3$	$P'_R = 2X + 1$
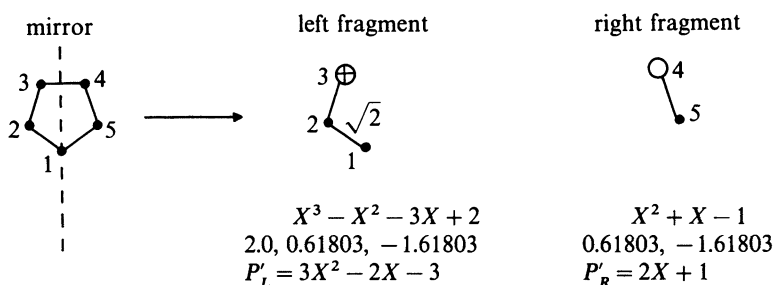
Using Eq. (10) in Table 1.2 gives

$$C_1^2 \equiv \quad = (X^2 - X - 1)/(3X^2 - 2X - 3)$$

$$C_2^2 \equiv \quad = (\tfrac{1}{2})(X^2 - X)/(3X^2 - 2X - 3)$$

$$C_3^2 \equiv \quad \sqrt{2} \quad = (\tfrac{1}{2})(X^2 - 2)/(3X^2 - 2X - 3)$$

$$C_4^2 \equiv \quad = (\tfrac{1}{2}) X/(2X + 1)$$

$$C_5^2 \equiv \quad = (\tfrac{1}{2})(X + 1)/(2X + 1)$$

Note that C_1^2 is not multiplied by $\tfrac{1}{2}$ because atom 1 is on the mirror plane in the fragmentation of cyclopentadienyl. To obtain the specific values one must evaluate C_1^2, C_2^2, and C_3^2 with only the eigenvalues associated with the left-hand fragment (2.0, 0.61803, -1.61803) and C_4^2 and C_5^2 with only the eigenvalues associated with the right-hand fragment (0.61803, -1.61803). Symmetry is used to obtain the remaining values. This is illustrated by the following eigenvector coefficient matrix.

	2.0	0.61803	0.61803	-1.61803	-1.61803
C_1	0.4472	a	-0.6324	a	0.6324
C_2	0.4472	b	-0.1954	b	-0.5117
C_3	0.4472	b	0.5117	b	0.1954
C_4	c	0.3718	c	-0.6015	c
C_5	c	0.6015	c	0.3718	c

a) Nodal plane positions give zero coefficients.
b) The values for these coefficients are determined by anti-symmetry.
c) The values for these coefficients are determined by symmetry.

Using the path deleting procedure, we obtain the following unnormalized coefficient polynomials

$$C_1 \equiv X^2 - X - 1 \qquad \text{for left mirror fragment}$$

$$C_2 \equiv \sqrt{2}(X - 1)$$

$$C_3 \equiv \sqrt{2}$$

$$C_4 \equiv X \qquad \text{for right mirror fragment}$$

$$C_5 \equiv 1$$

The normalization constant for C_1, C_2, and C_3 is 0.44721 for the eigenvalue of 2.0 and 0.51167 for 0.61803. The normalization constant for C_4 and C_5 is 0.85066 for the eigenvalue of 0.61803. Multiplying these coefficients by $1/\sqrt{2}$, except C_1, gives the normalized coefficients for cyclopentadienyl. It needs to be emphasized that the left-hand mirror fragment has a set of coefficients and associated eigenvalues, as does the right-hand fragment, and only the eigenvalues belonging to a given fragment can be used to evaluate the coefficients also belonging to that fragment. Symmetry/antisymmetry relationships have to be used to obtain the coefficient values at the other eigenvalues not associated with the fragment.

2.2.2 Common Right-Hand Mirror Plane Fragments

Table 2.1 Summarizes some common right-hand mirror plane fragments and their associated characteristic polynomials and eigenvalues. Some representative polyene families of these common mirror plane fragments are also shown. The identity of the atoms or substituents on the positions marked with an X of these structures have no effect on the given characteristic polynomials and eigenvalues that correspond to the tabulated mirror fragments. The total $p\pi$ energy (E_π, in β units) when X = CH are given near the respective structures. When the HOMO eigenvalue of the given structure for X = CH is among the mirror fragment eigenvalues, then the structure is marked with an asterisk. The HOMO value will be unchanged for X = CH or O. Because of the concept of
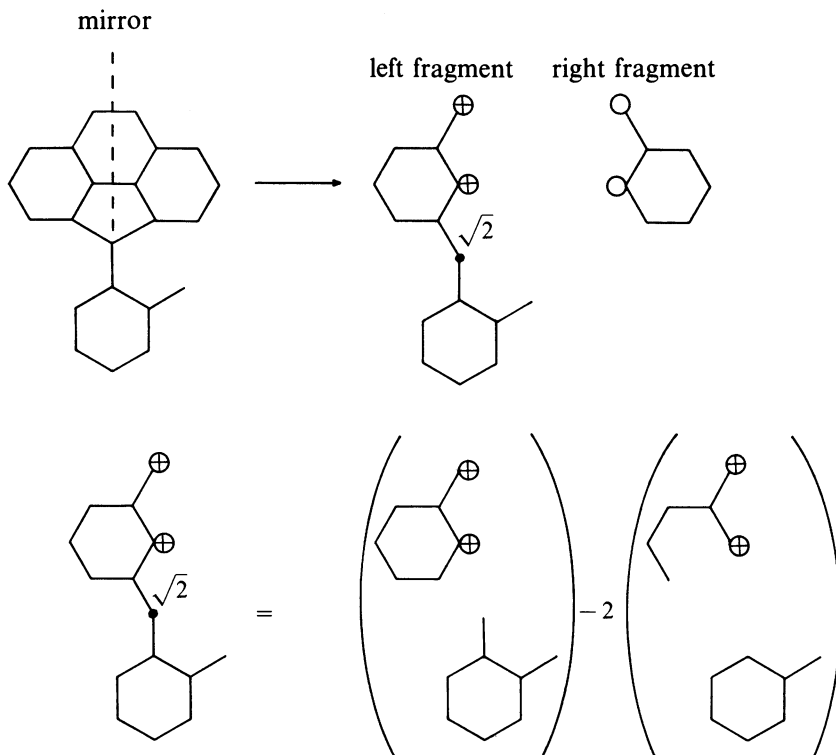
Fig. 2.1. Illustration of symmetry factoring using local 2-fold symmetry. The second decomposition of the left mirror fragment illustrates the application of Eq. (5) from Table 1.2 where $k = \sqrt{2}$. The characteristic polynomial and eigenvalues of the right fragment can be found in Table 2.1

local symmetry, substituents at **X** need not be symmetrical themselves [2–4]. As an example consider the molecule given in Fig. 2.1 Overall this molecule is devoid of symmetry but the cyclopenta[*def*]phenanthrene substructure has local symmetry and its mirror plane fragmentation gives a mirror fragment in Table 2.1. Mirror plane fragmentation of the symmetrical mirror fragments in Table 2.1 allows one to cross-check for internal consistency. Also, by difference the eigenvalues of many fragments additionally having weighted edges can be obtained. For example, the following mirror plane fragmentation allows us to
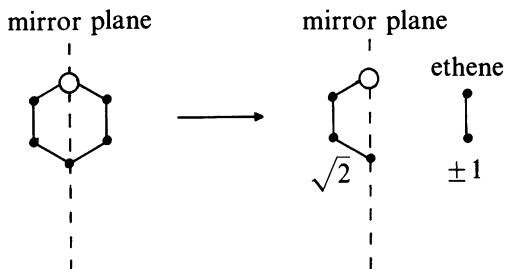
determine the eigenvalues for the middle (second) edge/vertex weighted fragment by substracting ± 1.0 from the eigenvalue set of the first fragment found in Table 2.1.

2.2.3 Factorization of Molecules with a Twofold Axis of Rotation

Molecules with a twofold axis of rotation but no symmetry mirror plane (C_{2h}) can be decomposed per the method of D'Amato [5–6]. Two types of molecular graphs are considered. The first type has the perpendicular twofold axis situated on the center of an even sided ring (ring-centric), and the second type has the twofold axis situated on a centrally located edge (edge-centric). In the former type, we will mainly be interested in tetragonal, hexagonal, and octagonal ring-centric twofold molecular graphs. Whenever a molecular graph G has a twofold axis of symmetry perpendicular to the molecular plane which defines two equivalent sets of vertices R and S, it is possible to factor G into two subspectral subgraphs G_+ and G_- whose eigenvalues, taken jointly, comprise the full spectrum of G. The following rules are given for constructing the components. 1) Identify the R set of vertices and all the edges connecting the members of the set, and repeat for the twofold symmetry-equivalent S set of vertices; performing the twofold rotation operation on G that is properly labelled should move r_1 into s_1, r_2 into s_2, etc. 2) Fragment G into G_+ and G_- components by parting the R set of vertices from the S set of vertices. 3) If vertices r_1 and s_1 were third degree vertices in G, then r_1 is weighted $+1$ in G_+ and s_1 is weighted -1 in G_-. 4) The weight of the edge between r_1 and r_2 in G ($+1$ if they are connected, zero if they if they are not) is increased by one unit in G_+, and the edge between s_1 and s_2 in G is decreased by one unit in G_-.

As it will be shown in the next section D'Amato factorization method [5–6] of 2-fold and 3-fold molecular graphs is subsumed by a more general factorization method first presented by Davidson [7] and which was also independently elaboratored by some Chinese workers [8]. Our follow-up work [6,9] which includes facile solution of the corresponding factor subgraphs is also noteworthy. Every molecular graph fragmentation has associated with it a factorization of its corresponding characteristic polynomial.

Factorization of a molecular graph with a twofold axis located at the center of an even sided ring is illustrated in with anthra-1,5-quinodimethane ($C_{16}H_{12}$) in Fig. 2.2. The characteristic polynomial of the edge weighted graph G_- in Fig. 2.2 is computed easily according to Eq. (5). The roots of the characteristic polynomials of G_- and G_+ taken together give the eigenvalues of G. An example of the factorization of a molecular graph with a twofold axis situated on a centrally located edge is provided by the molecular graph of naphtho-1,5-quinodimethane ($C_{12}H_{10}$) in Fig. 2.2. The characteristic polynomial of the first fragment (G_+) is readily computed with the use of Eq. (4) in Table 1.2 by setting $\underline{k} = 1$ and $h = 1$ as shown in Fig. 2.2. Since naphtho-1,5-quinodimethane is a bipartite graph (alternant hydrocarbon) and the first fragment graph G_+ gives six different eigenvalues, exactly half of those possessed by naphtho-1,5-quinodi-
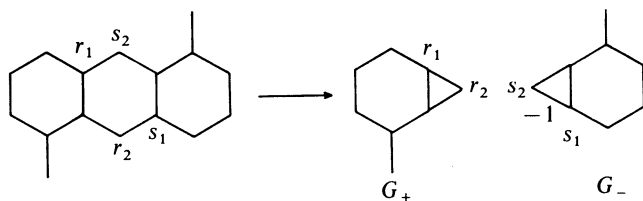
$P(G_+; X) = X^8 - 9X^6 - 2X^5 + 23X^4 + 8X^3 - 18X^2 - 8X + 1$

−2.10314		2.10314
−1.51834		1.51834
−1.0		1.0
−0.67124		0.67124
0.10268	by the pairing theorem →	−0.10268
1.23694		−1.23694
1.49343		−1.49343
2.45967		−2.45967
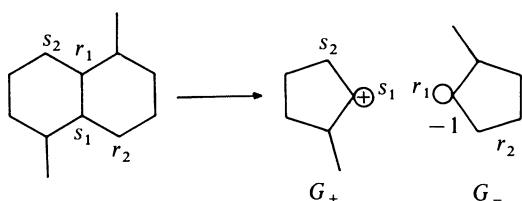
$P(G_+; X) = X^6 - X^5 - 6X^4 + 4X^3 - 8X^2 - 5X - 1$

−1.77222		1.77222
−1.4559		1.4559
−0.16215	by the pairing theorem →	0.16215
1.0		−1.0
1.0		−1.0
2.39026		−2.39026

Fig. 2.2. Factorization of anthra-1,5-quinodimethane and naphtho-1,5-quinodimethane into smaller graphs and their associated characteristic polynomials and eigenvalues. Using Eq. (4) in Table 1.2, the latter G_+ graph was decomposed to fulvene and L_5 to give the latter characteristic polynomial

methane, the pairing theorem allows one to deduce by inspection the other six without having to compute them directly from G_-.

If a molecular graph has a greater than twofold axis of symmetry, then it will possess at least one pair of degenerate eigenvalue subsets [5–7]. If a larger alternant hydrocarbon molecular graph can be embedded by a smaller subgraph in more than one mutally exclusive distinct way, then it will be degenerate in the eigenvalue subset associated with the embedding fragment. A node vertex position (zero eigenvector coefficient) is a vertex where the coefficients in a set of Hückel MO wavefunctions is zero and the sum of the coefficients of the

attached vertices equals zero [10]. Whenever an alternant hydrocarbon polyene has degenerate eigenvalue subsets, then one can obtain a (zero) node vertex at any select molecular graph position by taking an appropriate linear combination over these degenerate eigenvalue subsets. Thus, deletion of any atomic vertex or placement of any heteroatom or polyene substituent at any position on a molecular graph having doubly degenerate eigenvalue subsets will lead to successor molecular graphs still retaining one of these eigenvalue subsets. In the next section, we will present methods for factorization of molecular graphs having greater then twofold symmetry.

2.3 Molecules with n-Fold Symmetry

2.3.1 Introduction

The factorization of large symmetrical molecular graphs into smaller subgraphs for the purpose of simplifying their molecular orbital calculation has been the subject of several important contributions [1–9]. In general, if a conjugated polyene has $\mathbf{C}_n$ symmetry, its characteristic polynomial can be written as the product of n factors per [5–8]

$$P(\mathbf{C}_n; X) = \prod_{u=0}^{n-1} P(G_u; X)$$

where $P(G_u; X)$ is the characteristic polynomial of the irreducible subgraph G_u which is derived from the recurring unit R with the difference between G_u and R being determined as follows. For ring-centric molecular graphs, if in two neighboring units μ and $\mu + 1$, vertex μs is joined to $(\mu + 1)t$ $(s \neq t)$, then there will be two oppositely directed edges (called complex edge) connecting s and t in G_u whose values are respectively $\gamma_0 + \gamma e^{i\theta_k}$ and $\gamma_0 + \gamma e^{-i\theta_k}$, γ_0 being the value of edge $\mu s - \mu t$ and γ that of the edge $\mu s - (\mu + 1)t$. If $s = t$, then the weight of vertex s in G_u is $2\cos\theta_k$. For vertex-centric molecular graphs, one of the irreducible subgraphs G'_u possesses one more vertex (the central atom) than R with the weight of its connecting edge being $\sqrt{k}$ times the respective number of edges attached to the central vertex in the original molecular graph. The remaining rules for the changes in G'_u are the same as for G_u. The following relationships for complex exponentials will be needed in the application of the above factorization rules:

$$e^{i\theta_k} = \cos\theta_k + i\sin\theta_k = \omega$$
$$e^{-i\theta_k} = \cos\theta_k - i\sin\theta_k = \omega^*$$
$$e^{i\theta_k}e^{-i\theta_k} = 1 = \omega\omega^*$$
$$e^{i\theta_k} + e^{-i\theta_k} = 2\cos\theta_k = \omega + \omega^*$$
$$\theta_k = 2k\pi/n \text{ and } k = 0, 1, 2, \ldots, n-1.$$

The complex factor derives from the constant phase difference between repeating

units and always has real solutions because molecular graph eigenvalues are always real.

To illustrate the application of these general rules, consider benzene which has three different possible kinds of recurring unit R. The first recurring unit R_1 can be obtained as follows
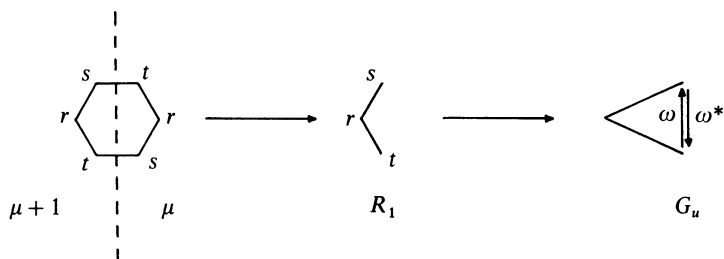
To obtain the characteristic polynomial of G_u, we apply Eq. (5) from Table 1.2 to the complex edge where $\underline{k}^2 = \omega\omega^*$ and $2\underline{k} = \omega + \omega^*$. This gives

$$\omega^* = L_3 - \omega\omega^* L_1 - (\omega + \omega^*)$$
$$= X^3 - 2X - X - 2\cos\theta_k$$
$$= X^3 - 3X - 2\cos\theta_k$$
$$\theta_k = 2k\pi/2, \; k = 0,1$$

Solution of this polynomial for $k = 0$ and 1 gives the six eigenvalues of benzene. The second recuring unit R_2 of benzene is
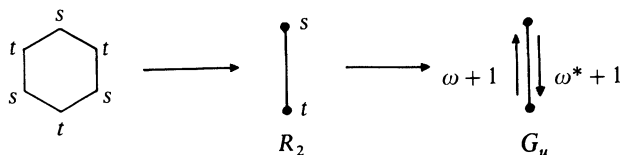
Using Eq. (5) on the complex edge of G_u where $\underline{k}^2 = (\omega + 1)(\omega^* + 1)$ and $2\underline{k} = (\omega + 1) + (\omega^* + 1)$ gives

$$\omega^* + 1 = L_1^2 - (\omega + 1)(\omega^* + 1)$$
$$= X^2 - 2(1 + \cos\theta_k)$$
$$\theta_k = 2k\pi/3, k = 0, 1, 2$$

Solution of this polynomial for $k = 0$, 1, and 2 gives the six eigenvalues of benzene. The third recurring unit R_3 is

$$2\cos\theta_k$$
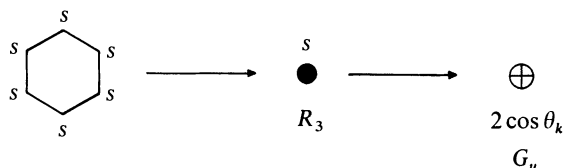
The characteristic polynomial of C_u is

$$\bigoplus_{2\cos\theta_k} = X - 2\cos\theta_k$$

$$\theta_k = 2k\pi/6 \quad k = 0, 1, 2, 3, 4, 5$$

which gives the six eigenvalues of benzene upon solution for $k = 0$, 1, 2, 3, 4, and 5. Only this last factorization of benzene truly gives an irreducible subgraph since it derives from the smallest possible recurring unit. Polycyclic irreducible subgraphs having multiple complex edges are not amenable to solution by Eq. (5). The reader needs to distinguish carefully between the phase factor $\omega = e^{i\theta_k}$ index k and the weighted edge factor of $\underline{k}$.

We will first give the specific method of D'Amato for factorization of molecular graphs with 3-fold symmetry [5]. Then a general method for factorization of molecular graphs having n-fold symmetry, which also includes 3-fold molecular graphs, will be presented [7–8]. Our method for solving the corresponding fragment subgraphs will also be merged with these discussions.

2.3.2 Factorization of Molecular Graphs with 3-Fold Symmetry

Two types of molecular graphs with a threefold axis of symmetry will be considered. The first type of molecular graph has the central atomic vertex situated on the threefold axis of symmetry and is called the phenalenyl-related series. The second type of molecular graph has the threefold axis of symmetry located at the center of the central hexagonal ring and is called the triphenylene-related series. The first type of molecular graph G has a threefold rotational operation defining three equivalent sets of vertices R, S, and T with a self equivalent vertex $\bar{q}$ lying on the axis or rotation. The following procedure may be used to construct two subgraphs G_a and G_e such that the eigenvalues of G_a and the eigenvalues of G_e taken twice comprise the complete spectrum of G for the phenalenyl series [11]. To construct G_a first draw the vertices of set R and vertex $\bar{q}$ together with all the edges connecting members of the set. Since a bridging vertex r_1 is connected to a vertex s_2 in G which is symmetry-equivalent to the second bridging vertex r_2 that is not adjacent to r_1, an undirected edge of weight one is connected between r_1 and r_2 in G_a. The weight of the undirected edge between r_1 and $\bar{q}$ becomes $\sqrt{3}$. In G_e the weight of the directed edge from s_2 to s_1 is ω and the weight of the directed edge from s_1 to s_2 is ω^* since s_1 and s_2 were not adjacent in G. This factorization procedure is illustrated on several examples in Figure 2.3.

For the triphenylene-related series, the following procedure may be used to construct the subgraphs of G_a and G_e from G. To construct G_a first draw the vertices of set R together with all the edges connecting members of the set. Since a bridging vertex r_1 is connected to a vertex s_2 in G which is symmetry-equivalent to a second bridging vertex r_2 that is adjacent to r_1, an undirected edge of weight two is connected between r_1 and r_2. In G_e the weight of the
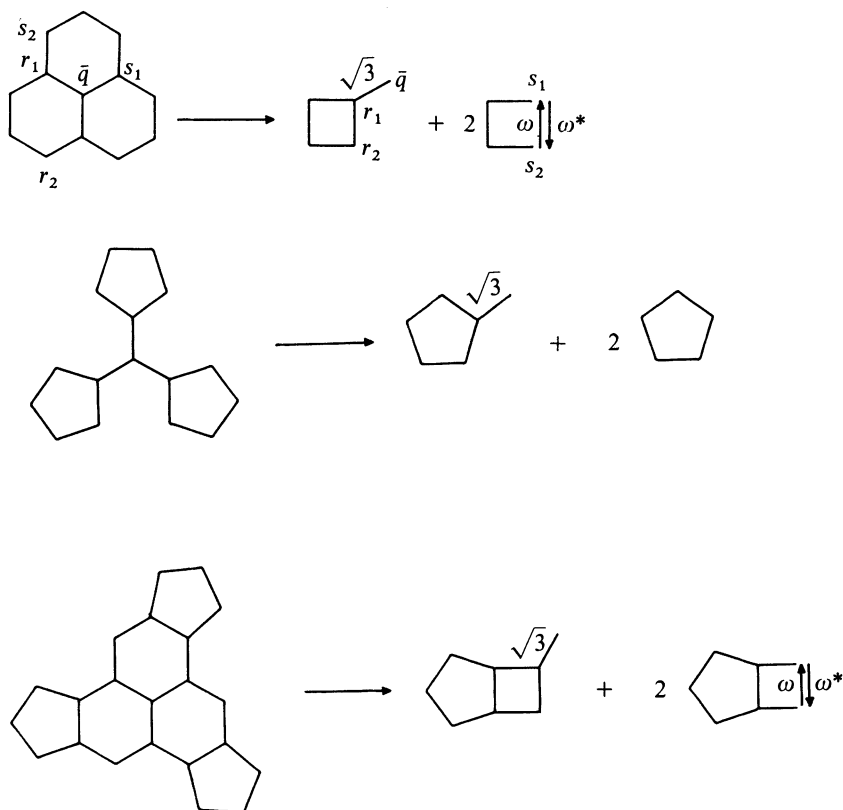
Fig. 2.3. General factorizations of 3-fold symmetrical vertex-centric molecular graphs of chemical interest

directed edge from s_2 to s_1 is $\omega + 1$ and the weight of the directed edge from s_1 to s_2 is $\omega^* + 1$. This factorization procedure is illustrated on several examples in Fig. 2.4. Recently published examples of 3-fold molecules and their doubly degenerate eigenvalues are listed in Fig. 2.5 [12]. Specific equations for solution of the complex edge weighted graph G_e [vertex-centric, Eq. (7)] and G_e [ring-centric, Eq. (8)] can be found in Table 1.2. Solution of the edge weighted subgraphs can be accomplished using Eq. (5) and the vertex weighted subgraphs by Eq. (4) and Eq. (6). Note that only 3-fold vertex-centric molecular graphs exist for hydrocarbon molecules.

2.3.3 Factorization of Molecular Graphs with 4-Fold Symmetry

Figure 2.6 illustrates the decomposition of the 4-fold cyclooctatetraene ring-centric molecular graph of [1,2]tetranaphthalene. In the succeeding section it will become evident that the four graph fragments of G_+, G_-, and G_{4i}, the latter
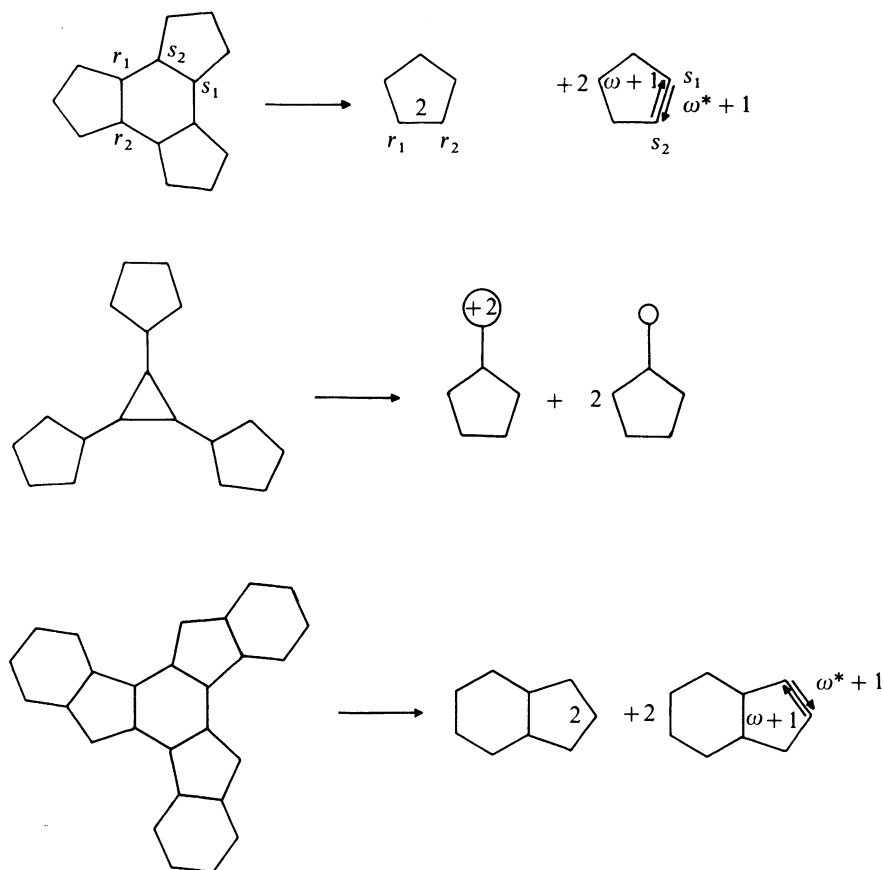
Fig. 2.4. General factorizations of 3-fold symmetrical ring-centric molecular graphs of chemical interest

twice, derive from the following general irreducible subgraph
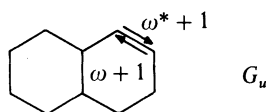
$$X^{10} - 10X^8 + 33X^6 - 44X^4 + 21X^2 - 1 - 2(1 + \cos\theta_k)$$
$$\cdot(X^8 - 8X^6 + 20X^4 - 19X^2 + 6)$$

$$\theta_k = \frac{2k\pi}{4} \quad \text{for} \quad k = 0, 1, 2, 3$$

where G_+ is given by $k = 2$, G_- by $k = 0$, and G_{4j} by $k = 1$ and $k = 3$. Some recent literature examples of 4-fold molecular graphs of chemical significance are listed in Fig. 2.7 [13] with their doubly degenerate eigenvalues.

2.3.4 A General Method for Factorization *n*-Fold Symmetrical Molecular Graphs

Chemically significant molecular graphs of 2-fold to 4-fold symmetry (Fig. 2.8) and 3-fold to 7-fold symmetry (Fig. 2.9) will be used to illustrate the general method for factorization of *n*-fold symmetrical molecular graphs. The recurring unit *R* for polyphenylenes (Fig. 2.8) can be transformed into the following

$C_{16}H_{12}$	$C_{18}H_{12}$	$C_{21}H_9$
2.0	± 2.0743	± 2.21635
± 1.61803	$- 1.61803$	± 1.51211
± 0.61803	± 0.8350	± 0.89516
	0.61803	0.0

$C_{22}H_{18}$	$C_{27}H_{15}$	$C_{27}H_{21}$
-1.8019	-2.2336	-2.0327
-1.8019	-1.6443	-1.8019
-0.4450	-1.2742	-1.1019
-0.4450	-0.8814	-0.4450
1.2470	0.1361	-0.3379
2.0	0.8078	0.8072
	1.2224	1.2470
	1.5708	1.5406
	2.2964	2.1248
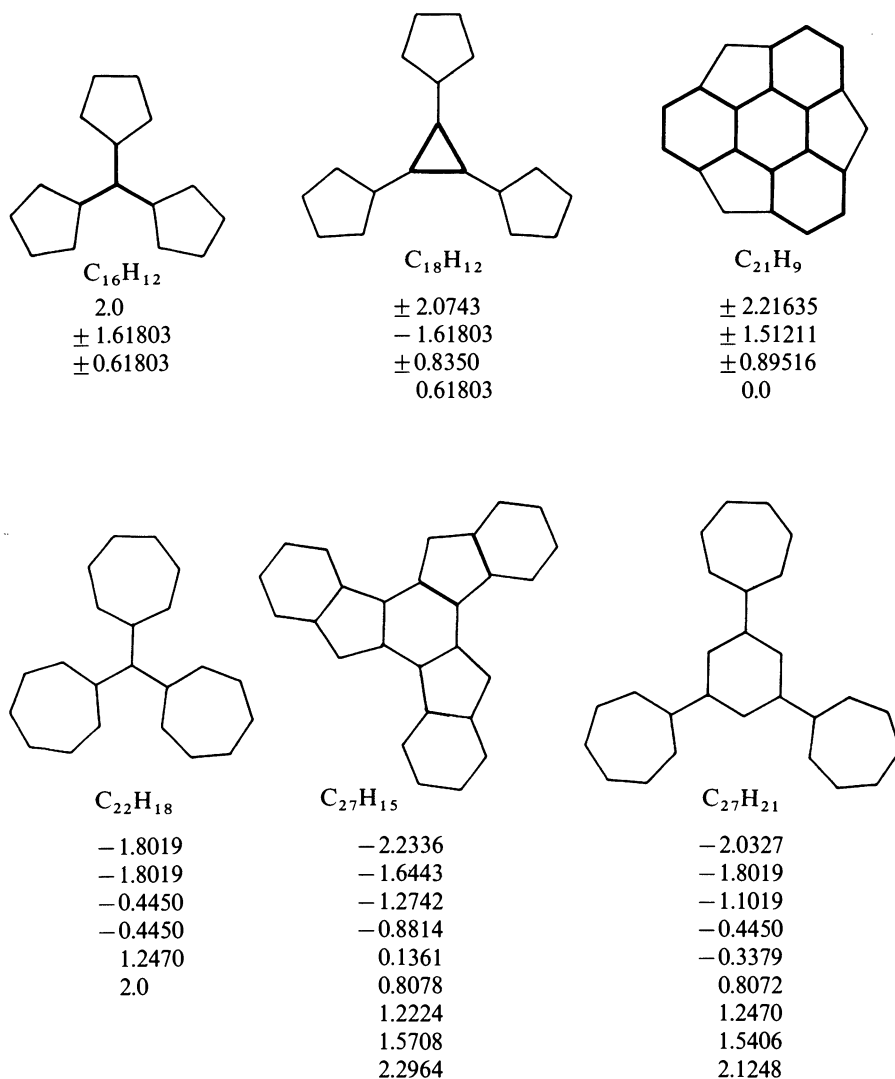
Fig. 2.5. Threefold nonalternant hydrocarbon molecular graphs and their doubly degenerate eigenvalues

$C_{33}H_{21}$
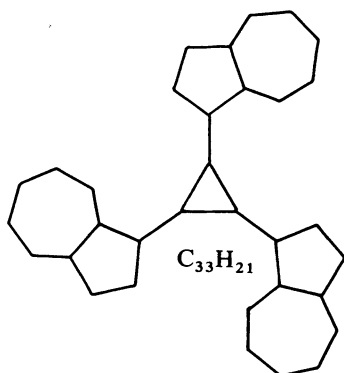
−2.2269	
−1.9609	0.6331
−1.7467	0.9345
−1.0664	1.3784
−0.5817	1.6836
−0.3937	2.3465

guaiazulene

$C_{42}H_{24}$
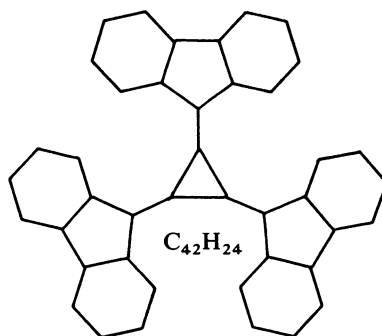
−2.3028	0.4249
−2.2784	0.7046
−1.6624	1.3028
−1.3174	1.4959
±1.0	1.8912
−0.7574	2.4989

tris(9-fluorenylidene)cyclopropane

$C_{45}H_{27}$
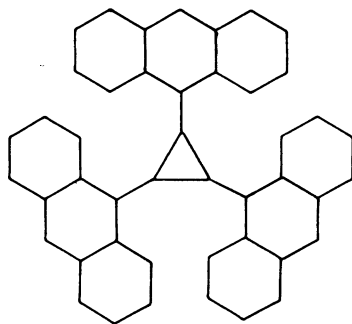
−2.5005	−0.2249
±2.0	0.5434
−1.7731	1.5099
$\pm\sqrt{2}$	2.4450
±1.0, ±1.0	

tris(9-anthrylidene)cyclopropane

$C_{67}H_{39}$
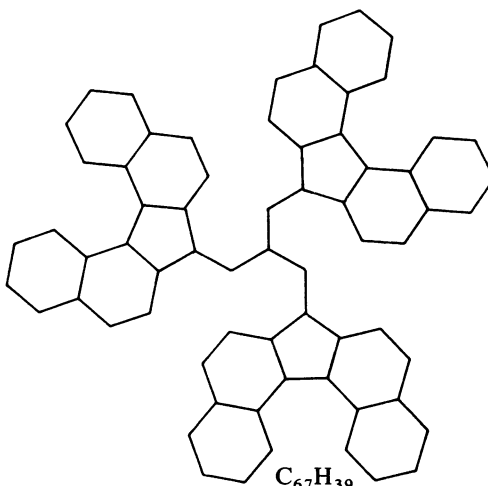
−2.4679	−0.7719	1.3417
−2.3371	−0.7569	1.4674
−1.9791	−0.3033	1.5801
−1.7598	0.4433	1.9974
−1.4478	0.6783	2.2440
−1.3697	0.7882	2.6035
−1.1303	1.1799	±1.0

tris(7*H*-dibenzo[*c, g*]fluorenylidenemethyl)methyl

Fig. 2.5. (*Continued*)
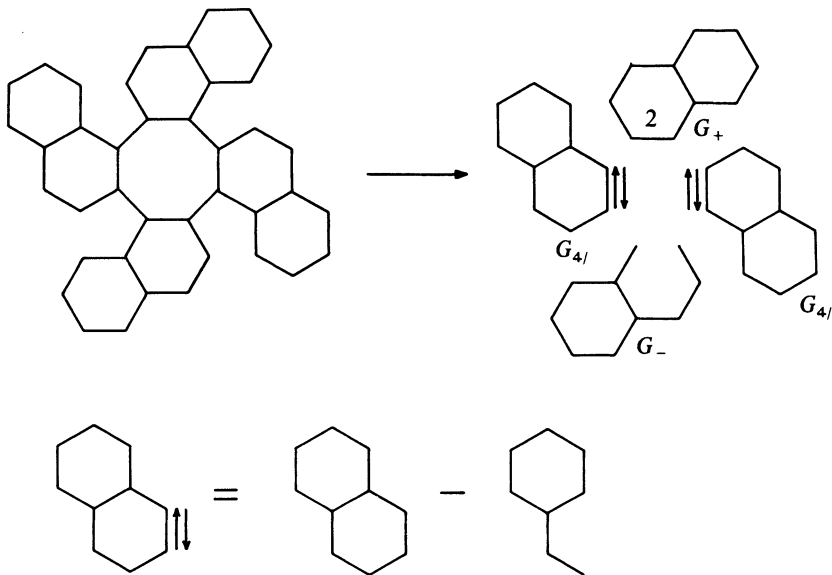
$$P(G_{4l}; X) = P(\text{naphthalene}; X) - P(\text{styrene}; X)$$
$$= (X^{10} - 11X^8 + 41X^6 - 65X^4 + 43X^2 - 9) - (X^8 - 8X^6 + 19X^4 - 16X^2 + 4)$$
$$= X^{10} - 12X^8 + 49X^6 - 84X^4 + 59X^2 - 13$$

$$\pm 0.63252$$
$$\pm 1.0$$
$$\pm 1.35906$$
$$\pm 1.76835$$
$$\pm 2.37188$$

Fig. 2.6. Factorization of [1,2]tetranaphthalene into fragment subgraphs

general irreducible subgraph G_u
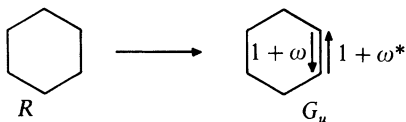
Using Eq. (5) in Table 1.2 on the complex edge where

$$\underline{k}^2 = (1 + \omega)(1 + \omega^*) \quad \text{and} \quad 2\underline{k} = (1 + \omega) + (1 + \omega^*)$$

gives

$$P(G_u; X) = X^6 - (7 + 2\cos\theta_k)X^4 + (12 + 6\cos\theta_k)X^2 - (5 + 4\cos\theta_k)$$
$$\theta_k = 2k\pi/n \quad \text{for} \quad k = 0, 1, 2, \ldots n - 1.$$

$C_{16}H_8$

± 1.93185
± 0.51764

$C_{32}H_{16}$

± 2.30725
± 2.0
± 1.53555
$\pm 1.0, \pm 1.0$
± 0.56451

$C_{40}H_{24}$

± 2.3546
± 1.8177
± 1.3004
± 1.0907
± 0.5209

Ph   Ph
Ph   Ph
Ph   Ph
Ph   Ph

$C_{56}H_{40}$

± 2.30725
$\pm 2.0, \pm 2.0, \pm 2.0, \pm 2.0$
± 1.53555
$\pm 1.0, \pm 1.0, \pm 1.0, \pm 1.0$
$\pm 1.0, \pm 1.0, \pm 1.0, \pm 1.0$
± 0.56451
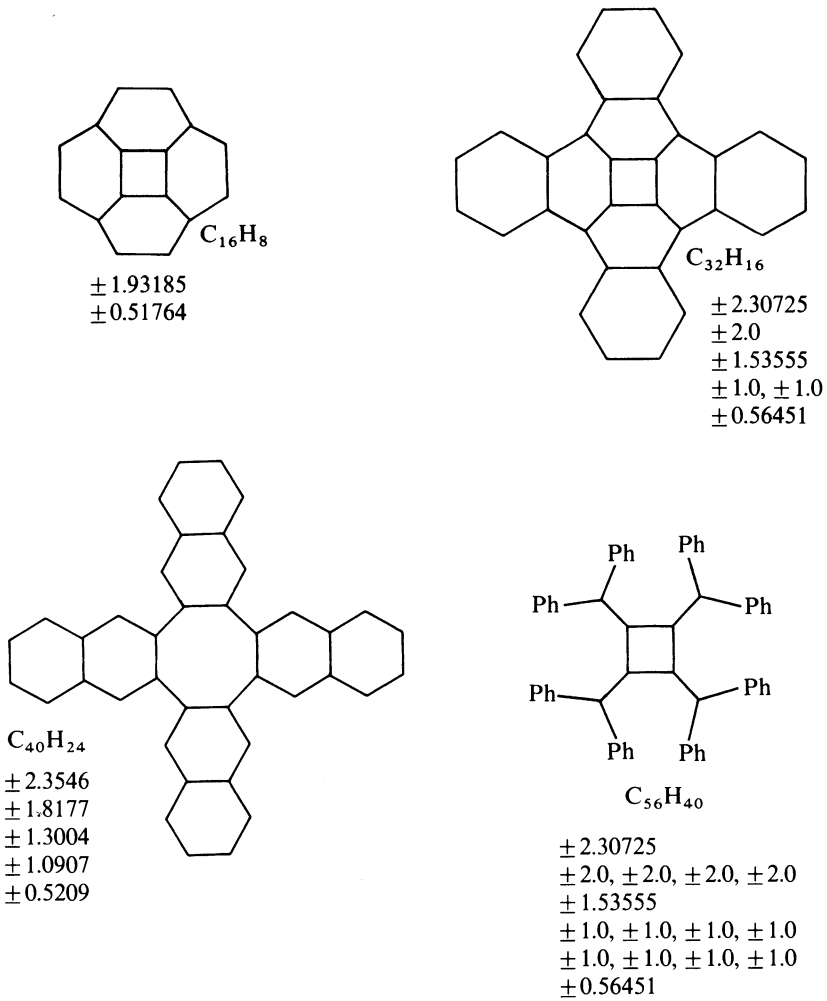
Fig. 2.7. Molecular graphs of 4-fold symmetry with their doubly degenerate eigenvalues

Similarly, the recurring unit R for circulenes (Fig. 2.9) can be transformed into the following general irreducible subgraph G_u

R

ω^*
ω

$2 \cos \theta_k$
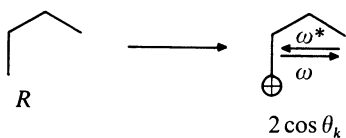
Again, using Eq. (5) on the complex edge where $\underline{k}^2 = \omega\omega^*$ and $2\underline{k} = \omega + \omega^*$ and

biphenylene

$n = 2$

triphenylene

$n = 3$

tetraphenylene

$n = 4$
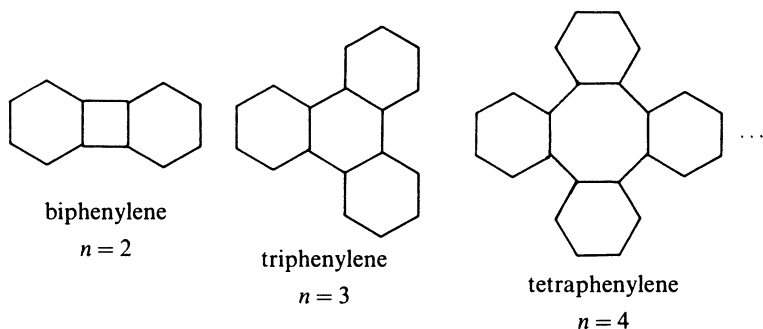
irreducible
subgraph
G_u

$1 + \omega^* = L_6 - (1 + \omega)(1 + \omega^*)L_4 - [(1 + \omega) + (1 + \omega^*)]$

$= L_6 - 2(1 + \cos \theta_k)L_4 - 2(1 + \cos \theta_k)$

$= X^6 - (7 + 2\cos \theta_k)X^4 + (12 + 6\cos \theta_k)X^2 - (5 + 4\cos \theta_k)$

$\theta_k = \dfrac{2k\pi}{n}$ for $k = 0, 1, 2, \ldots, n - 1$

For $k = 0$, $\theta_k = 0$ and $\cos \theta_k = 1$ for all values of n which gives the following characteristic polynomial and eigenvalues present in all polyphenylenes.

$$X^6 - 9X^4 + 18X^2 - 9 = 0$$

$$\pm 2.5321$$
$$\pm 1.3473$$
$$\pm 0.8794$$

Fig. 2.8. The general irreducible subgraph of polyphenylenes

then using Eq. (4) on the remaining weighted vertex $(X - 2\cos \theta_k)$ gives

$$P(G_u; X) = X^4 - 2X^3 \cos \theta_k - 4X^2 + 4X \cos \theta_k + 4\cos^2 \theta_k + 1$$
$$\theta_k = 2k\pi/n \text{ for } k = 0, 1, 2, \ldots, n - 1.$$

Thus, these characteristic polynomials of the above irreducible subgraphs allow one to quickly solve for the eigenvalues of series of related molecular graphs of n-fold symmetry. Since $k = 0$ gives $\cos \theta_k = 1$ regardless of the value of n, each series of related molecular graphs will be subspectral (have a common subset of eigenvalues) in the corresponding eigenvalues obtained for $k = 0$. For $n \to \infty$ one should obtain an energy continuum corresponding to energy valence bands. If a conduction band exists X should have zero as one of its values. No conduction band occurs in the infinite polyphenylene system, since $\cos \theta_k \neq -5/4$ for $X = 0$, and no conduction band exists in the infinite circulene because for $X = 0$, $\cos^2 \theta_k = -1/4$ has no real solution.

<div align="center">

[3]circulene
$n = 3$

[4]circulene
$n = 4$

corannulene
$n = 5$

</div>

<div align="center">

coronene
$n = 6$

[7]circulene
$n = 7$

</div>

$2 \cos \theta_k$
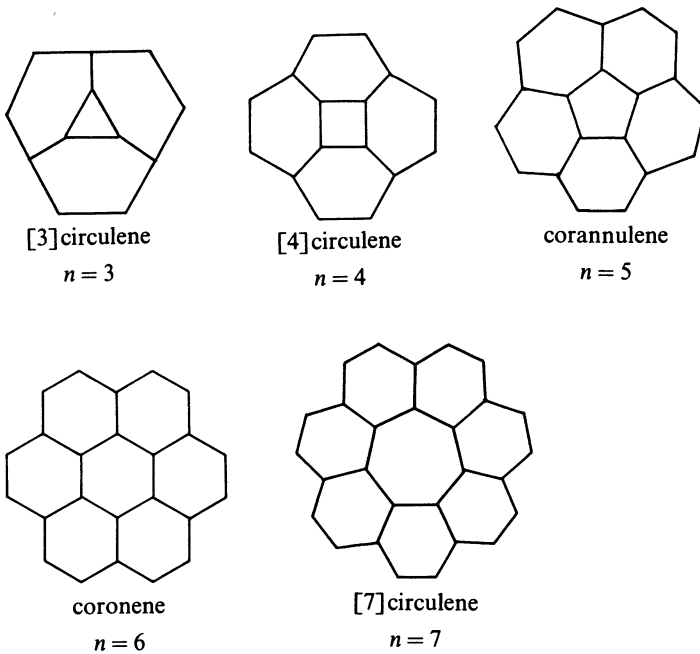
irreducible
subgraph
G_u

$$= L_4 - 2 \cos \theta_k L_3 - (X - 2 \cos \theta_k)(X + 2 \cos \theta_k)$$

$$= X^4 - 2X^3 \cos \theta_k - 4X^2 + 4X \cos \theta_k + 4 \cos^2 \theta_k + 1$$

$$\oplus = (X - 2 \cos \theta_k)$$

$$\theta_k = \frac{2k\pi}{n} \text{ for } k = 0, 1, 2, \ldots, n-1$$

For $k = 0$, $\theta_k = 0$ and $\cos \theta_k = 1$ for all values of n which gives the following characteristic polynomial and eigenvalues present in all circulenes.

$$X^4 - 2X^3 - 4X^2 + 4X + 5$$

<div align="center">

2.6751
1.5392
-1.0
-1.2143

</div>

Fig. 2.9. A general irreducible subgraph of [n]circulenes
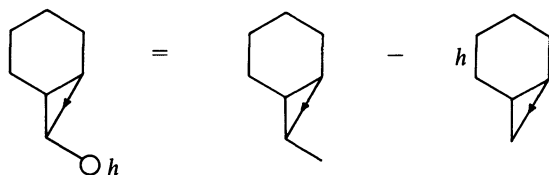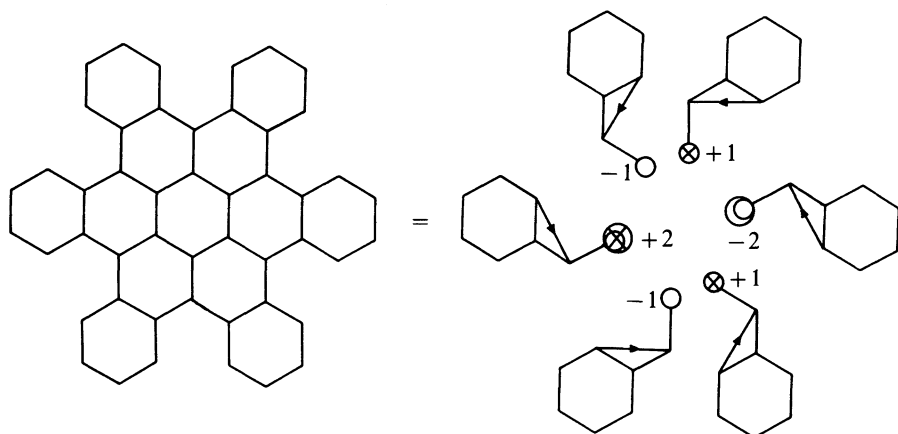
$$= X^8 - 9X^6 + 23X^4 - 19X^2 + 4 - h(X^7 - 7X^5 + 14X^3 - 8X) + h^2(X^4 - 3X^2 + 2)$$

$h = -1$	$h = -2$
0.45050	0.55241
$\pm 1.0, -1.0$	± 1.0
1.51079	-1.28733
-1.64750	1.51658
2.16163	± 2.0
-2.47541	-2.78165

Fig. 2.10. The 6 irreducible subgraphs of hexabenzocoronene

Figure 2.10 shows the solution for hexabenzocoronene $(n = 6)$ with the following irreducible subgraph
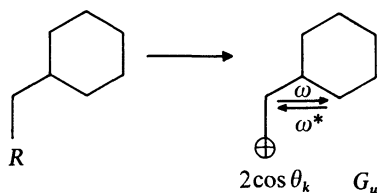
The various weights of the $\oplus$ vertex are

$$2\cos\theta_k = 2,\ 1,\ -1,\ -2,\ -1,\ 1$$

C$_{20}$H$_{10}$

−2.4667	0.7376
−1.7775	0.7775
−1.3557	1.4667
−0.4773	2.0953

C$_{40}$H$_{20}$

−2.6333	0.5003
−2.2175	0.8175
−1.8436	±1.0, ±1.0
−1.5158	1.5110
−1.2182	1.5844
−0.4551	2.0658
	2.4045

C$_{28}$H$_{14}$

−2.5616	0.4677
−2.0470	0.8312
−1.6013	1.1474
−1.4486	1.3770
−0.6870	1.8213
−0.6034	2.0304

C$_{56}$H$_{28}$

−2.6983	−0.7363	1.5130
−2.3758	−0.4639	1.5196
−2.1244	0.4709	1.7113
−1.9190	0.5239	2.0350
−1.5659	1.1037	2.2424
−1.5097	±1.0, ±1.0, ±1.0	2.5299
−1.2565		
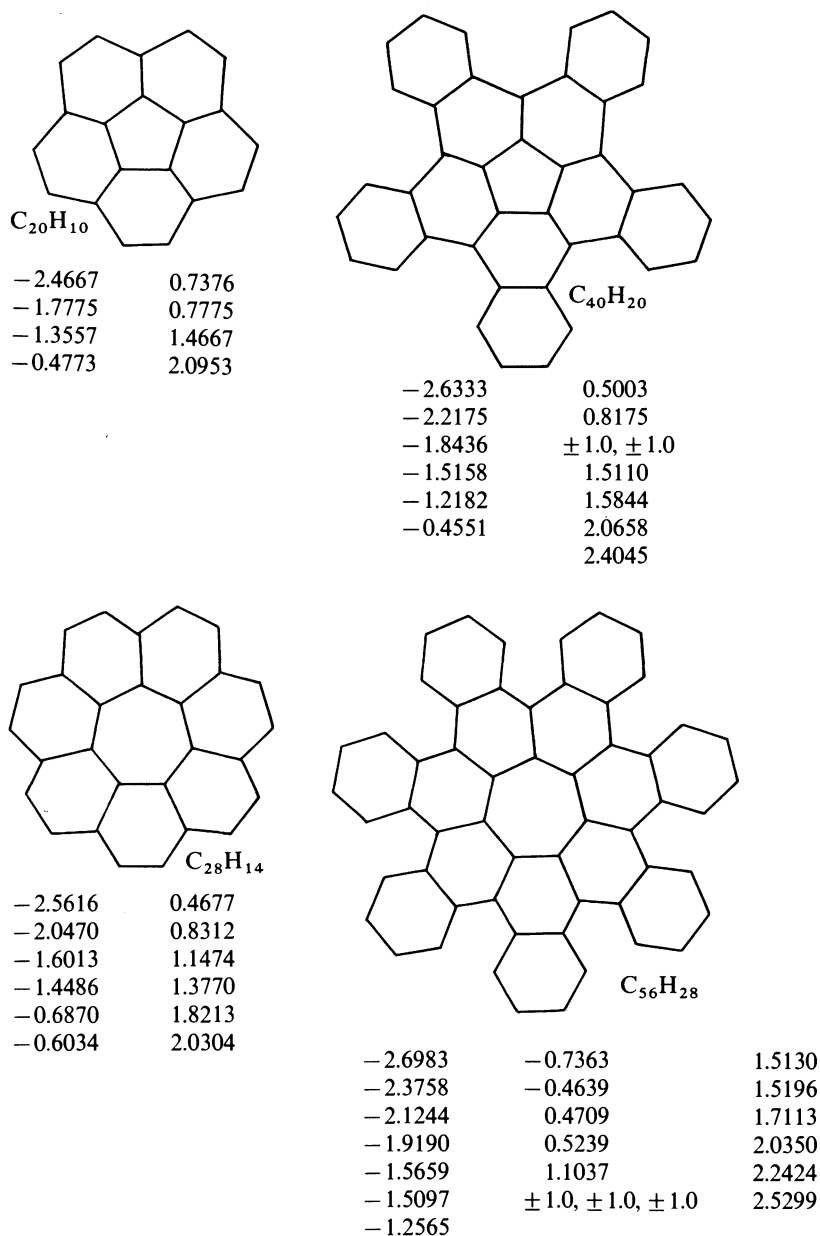
Fig. 2.11. The doubly degenerate eigenvalues of the two known circulenes and their unknown benzo derivatives

for $\theta_k = 2\pi k/6$ and $k = 0, 1, 2, 3, 4, 5$ as shown explicitly in Fig. 2.10 for the six corresponding irreducible subgraphs. Fig. 2.11 presents one set of doubly degenerate eigenvalues for some circulenes and perbenzocirculenes. Fig. 2.12 shows the general irreducible subgraph of the infinite ring acene which has no energy gap between its valence and conduction bands. Thus, the infinite ring acene is predicted to be an organic conductor [14].

The same general irreducible subgraph is obtained for an n-fold related series of molecular graphs (e.g., Figs. 2.8 and 2.9). Regardless of the value of n, all such molecular graphs will be subspectral in the eigenvalues obtained for $k = 0$. Using the vertex deletion procedure, one can easily determine the eigenvector coefficients for this common set of eigenvalues belonging to all the

ring acene of n-fold symmetry
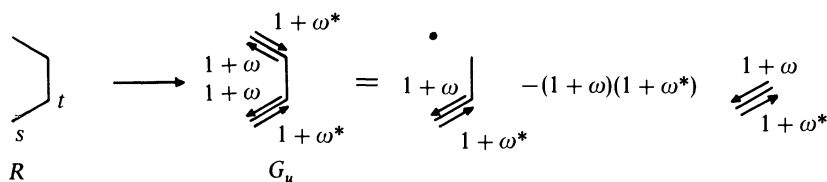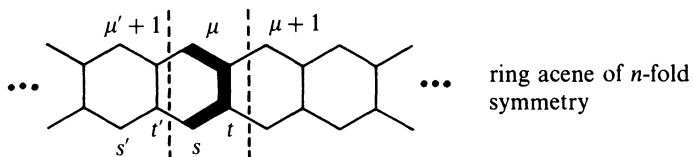
$$= L_1^2 L_2 - 2(1 + \omega)(1 + \omega^*)L_1^2 + (1 + \omega)^2(1 + \omega^*)^2$$
$$= X^4 - X^2(5 + 4\cos\theta_k) + 4(1 + \cos\theta_k)^2$$

$$\theta_k = \frac{2k\pi}{n} \text{ for } k = 0, 1, 2, \ldots, n - 1$$

For $k = 0$, $\theta_k = 0$ and $\cos\theta_k = 1$ for all values of n which gives the following characteristic polynomial and eigenvalues present in all ring acenes.

$$X^4 - 9X^2 + 8$$
$$\pm 2.8284$$
$$\pm 1.0$$

For $n = \infty$ and $X = 0$, $\cos\theta_k = -1$ and, therefore, the infinite ring acene possesses a conduction band adjacent to its valence band.

Fig. 2.12. The general irreducible subgraph of the n-fold ring acene which is predicted to be an organic conductor for $n = \infty$

members of an n-fold related series. We now illustrate this method for the polyphenylene. Consider specifically triphenylene ($n = 3$) which has the irreducible subgraph given in Fig. 2.8 numbered as follows:

$$G_u \to G_o \text{ for } k = 0$$

$$P(G_o; X) = X^6 - 9X^4 + 18X^2 - 9 = 0$$

$$\pm 2.5321, \ \pm 1.3473, \ \pm 0.8794$$

$$P'(G_o; X) = 6X^5 - 36X^3 + 36X$$
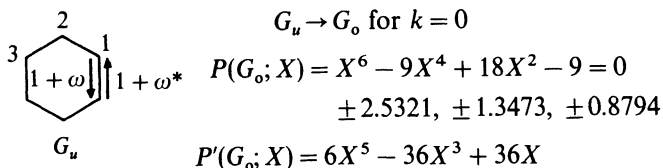
Using the vertex deletion method and Eq. (5) from Table 1.2 on the complex edge of resulting Ulam subgraphs gives the following eigenvector polynomials.

$$C_1^2 \equiv \qquad = L_5 = X^5 - 4X^3 + 3X$$

$$C_2^2 \equiv \qquad \begin{aligned} &= L_1 L_4 - (1 + \omega)(1 + \omega^*)L_3 \\ &= X^5 - (5 + 2\cos\theta_k)X^3 + (5 + 4\cos\theta_k)X \end{aligned}$$

$$C_3^2 \equiv \qquad \begin{aligned} &= L_2 L_3 - (1 + \omega)(1 + \omega^*)L_1 L_2 \\ &= X^5 - (5 + 2\cos\theta_k)X^3 + (4 + 2\cos\theta_k)X \end{aligned}$$
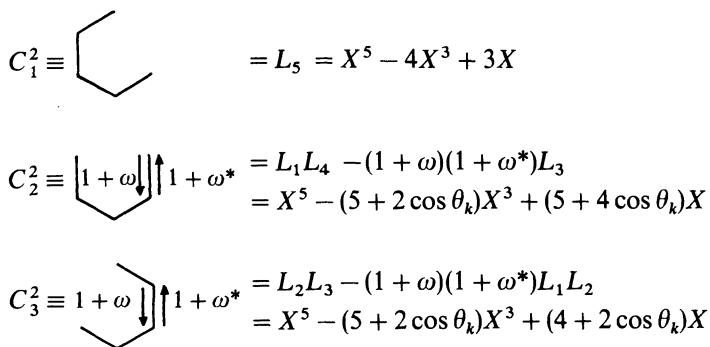
For $k = 0$, $\theta_k = 0$ and $\cos\theta_k = 1$, the above equations become

$$C_1^2 = X^5 - 4X^3 + 3X$$
$$C_2^2 = X^5 - 7X^3 + 9X$$
$$C_3^2 = X^5 - 7X^3 + 6X$$

Solution of these eigenvector polynomials give

	2.5321	1.3473	0.8794
C_1^2	0.3562	0.1008	0.04296
C_1	0.5968	-0.3176	0.2073
C_2^2	0.1008	0.04296	0.3562
C_2	0.3176	0.2073	-0.5968
C_3^2	0.04296	0.3562	0.1008
C_3	0.2073	0.5968	-0.3176
$P'(G_o; X)$	131.24	-12.904	10.331

where the signs are determined by symmetry/antisymmetry relationships. All these coefficients are normalized for the subgraph unit. To obtain the normalized coefficients for triphenylene, itself, these coefficients are divided by $\sqrt{3}$. The doubly degenerate eigenvalue subset for triphenylene (Fig. 2.8) is comprised of

± 1.9696, ± 1.2856, ± 0.6840 where the latter eigenvalues belong to the frontier orbital set (HOMO/LUMO) leading to a doubly intense peak for its first ionization potential.

The determination of the eigenvectors for the $k = 0$ fragment present in all [n]circulenes of Fig. 2.9 will now be illustrated. The general irreducible subgraph of [n]circulenes is numbered as follows

$$G_u \to G_o \text{ for } k = 0$$

$$P(G_o; X) = X^4 - 2X^3 - 4X^2 + 4X + 5$$

$$2.6751,\ 1.5392,\ -1.0,\ -1.2143$$

$$P'(G_o; X) = 4X^3 - 6X^2 - 8X + 4$$

$$\text{for } k = 0,\ 2\cos\theta_k = 2$$

Using the vertex deletion procedure gives the following eigenvector coefficient polynomials where Eq. (5) for $\underline{k}^2 = \omega\omega^*$ and $2\underline{k} = \omega + \omega^*$ is employed

$$C_1^2 \equiv \qquad = \qquad -\omega\omega^*(X - 2\cos\theta_k) = X^3 - 2X^2\cos\theta_k - 2X + 2\cos\theta_k$$

$$= X^3 - 2X^2 - 2X + 2$$

$$C_2^2 \equiv \qquad = L_3 - 2L_2\cos\theta_k = X^3 - 2X^2\cos\theta_k - 2X + 2\cos\theta_k$$

$$= X^3 - 2X^2 - 2X + 2$$

$$C_3^2 \equiv \qquad = L_2(X - 2\cos\theta_k) = X^2 - 2X^2\cos\theta_k - X + 2\cos\theta_k$$

$$= X^3 - 2X^2 - X + 2$$

$$C_4^2 \equiv \qquad = L_3 - \omega\omega^* L_1 - (\omega + \omega^*)$$

$$= X^2 - 3X - 2\cos\theta_k = X^3 - 3X - 2$$

Solution of these eigenvector polynomials gives the following eigenvector/eigen-value array

	2.6751	1.5392	−1.0	−1.2143
C_1^2	0.09122	0.2732	0.5	0.1355
C_1	0.30203	0.5227	0.7071	0.3682
C_2^2	0.09122	0.2732	0.5	0.1355
C_2	0.30203	0.5227	0.7071	0.3682
C_3^2	0.2560	0.07944	0	0.6646
C_3	0.5059	0.28184	0	0.8152
C_4^2	0.5616	0.3741	0	0.06432
C_4	0.7494	0.6116	0	0.2536
$P'(G_0; X)$	16.2374	−7.9421	2.0	−2.2952

Note that this $k = 0$ fragment is normalized within each row and column of the above array; the signs of the coefficients have not been determined. The pairing theorem requires that the complementary eigenvalues of -2.6751, -1.5392, ± 1.0, and $+1.2143$ occur when n is even. To obtain the normalized coefficients at these eigenvalues for some particular [n]circulene, one needs to divide the above coefficients by $\sqrt{n}$.

Since the $k = 0$ ($\theta_k = 0$) fragment is subspectral to all members of a series having the same general irreducible subgraph regardless of the value of n, the following generalizations about the $k = 0$ graph (G_o) will be useful. The specific

$$X^5 - 8X^3 + 11X - 4$$

2.5616
1.0
0.4142
-1.5616
-2.4142

$$X^7 - 10X^5 + 26X^3 - 16X - 4$$

2.5166
1.5524
1.1701
-0.2873
-0.6889
-1.7817
-2.4812

$$X^{10} - 14X^8 + 65X^6 - 121X^4 + 88X^2 - 16$$

± 2.5962
± 2.0
± 1.2631
± 1.1826
± 0.5157

$$X^{10} - 14X^8 + 65X^6 - 124X^4 + 97X^2 - 25$$

± 2.6267
± 1.9150
± 1.3848
± 1.0
± 0.7178
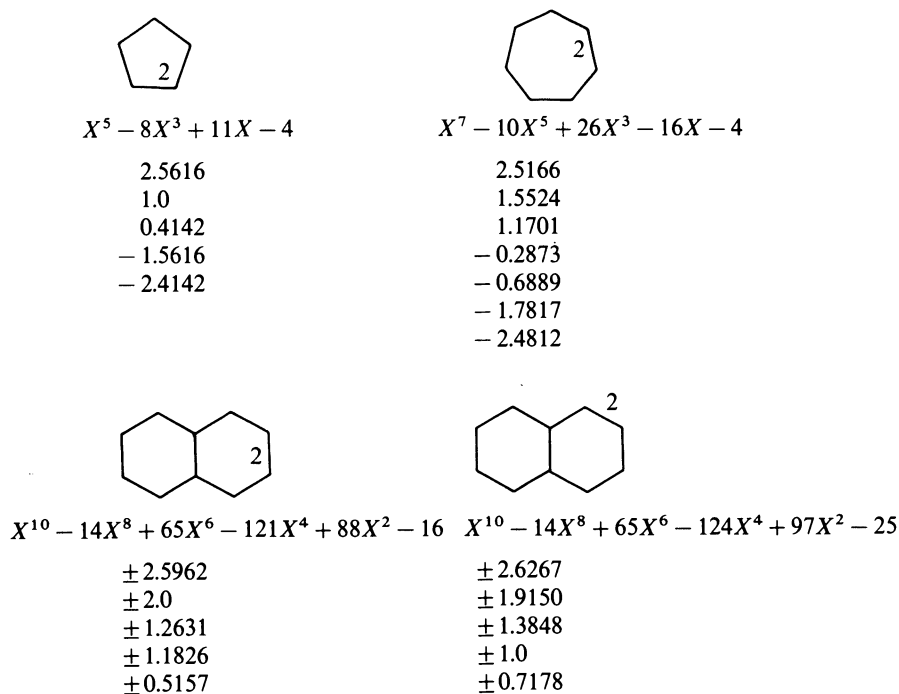
Fig. 2.13. Some typical $k = 0$ fragment subgraphs for molecular graphs of *n*-fold symmetry and their eigenvalues

G_o subgraph is obtained from the general irreducible subgraph G_u by replacing each $1 + \omega/1 + \omega^*$ complex edge by the weight of two and each ω/ω^* complex edge by the weight of one. Thus, for the prior examples above one has the following correspondences.

$$X^6 - 9X^4 + 18X^2 - 9$$

$$k = 0 \qquad \xrightarrow{\text{eq (4)}} \qquad X^4 - 2X^3 - 4X^2 + 4X + 5$$

$2\cos\theta_k$

G_u

2

G_o
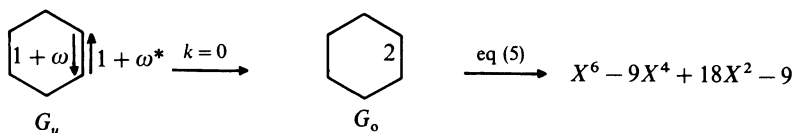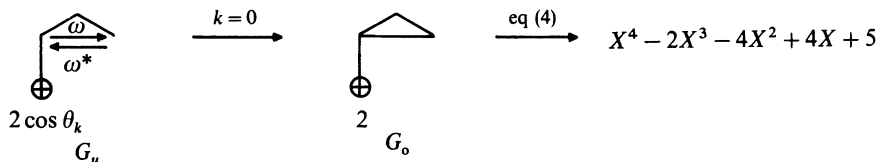
Using Eq. (5) from Table 1.2, one can quickly obtain the characteristic polynomial for the former G_o fragment, and using Eq. (4), one can obtain the characteristic polynomial for the latter G_o fragment. For vertex centric molecular graphs, the $k = 0$ fragment will contain the additional central vertex of $\sqrt{3}$ edge weight. Other $k = 0$ fragments are given in Fig. 2.13.

It has been shown in this chapter that the spectrum of eigenvalues of many molecular graphs of $\mathbf{C}_n$ symmetry devolves to the consideration of a single monomer-derived elementary substructure, i.e., recurring unit to irreducible subgraph. A molecular graph having greater than 2-fold symmetry will have a doubly degenerate subset of eigenvalues. Deletion of a carbon vertex or replacement with a heteroatom or polyene substituent on any position in molecular possessing a doubly degenerate eigenvalue subset will produce a successor molecular graph still possessing these eigenvalues once. Coupling two molecules together, each with the same doubly degenerate eigenvalue subset, through a single link gives a successor molecule still doubly degenerate in these same eigenvalues.

2.3.5 Spectroscopic Evidence for Electronic Degeneracy in Molecules with Greater than 2-Fold Symmetry

Many aromatic molecules with 3-fold and 6-fold symmetry have been shown to give doubly intense first ionization potential (IP$_1$) peaks in their photoionization spectra [15] in agreement with them having doubly degenerate HOMOs. The first ionization potentials of triphenylene ($C_{18}H_{12}$; 7.88 eV), tribenzo[c, i, o] triphenylene ($C_{30}H_{18}$; 7.19 eV), and hexabenzotriphenylene ($C_{42}H_{24}$; 7.52 eV) correspond to doubly intense peaks. In contrast, the first ionization band of [3.3.3]decastarphene ($C_{42}H_{24}$; 6.85 eV) is nondegenerate followed by a doubly degenerate band (7.04 eV) which is consistent with the HOMO level of $\varepsilon = 0.3405\beta$ compared to the doubly degenerate one at $\varepsilon = 0.3918\beta$. The first two ionization bands of coronene are both doubly degenerate. Schmidt [15] has also shown that an excellent correlation between IP$_1$ bands and the corresponding HOMOs exists.

From this chapter, symmetry has been shown to be an important concept which allows one to identify common eigenvalue subsets among molecules having an identical right-hand mirror plane fragment and among series of molecules having the same $k = 0$ irreducible subgraph. As it will be discussed in Chapter 4, right-hand mirror plane fragments and $k = 0$ irreducible subgraphs are elementary substructures.

2.4 References

1. McClelland BJ (1974) J Chem Soc Faraday Tran 2 70: 1453
2. McClelland BJ (1982) J Chem Soc Faraday Tran 2 78: 911; Mol Phys 45: 189
3. Dias JR (1987) In: King RB, Rouvray DH (eds) Graph Theory and Topology in Chemistry, Elsevier, Amsterdam: 466
4. King RB (1992) In: Bonchev D, Rouvray DH Chemical Graph Theory,
5. D'Amato SS (1979) Molec Phys 37: 1363; Theor Chim Acta 53: 319
6. Dias JR (1988) J Molec Struct (Theochem) 165: 125; Handbook of Polycyclic Hydrocarbons, Part B. Elsevier, Amsterdam
7. Davidson RA (1981) Theor Chim Acta 58: 193
8. Tang A, Kiang Y, Yan G, Tai S (1986) Graph Theoretical Molecular Orbitals. Sci Press, Beijing
9. Dias JR (1989) Theor Chim Acta 76: 153; J Molec Struct (Theochem) 185: 57
10. Dewar MJS (1969) The Molecular Theory of Organic Chemistry. McGraw-Hill, St. Louis
11. D'Amato SS, Gimarc BM, Trinajstic' N (1981) Croat Chem Acta 54: 1
12. Mizumoto K, Kawai H, Okada K, Oda M (1986) Angew Chem Int Ed Engl 25: 916; Murray RW, Kaplan ML (1967) Tetrahedron Lett 14: 1307; Agranat I, Aharon-Shalom E (1976) J Org Chem 41: 2379; Iyoda M, Otani H, Oda M (1988) Angew Chem Int Ed Engl 27: 1080; Sugimoto T, Misaka Y, Kajita T, Nagatomi T, Yoshida Z, Yamauchi J (1988) Angew Chem Int Ed Engl 27: 1078; Okamoto K, Kitagawa T, Takeuchi K, Komatsu K, Takahashi K (1985) J Chem Soc, Chem Commun: 173
13. Waitkus PA, Sanders EB, Peterson LI, Griffen GW (1967) J Am Chem Soc 89: 6318; Wong HNC (1989) Acc Chem Res 22: 145
14. Kivelson S, Chapman OL (1983) Phys Rev 28: 7236
15. Schmidt W (1977) J Chem Phys 66: 828

2.5 Problems

1   Mirror plane fragment naphthalene and obtain the eigenvector coefficients for the left-hand and right-hand fragments by the vertex-deletion method. Verify that the vertices on the mirror plane do not have to be multiplied by $1/\sqrt{2}$ to obtain the eigenvector coefficients of naphthalene from the fragment subgraphs.

2   Discuss the plausibility that the following resonance contributor may make bicyclobutadiene more stable than initially anticipated.
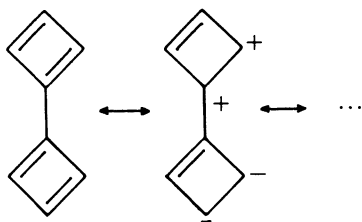
3   Show that the following is a general irreducible subgraph for the molecular graphs in Fig. 2.9 by determining its characteristic polynomial using Eq. (5) and $\underline{k}^2 = \omega\omega^*$ and $2\underline{k} = \omega + \omega^*$ (cf. with Table 1.2).
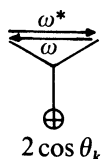
4   For $n = \infty$, plot X versus θ_k for the general irreducible subgraph given above in problem 3.

5   Compute the eigenvalues and eigenvectors for the following molecules. Determine the bond orders for the central benzene ring and compare them to those of venzene, itself. Do your results suggest that ring strain causes bond fixation [Stanger A (1991) J Am Chem Soc 113: 8277]?
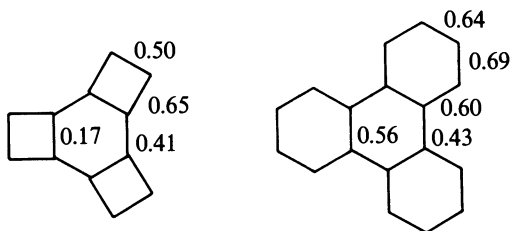
6   Compare the eigenvalues and eigenvectors of the following molecules with those in problem 5. Note that the bond orders are given for each structure.
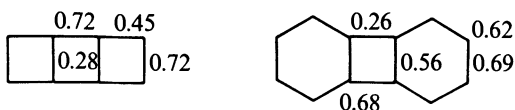
7   Show that coronene and the isomer below are subspectral in eigenvalues belonging to their $k = 0 (\theta_k = 0)$ fragment.
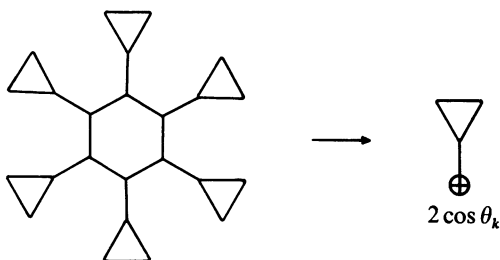
8   Calculate the bond lengths and electron densities of the following analog of calicene and compare your results with (1992) Tetrahedron Lett 33: 6819.
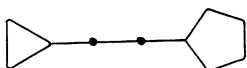
9   Calicene has not yet been synthesized but bicalicene has already been prepared [(1984) Angew Chem Acta, Int Ed Engl 23: 63]. Calculate the charge densities and bond orders of bicalicene, and compare these results

with those obtained for calicene. Compare the E_π of bicalicene with two times that of calicene. Take a linear regression of the bond orders for bicalicene against its experimental bond distances. Note that bicalicene can be decomposed by perpendicular mirror planes into four fragments. Discuss these results while considering further more recent results [(1991) Angew Chem Acta, Int Ed Engl 30: 446].

calicene
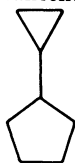
bicalicene
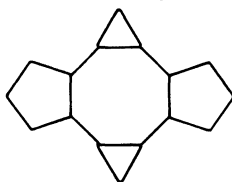
10   Using mirror plane fragmentation, calculate the MO parameters of the following molecule and compare your results with (1981) Tetrahedron Lett 22: 3879.
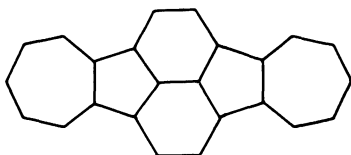
11   Read the following papers on spectral moments and calculate these quantities for calicene. (1991) J Molec Struct (Theochem) 235: 81; (1992) Theor Chim Acta 81: 237; (1992) Int J Quant Chem 41: 667.

12.   Using the results of Figure 2.9 for $n = 5$, show that the LUMO value for corannulene published in (1992) Angew Chem Int Ed Engl 31: 1636 is incorrect.

Chapter 3
Heterocyclic and Organometallic Molecules

3.1 Introduction

In this chapter, edge/vertex weighted molecular graphs that correspond to heterocyclic and organometallic compounds will be studied. The distinction between the term *molecular graph* for a heterocyclic molecule and *orbital network diagram* for a π-hydrocarbon-metal complex must be carefully made. Another unique feature characteristic of π-hydrocarbon-metal complexes is the presence of Möbius circuits in which an odd number of negative weighted edges ($\underline{k} = -1$) occurs. Circuits with an even number (including zero) of negative unit weighted edges are called Hückel circuits. In electronically neutral AH molecular graphs, there are $4n$ and $4n + 2$ $(n = 0, 1, 2, ...)$ circuits. Möbius circuits of $4n$ and Hückel circuits of $4n + 2$ are regarded as being aromatic circuits.

Several generalizations can made about heterocyclic molecules based on the results discussed in Chapters 1 and 2. Placement of a heteroatom in an isoconjugate molecular graph possessing zero node positions (zero eigenvector coefficients) for given set of eigenvalues generates a successor edge/vertex weighted molecular graph which still has these same eigenvalues. The location of zero node positions are easily determined (assigned) for molecular graphs capable of being embedded (Table 1.4), having carbon vertices located on a mirror symmetry plane (Table 2.1), or molecular graphs having a doubly degenerate eigenvalue subset (Figs. 2.5–2.11).

Figure 3.1 presents the heteroatom/heterocyclic examples of pyridine, aniline, and quinoline. It should be noted that benzene and naphthalene are isoconjugated to pyridine and quinoline, respectively, and all these molecules can be embedded by ethene (Table 1.4). Benzyl is isoconjugated (has the same number of conjugated atoms) to aniline, and the benzyl carbanion is isoelectronic to aniline. Both benzyl and aniline can also be embedded by ethene. All the graphs in Fig. 3.1 are subspectral in the eigenvalues of ± 1. For convenience, unless otherwise stated, we will assume that $h = \underline{k} = 1$ for edge/vertex weighted molecular graphs corresponding to nitrogen and oxygen containing molecules.

Table 2.1 lists all the right-hand fragments and their eigenvalues for most 2-fold molecular graphs of chemical significance. These roots are invariant in regard to the identity of the heteroatom located at the positions designated by X. This means that the values of h and $\underline{k}$ in Eq. (4) of Table 1.2 have no effect on these roots but only determine the magnitude of the roots associated with the left-hand fragment. In general, electronegative atoms ($h > 0$) cause all the
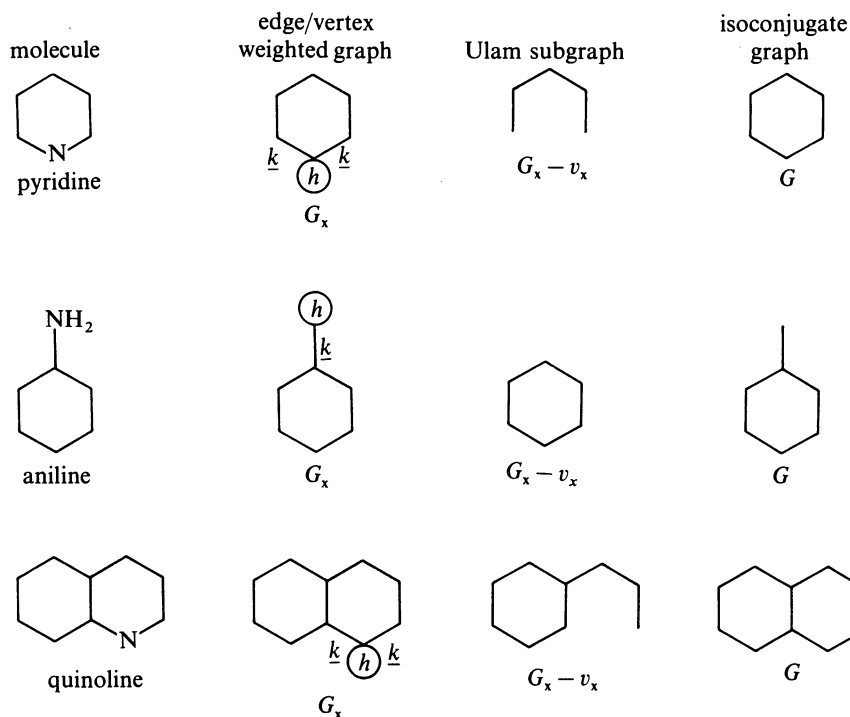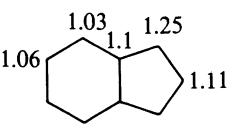
$$P(G_x; X) = XP(G_x - v_x; X) - hP(G_x - v_x; X) - \underline{k}^2[XP(G_x - v_x; X) - P(G; X)]$$

Fig. 3.1. Some heteroatom molecules and their molecular graphs, Ulam subgraphs, and isoconjugate molecular graphs

roots associated with the left-hand fragment to become more positive. Thus, if the HOMO frontier orbital is among the right-hand fragment eigenvalues, it will remain the HOMO regardless of the identity of the electronegative heteroatom at X on the nodal mirror plane of the 2-fold molecular graph. For example, consider the isoconjugated series of cyclopentadienyl anion, furan, thiophene, selenole, tellurole, and pyrrole, all which have the same right-hand mirror fragment and corresponding eigenvalue of $X = \frac{1}{2}(\sqrt{5} - 1)$. Furan, thiophene, and selenole have the same first ionization energies (IP_1) of 8.9 eV consistent with the same HOMO value. The electronegativity of tellurium is sufficiently lower that tellurole has $IP_1 = 8.4$ eV probably because it has an elevated HOMO from the left-hand fragment. The exceptionally low $IP_1 = 8.2$ eV for pyrrole probably results from a unique factor associated with the N—H bonding electrons.

The pattern of charge densities $(1 - Q)$ in a molecule is determined, at least in part, by the connectivity or the topology of the molecule [1]. For planar alternant hydrocarbons (AHs), the calculated π-electron densities (Q) are all

equal. In nonAH systems, the π-electron densities are not uniform. Substitution of a heteroatom of greater electronegativity into an isoelectronic (anionic) nonAH will lead to greater stabilization if the heteroatom is placed into those positions of greater π-electron densities [1]. Similarly, if one deletes that position of greater electron density in an anionic nonAH, then that neutral successor molecule should be more stable than those isomers obtained by deleting other positions. For example, consider the following indenyl anion having the electron densities shown.

positions	Q
1, 3	1.25
2	1.11
4, 7	1.03
5, 6	1.06
3a, 7a	1.1
total	10.0

Clearly, substitution of N or O into any of the five given nonequivalent positions leads to five different heterocyclic molecules. By the above rule of *topological charge stabilization*, indole or benzo[b]furan is predicted to be the most stable isomer in each set. Similarly, vertex deletion gives five different hydrocarbon isomers, with styrene being the most stable.

While AHs have $Q = 1$ at every pi electronic center, heteroatomic analogs to AHs have $Q > 1$ at the electronegative atomic centers. The pattern of charge densities on heterocyclic alternant molecules tend to alternate between plus and minus charge starting with negative charge on the electronegative atomic center. This leads to greater electrostatic stabilization of molecules in which carbon and the electronegative atoms are found on alternant positions.

The magnitude of the eigenvector coefficient at a given position in an AH for a given eigenvalue determines the magnitude of the respective eigenvalue change invoked in a successor molecule generated by placement of a substituent at that position. We have already seen that placement of a heteroatom or polyene substituent at a node position (having a zero eigenvector coefficient) in a molecular graph that can be embedded (Table 1.4) leaves the respective eigenvalues unchanged. This is nicely illustrated by going from naphthalene to quinoline, both which are embeddable by ethene where nitrogen in the latter occupies a node position. Vertices lying on a mirror plane of symmetry are always nodes (have zero eigenvectors) for the eigenvalues associated with the right-hand fragment (subgraph). For odd alternant hydrocarbons (OAHs), the starred positions coincide with the positions that can be embedded by methyl radical and the nonstarred positions are node positions for the zero eigenvalue (i.e., the NBMO). Placement of substituents on the nonstarred positions of an OAH leaves the relevant NBMO coefficients unchanged. Consider dibenzo[a, c]-anthracene with its largest and smallest eigenvector coefficients for its HOMO

($X = 0.499$) shown. For $h = 0.5$ and $\underline{k} = 1.0$, substitution of the 9, 14-CHs ($C_9 = C_{14} = 0.423$) by Ns leads to a larger change in the HOMO value than does the substitution of the 1, 8-CHs ($C_1 = C_8 = -0.063$) by Ns ($X = 0.646$ versus $X = 0.502$). Thus, one would predict that dibenzo[a, c]phenazine should have a higher first ionization potential (IP$_1$) than 1, 8-diazadibenzo[a, c]-anthracene [2].
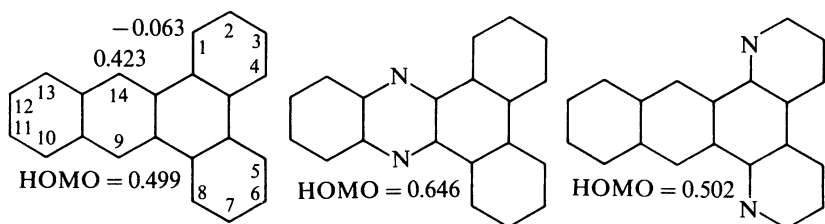
dibenzo[a, c]anthracene   1,8-diazadibenzo[a, c]anthracene
                    dibenzo[a, c]phenazine

The zero-sum rule states that for OAHs the eigenvector coefficients to each nonstarred position of the NBMO will sum to zero [3, 4]. An OAH is maximally starred so that no two starred positions are adjacent. To illustrate, consider the benzyl radical arbitrarily numbered starting with 1 on the methylenyl and continuing in sequence clockwise on the ring. Putting an asterisk on positions 1, 3, 5, and 7 maximally stars benzyl. To obtain a minimum integer eigenvector set, apply the zero-sum rule to each nonstarred position in succession. This process is summarized by the sequence.
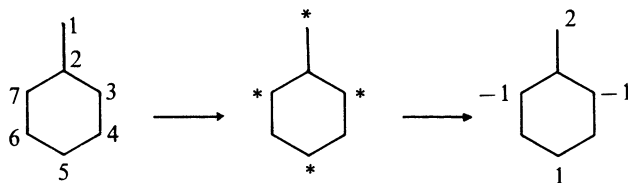
These latter integers are the unnormalized eigenvector set for $X = 0$. To obtain the normalization constant, take the inverse of the square root of the sum of the squares of these integers.

Thus,

$$\psi_{NBMO} = (1/\sqrt{7})(2\phi_1 - \phi_3 + \phi_5 - \phi_7).$$

The characteristic polynomial of benzyl is

$$P(\text{benzyl}; X) = X^7 - 7X^5 + 13X^3 - 7X$$

where Eq. (1) to Eq. (3) were used. However, note that the sum of the squares of the unnormalized coefficients also give the tail coefficient (a_6). Adding an electron into the above NBMO leads to the anion of benzyl. The charge density ($1 - Q$) for each nonstarred position is zero and for each starred position is

given by the square of the relevant NBMO coefficient. From the rule of topological charge stabilization [1], one would predict that of the three successor heteroatom analogs of benzyl carbanion produced by substituting nitrogen into its three distinct anionic positions, aniline should be the most stable. We would expect the other two analogs to gain greater stability by tautomerizing to α- and γ-picoline.

aniline

tautomerization

α-picoline γ-picoline
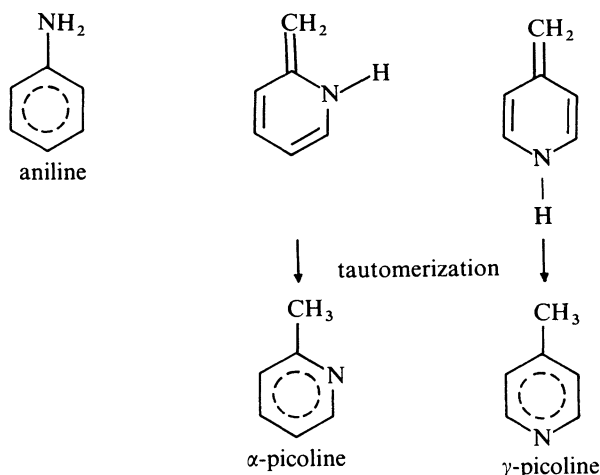
Using the factorization methods of Chapter 2, one can decompose 3-fold symmetrical phenalenyl into its irreducible subgraphs as follows

$n = 3$

phenalenyl

$k = 0$

G'_u

$k = 1,2$

G_u
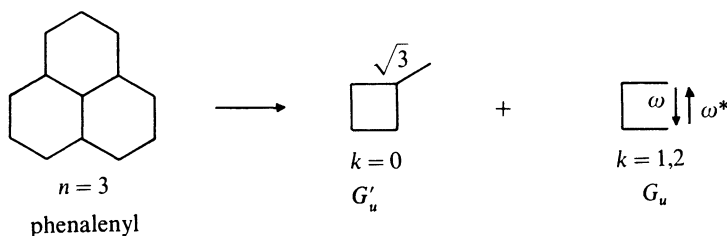
Application of Eq. (5) to the weighted edges, $\underline{k} = \sqrt{3}$ for G'_u and $\underline{k}^2 = \omega\omega^* = 1$ and $2\underline{k} = \omega + \omega^* = 2\cos\theta_k$ for G_u gives

$$P(G'_u; X) = L_1 C_4 - 3L_3 = X^5 - 7X^3 + 6X$$

$$0, \pm 1.0, \pm\sqrt{6}$$

$$P(G_u; X) = L_4 - L_2 - 2\cos\theta_k = X^4 - 4X^2 + 2 - 2\cos\theta_k$$

$$\theta_k = 2\pi k/3 \text{ and } k = 1, 2$$

$$\pm 1.0, \pm\sqrt{3}, \pm 1.0, \pm\sqrt{3}$$

Mirror plane fragmentation of phenalenyl gives L_5 (Table 1.4) as the right-hand fragment.

Odd carbon benzenoids, like phenalenyl ($C_{13}H_9$), are less stable than even carbon benzenoids. Odd carbon benzenoids are always odd radical species with

a corresponding number of nonbonding MOs (NBMOs). Also, odd carbon benzenoids always have a $4n$ perimeter possessing antiaromatic character. Even carbon benzenoids always have an aromatic $4n + 2$ pπ electronic perimeter. Phenalenyl has 3-fold symmetry and is doubly degenerate in the eigenvalues of $\pm\sqrt{3}$ and ± 1.0, and deletion of its central vertex gives [12]annulene $(C_{12}H_{12})$ with 12-fold symmetry. [12]Annulene is antiaromatic and possesses $\pm\sqrt{3}$ and ± 1.0 among its doubly degenerate eigenvalue subset. Using the zero-sum rule, one can show that while the central vertex of phenalenyl is starred, its corresponding NBMO eigenvector coefficient equals zero. Thus, from the rule of topological charge stabilization [1], one would predict that substitution of a carbon by a nitrogen at the central vertex of phenalenyl would be least stabilizing. However, a closer inspection shows that it is more stabilizing than one would expect based on this rule because this molecule has contributors where the nitrogen at this starred position is positively charged while the negative charge is delocalized over the starred positions of the perimeter.

maximally
starred

eigenvector
by zero sum
rule for $X = 0$

$SC = 3 \cdot 6 = 18$

3 contributors
have radical
electron fixed
at position shown

important
polar contributor
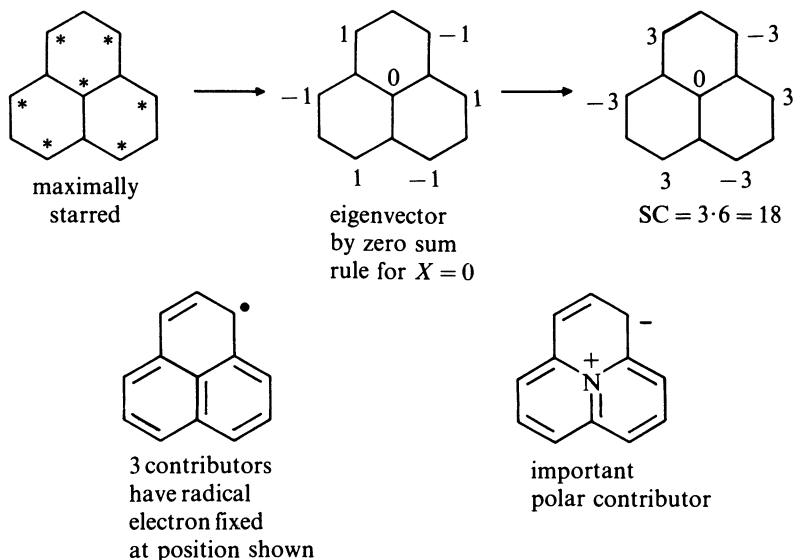
3.2 Heterocyclic and Related Molecules

3.2.1 Characteristic Polynomials of Small Molecular Graphs with one Heteroatom

If one wishes to compute the characteristic polynomial of a small molecular graph possessing one heteroatom utilizing Eq. (1) to Eq. (3) from Table 1.2, then the following relationship will be needed [5]

$$P(G_x; X) = XP(G_x - v_x; X) - hP(G_x - v_x; X) - \underline{k}^2[XP(G_x - v_x; G) - P(G; X)]$$

$$(4)$$

where G_x is the graph containing the heteroatom, G is its isoconjugate graph, $G_x - v_x$ is the graph obtained upon deletion of heteroatom vertex with its adjacent edges, h comes from $\alpha_x = \alpha_c + h\beta$, $\underline{k}$ comes from $\beta_{cx} = \underline{k}\beta_{cc'}$ and $X = (\varepsilon - \alpha)/\beta$. Equation (4) is valid for both the acyclic and characteristic polynomials. The application of Eq. (4) will be illustrated with the molecular graphs in Fig. 3.1. Computation of the HMO characteristic polynomial for the pyridine-like structure is equivalent to the graph theoretical determination of the characteristic polynomial of the following edge/vertex weighted molecular graph.
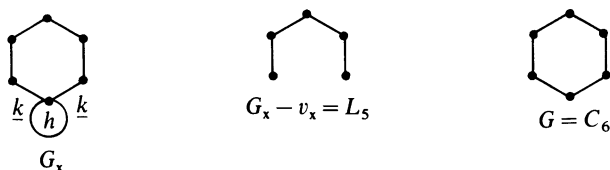
The characteristic polynomial of both $G_x - v_x$ and G can be easily computed using Eq. (1) and Eq. (2) giving

$$P(G_x - v_x; X) = X^5 - 4X^3 + 3X$$
$$P(G; X) = X^6 - 6X^4 + 9X^2 - 4$$

which when combined according to Eq. (4) gives

$$P(G_x; X) = (X^6 - 4X^4 + 3X^2) - h(X^5 - 4X^3 + 3X) - \underline{k}^2(2X^4 - 6X^2 + 4).$$

Note that if $h = 0$ and $\underline{k} = 1$, this latter equation gives $P(C_6H_6; X) = X^6 - 6X^4 + 9X^2 - 4$ which is the characteristic polynomial for benzene. Computation of the characteristic polynomial of the quinoline-like structure is achieved as follows.
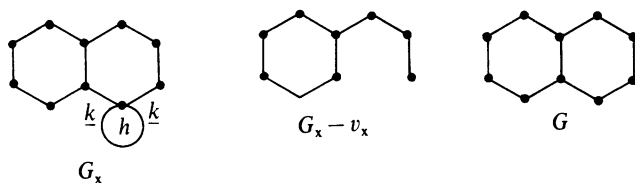
From Eq. (1) and Eq. (2) and ethene embedding of $G_x - v_x$ and G, it is determined that

$$P(G_x - v_x; X) = X^9 - 9X^7 + 26X^5 - 29X^3 + 11X$$
$$P(G; X) = X^{10} - 11X^8 + 41X^4 - 65X^4 + 43X^2 - 9$$

which when combined per Eq. (4) gives

$$P(G_x; X) = (X^{10} - 9X^8 + 26X^6 - 29X^4 + 11X^2) - h(X^9 - 9X^7 + 26X^5 - 29X^3 + 11X) - \underline{k}^2(2X^8 - 15X^6 + 36X^4 - 32X^2 + 9).$$

The $G_x - v_x$ subgraph of the isoquinoline-like structure can be embedded by

allyl fragments as shown by the following.
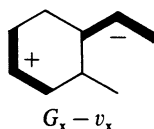
$$G_x - v_x$$

Thus from Eq. (1) and Eq. (2), we get

$$P(G_x - v_x; X) = X^9 - 9X^7 + 25X^5 - 26X^3 + 8X$$

which when combined with Eq. (3) gives

$$P(G_x; X) = (X^{10} - 9X^8 + 25X^6 - 26X^4 + 8X^2) - h(X^9 - 9X^7 + 25X^5$$
$$- 26X^3 + 8X) - \underline{k}^2(2X^8 - 16X^6 + 39X^4 - 35X^2 + 9).$$

From these examples, it is evident that a weighted graph vertex makes no contribution to the even terms of a characteristic polynomial. Since in a set of Sach's graphs a weighted vertex (h) excludes a K_2 component from the same two edge sites as excluded when the number of non-edge-weighted K_2 and C_n combinations are counted in $G_x - v_x$, then the combinatorial possibilities for both cases become identical and, therefore, the two associated polynomial parts will have the same set of coefficients.

3.2.2 Characteristic Polynomials of Small Molecular Graphs with Multiple Heteroatoms

Successive use of Eq. (4) on molecular graphs possessing multiple heteroatoms will be illustrated. Consider the pyrazine-like structure G_{xx} and its subgraphs.
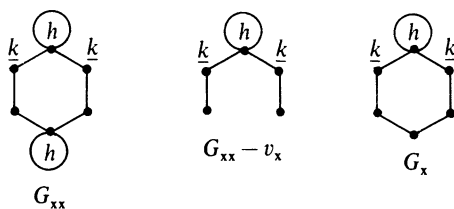
To compute $P(G_{xx}; X)$ using Eq. (4), one needs to know $P(G_{xx} - v_x; X)$ and $P(G_x; X)$ which are obtained per the method outlined above for molecular graphs containing a single heteroatom. Thus,

$$P(G_{xx} - v_x; X) = (X^5 - 2X^3 + X) - h(X^4 - 2X^2 + 1) - \underline{k}^2(2X^3 - 2X)$$
$$P(G_x; X) = (X^6 - 4X^4 + 3X^2) - h(X^5 - 4X^3 + 3X) - \underline{k}^2(2X^4 - 6X^2 + 4)$$

Incorporation of these quantities into Eq. (4) leads to

$$P(G_{xx}; X) = [(X^6 - 2X^4 + X^2) - h(X^5 - 2X^3 + X) - \underline{k}^2(2X^4 - 2X^2)]$$
$$- h[(X^5 - 2X^3 + X) - h(X^4 - 2X^2 + 1) - \underline{k}^2(2X^3 - 2X)]$$
$$- \underline{k}^2[(2X^4 - 2X^2) - h(2X^3 - 2X) - \underline{k}^2(4X^2 - 4)]$$

For $h = 1$ and $\underline{k} = 1$, this latter equation becomes

$$P(G_{xx}; X) = X^6 - 2X^5 - 5X^4 + 8X^3 + 7X^2 - 6X - 3$$

having eigenvalues of $X = \pm\sqrt{3}, \pm 1, 1 - \sqrt{2},$ and $1 + \sqrt{2}$. Although the weighted vertices in this example both had the same values of h and $\underline{k}$, this method is still valid for molecular graphs having multiple heteroatoms with different values for h and $\underline{k}$. Successive use of Eq. (4) per this procedure will yield the characteristic polynomial of molecular graphs having multiple heteroatoms of different kinds.

Computation of the characteristic polynomial of the aniline-like structure (Fig. 3.1) is achieved as follows. From Eq. (1) and Eq. (2), it is determined that

$$P(\text{benzyl}; X) = X^7 - 7X^5 + 13X^3 - 7X$$
$$P(\text{benzene}; X) = X^6 - 6X^4 + 9X^2 - 4$$

which when combined per Eq. (4) gives

$$P(G_x; X) = (X^7 - 6X^5 + 9X^3 - 4X) - h(X^6 - 6X^4 + 9X^2 - 4)$$
$$- \underline{k}^2(X^5 - 4X^3 + 3X).$$

3.2.3 Eigenvectors corresponding to heterocyclic molecules

We will now obtain the eigenvector polynomials for pyridine-like molecular graphs using first the vertex deletion procedure and then the path deletion procedure. Assuming $h = \underline{k} = 1$, we obtain the following charge densities for pyridine.
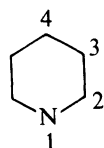
$$P(\text{Py}; X) = X^6 - X^5 - 6X^4 + 4X^3 + 9X^2 - 3X - 4$$
$$- 1.8912, \pm 1.0, -0.7046, 1.3174, 2.2784$$
$$P'(\text{Py}; X) = 6X^5 - 5X^4 - 24X^3 + 12X^2 + 18X - 3 = P'$$

$$P'C_1^2 = L_5 = X^5 - 4X^3 + 3X$$
$$P'C_2^2 = L_5 - L_4 = X^5 - X^4 - 4X^3 + 3X^2 + 3X - 1$$
$$P'C_3^2 = L_5 - L_1L_3 = X^5 - X^4 - 4X^3 + 2X^2 + 3X$$
$$P'C_4^2 = L_5 - L_2^2 = X^5 - X^4 - 4X^3 + 2X^2 + 3X - 1$$

	2.2784	1.31743	1.0	Q	1−Q
C_1^2	0.4177	0.2672	0	1.37	−0.37
C_1	0.6463	0.5169	0		
C_2^2	0.1707	0.0067	0.25	0.85	0.15
C_2	0.4131	0.0820	0.5		
C_3^2	0.0870	0.1671	0.25	1.01	−0.01
C_3	0.2950	0.4088	0.5		
C_4^2	0.0670	0.3851	0	0.90	0.10
C_4	0.2589	0.6206	0		
$P'(\text{Py}; X)$	50.10	−4.587	4.0		

These HMO electron density results for pyridine can be compared with those calculated by the Pople method which gives 1.38, 0.75, 1.12, and 0.87, respectively. Note that these sets of electron density values sum to 6.0, as they should. From the alternating polarity effect observed here for pyridine, one would predict that pyrimidine (1,3-diazine) will be more stable than pyrazine (1,4-diazine) because of electrostatic stabilization.

Determination of the eigenvectors of the pyridine-like molecular graph by the path deletion procedure will now be illustrated. Number pyridine in succession starting with 1 at nitrogen and let $h = \underline{k} = 1$ as done above. The path deletion procedure gives the following eigenvector polynomials.

$$C_1 = L_5 = X^5 - 4X^3 + 3X$$
$$C_2 = L_4 + 1 = X^4 - 3X^2 + 2$$
$$C_3 = L_3 + L_1 = X^3 - X$$
$$C_4 = 2L_2 = 2X^2 - 2$$

These equations lead to the following coefficient array.

	2.2784	1.31174	1.0
C_1	0.6463	−0.5169	0
C_2	0.4131	−0.0820	0.25
C_3	0.2949	0.4088	0.25
C_4	0.2589	0.6206	0
N	0.03089	0.4218	

In this case, solution of all these polynomials for the eigenvalue of 1.0 leads to a column of zeros because the numbering of pyridine was initiated at a node position for this eigenvalue. However, these coefficients can be easily obtained by ethene embedding (Table 1.4).

At this point it should be noted that in Eq. (4), the precision of the value for h effects the electron density to greater extent than bond order, and the precision of $\underline{k}$ affects the bond order to a greater extent than electron density.

Comparison of the eigenvalues of benzene versus those obtained above for pyridine gives the following correspondences where one pair of ± 1.0 eigenvalues remains unchanged.

$$-2.0 \rightarrow -1.8912$$
$$-1.0 \rightarrow -0.7046$$
$$1.0 \rightarrow 1.3174$$
$$2.0 \rightarrow 2.2784$$

Thus, in general, replacement of CH in a carbon skeleton by electronegative atoms leads to a general lowering of eigenvalues in going from an isoconjugate to a heterocyclic analog.

3.2.4 3-Fold Polyazaheterocyclic Molecules

Figure 3.2 presents the doubly degenerate eigenvalues of a number of chemically relevant heterocyclic molecules [6–7]. Deletion of any vertex, including a weighted one, or placing a heteroatom or polyene substituent at any position in any molecular graph listed in Fig. 3.2 generates a successor molecular graph still having these eigenvalues once [8–9]. There are 29 molecular graphs in Fig. 3.2 having a total of over 125 different vertices. Thus, Fig. 3.2 represents a compact compendium of select eigenvalues for well over 1000 heterocyclic molecules. A number of interesting observations from Fig. 3.2 can be rendered. For the ring-centric structures with formulas of $C_{12}H_9N_3$ and $C_{15}H_9N_3$ and the vertex-centric structures with formulas of $C_{10}H_6N_3$ and $C_{13}H_9N_3$, the doubly degenerate eigenvalue subset is identical for the positional isomers with different nitrogen locations. The vertex-centric $C_{19}H_9N_3$ molecular graph with three different possible nitrogen locations has one pair of isomers with identical doubly degenerate eigenvalues. Deletion of the central vertex of these three $C_{19}H_9N_3$ molecular graphs leads to two $C_{18}H_9N_3$ isomers of 3-fold symmetry with exactly the same set of doubly degenerate eigenvalues listed. Deletion of the central vertex of the other vertex-centric molecular graphs of the formulas $C_7H_3N_3$, $C_{10}H_6N_3$, $C_{13}H_9N_3$, $C_{16}H_6N_3$, $C_{19}H_9N_3$, and $C_{22}H_{12}N_3$, likewise produces 3-fold symmetrical molecules with the same set of doubly degenerate eigenvalues listed. Substitution of an aza group into the central vertex of all the vertex-centric molecular graphs in Fig. 3.2 leads to successor 3-fold molecular graphs still doubly degenerate in the eigenvalues listed. A number of these heterocyclic compounds have been synthesized [7].

   The results summarized in Fig. 3.2 can be obtained by using Eq. (7) from Table 1.2 for vertex-centric and Eq. (8) for the ring-centric molecular graphs. By way of review of our approach presented in Chapter 2, consider the $C_{15}H_9N_3$ ring-centric molecular graph given in Fig. 3.2. Its general irreducible subgraph (G_u) is presented on the top left-hand corner of Fig. 3.3.

   Application of Eq. (5) from Table 1.2 to the complex edge with $\underline{k}^2 = (1 + \omega)(1 + \omega^*) = 2(1 + \cos \theta_k)$ and $2\underline{k} = (1 + \omega) + (1 + \omega^*) = 2(1 + \cos \theta_k)$ gives

$$P(G_u; X) = X^6 - 0.5X^5 - (7 + 2\cos \theta_k)X^4 + (2.5 + \cos \theta_k)X^3$$
$$+ (12 + 6\cos \theta_k)X^2 - (2.5 + 2\cos \theta_k)X - (5 + 4\cos \theta_k)$$

which for 3-fold symmetry uses

$$\theta_k = 2k\pi/3 \text{ for } k = 0, 1, 2.$$

Regardless of the value of n, the same edge weighted graph exists for $k = 0$ which is the third subgraph in Fig. 3.3.

   As a second example, consider the $C_{10}H_6N_3$ vertex centric molecular graph in Fig. 3.2. Its irreducible subgraph is shown in Fig. 3.3. Application of Eq. (5) to the complex edge with $\underline{k}^2 = \omega\omega^* = 1$ and $2\underline{k} = \omega + \omega^* = 2\cos \theta_k$ gives

$$P(G_u; X) = X^4 - 0.5X^3 - 4X^2 + X + 2 - 2\cos \theta_k$$

$C_3H_3N_3$

$(X + 1)(X - h) - \underline{k}^2 = 0$

for $h = 0.5$ & $\underline{k} = 1$

1.0

−1.5

$C_3H_3N_3$

1.2807764

−0.7807764

$C_6H_9N_3$

1.57067

0.24243

−1.31310

$C_7H_3N_3$

$\pm\sqrt{3}$

0.5

$C_{10}H_6N_3$

1.89187
1.11372
−0.87108
−1.63451

$C_{12}H_9N_3$

1 − N's or 2 − N's

2.08140
1.10735
0.30035
−1.23581
−1.75329

$C_{13}H_9N_3$

1 − N's or 2 − N's

1.96320
1.42766
−0.10439
−0.91132
−1.87515

$C_{15}H_9N_3$

1 − N's or 2 − N's

2.07929
1.37584
0.75990
−0.59723
−1.21316
−1.90464

$C_{12}H_6N_6$
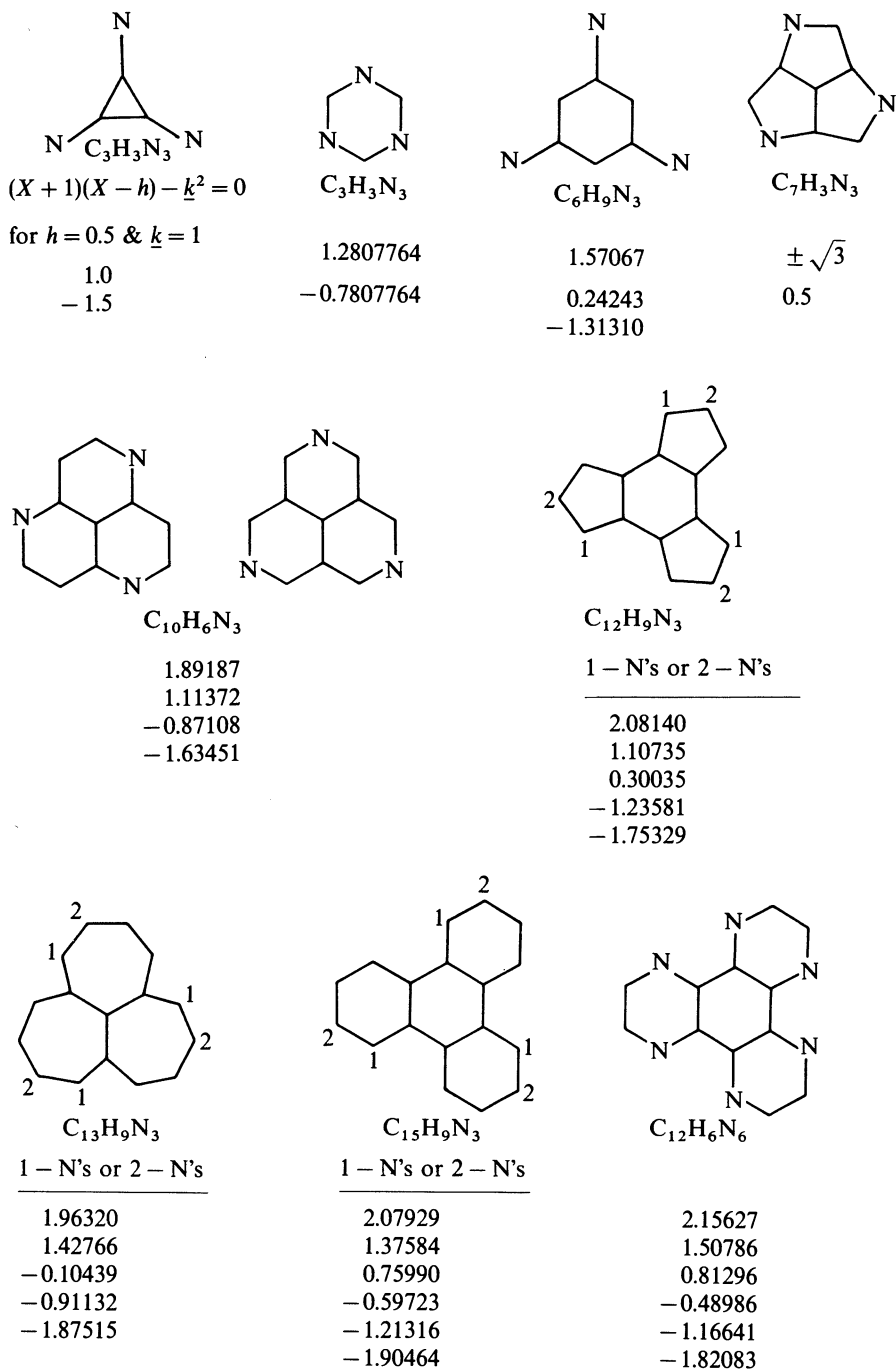
2.15627
1.50786
0.81296
−0.48986
−1.16641
−1.82083

Fig. 3.2. 3-Fold symmetrical heterocyclic molecules ($h = 0.5$, $\underline{k} = 1.0$) and their doubly degenerate eigenvalues
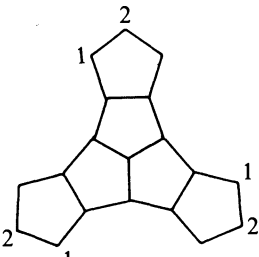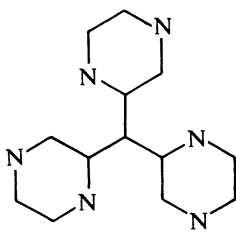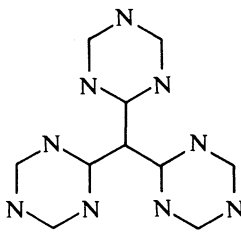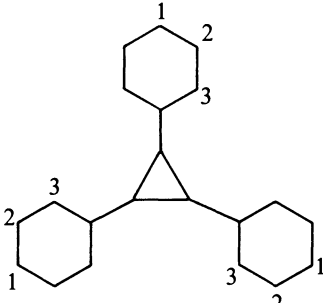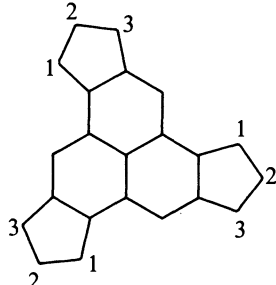
$C_{16}H_6N_3$

1 – N's	2 – N's
2.24044	2.18074
1.31484	1.48557
0.70034	0.61057
−0.07401	−0.16400
−1.50278	−1.38142
−2.17882	−2.23145

$C_{13}H_9N_6$

2.18614
1.35078
1.0
−0.686141
−1.0
−1.85078

$C_{10}H_6N_9$

2.26556
1.28078
1.28078
−0.78078
−0.78078
−1.76556

$C_{18}H_{12}N_3$

1 – N's	2 – N's	3 – N's
2.15210	2.15628	2.17089
1.32502	1.26304	1.20529
1.0	1.07542	1.09781
−0.40497	−0.49642	−0.41884
−1.0	−0.87278	−0.89888
−1.38696	−1.44660	−1.50285
−2.18519	−2.17893	−2.15343

$C_{19}H_9N_3$

1 – N's or 3 – N's	2 – N's
2.30573	2.28681
1.49663	1.54154
0.91542	0.92763
0.42770	0.37254
−1.03668	1.03975
−1.59673	−1.54533
−2.01207	−2.04344

Fig. 3.2. (*Continued*)

which for 3-fold symmetry uses

$$\theta_k = 2k\pi/3 \text{ for } k = 1, 2.$$

The $k = 0$ fragment possesses the additional unique central vertex linked by a $\sqrt{3}$ weighted edge.

There are two $C_{10}H_6N_3$ 3-fold molecular graphs with the phenalenyl skeleton in Fig. 3.2 (second row) and both have the same doubly degenerate

$C_{19}H_9N_3$

1 – N's	2 – N's
2.21727	2.20013
1.48225	1.52087
1.07865	1.07230
0.25842	0.24836
−0.85739	−0.93808
−1.39079	−1.29591
−2.28842	−2.30768

$C_{19}H_{15}N_3$

2.13891
1.35910
1.0
0.27672
−1.0
−1.19613
−2.07860

$C_{21}H_{15}N_3$

2.17811
1.47378
1.0
0.55598
−1.0
−1.0
−1.57962
−2.12824

$C_{21}H_{15}N_3$

2.15033
1.50352
1.0
0.84491
−0.50310
−1.0
−1.36792
−2.12775

$C_{22}H_{12}N_3$

2.25011
1.66578
1.18160
0.74923
−0.58949
−1.14222
−1.44133
−2.17369
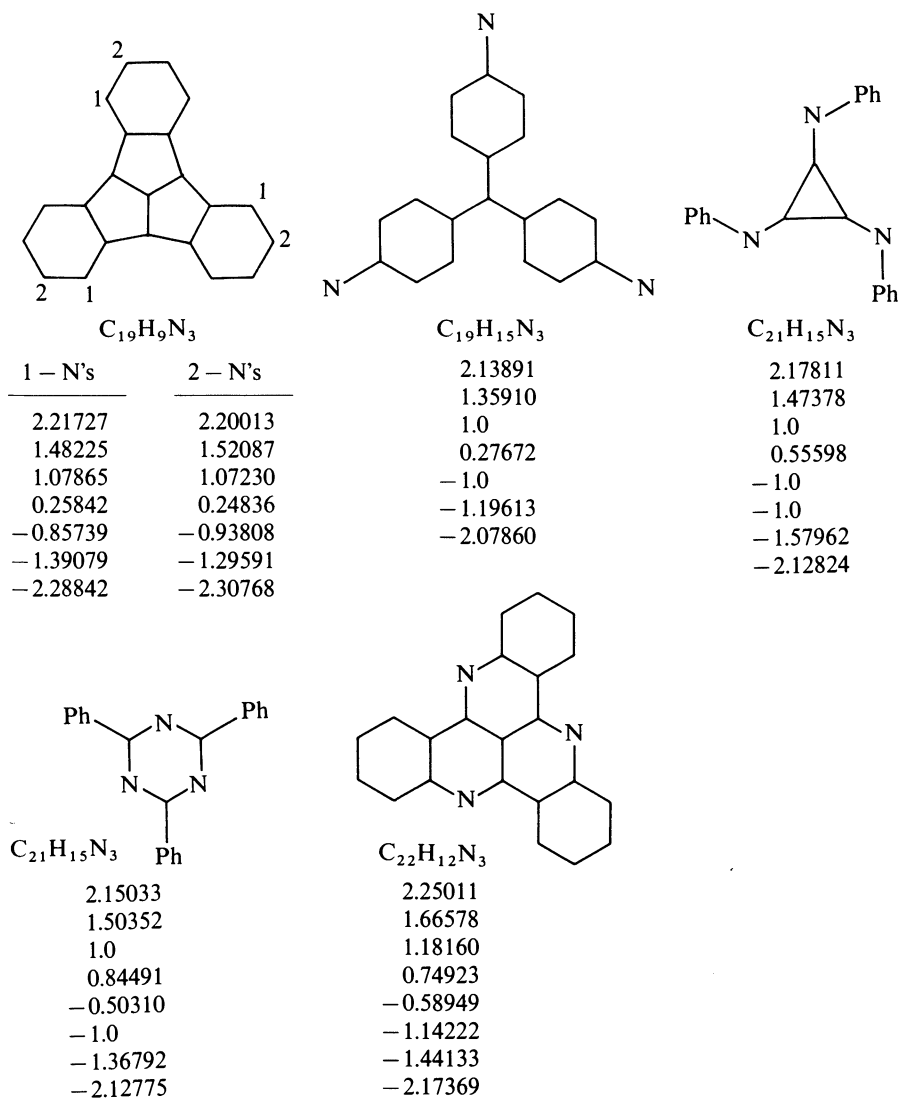
Fig. 3.2. (*Continued*)

eigenvalue subset. By the rule of topological charge stabilization, the first one with the nitrogens in the starred positions of the anionic phenalenyl skeleton is predicted to be the more stable. The last six irreducible subgraphs in Fig. 3.3 do not have their corresponding molecular graphs listed in Fig. 3.2.

In the molecules thus far treated, there was one interacting orbital per atom leading to molecular graphs in which the vertices coincided with the atoms. In the next section, we will show the treatment of molecular systems having more

$\omega^* + 1$

$\omega + 1$ $\omega^* + 1$ $\omega + 1$

N   N

2.07929
1.37584
0.75990
−0.59723
−1.21316
−1.90464

2

N

2.59415
1.38362
1.05860
−0.71388
−1.33250
−2.48999

2

N

2.56040
1.55440
0.91772
−0.81407
−1.20357
−2.51488

N

$\omega + 1$ $\omega^* + 1$

N

2.15627
1.50786
0.81296
−0.48986
−1.16641
−1.82083

N

2

N

2.64853
1.39340
1.25165
−0.54193
−1.30753
−2.44411

ω^*

ω ω^* ω

N   N

$X^4 - 4X^2 + 3 - h(X^3 - 2X)$
1.89187
1.11372
− 0.87108
− 1.63451

$\omega^* + 1$ $\omega + 1$
N

$\omega^* + 1$ $\omega + 1$
N

$\omega^* + 1$ $\omega + 1$
N

$\omega + 1$
N

$\omega^* + 1$

$\omega + 1$
N

$\omega^* + 1$

$\omega + 1$
N

$\omega^* + 1$

2.34493
1.71880
1.39068
1.0
0.61803
−0.43922
−1.0
−1.26174
−1.61803
−2.25345

$h = 0.5$ and $\underline{k} = 1.0$

2.34968
1.69634
1.38611
1.05904
0.57988
−0.46537
−0.94055
−1.28455
−1.63111
−2.24950

2.32734
1.74062
1.39043
1.05286
0.55781
−0.48893
−0.93307
−1.27156
−1.61034
−2.26516

Fig. 3.3. Irreducible subgraphs for C_n heterocyclic molecular graphs and their eigenvalues for $n = 3$

than one interacting orbital per atom. Orbital network diagrams have more vertices than there are atoms in the molecule to which they correspond. The work of Herndon on MO and PMO calculations of saturated organic compounds is highly relevant [15].

3.3 Characteristic Polynomials of π-Hydrocarbon-Iron Tricarbonyl Complexes

3.3.1 Basis Orbitals for π-Hydrocarbonyl-Iron Tricarbonyl Complexes

Merging the graph-theoretical methods previously developed by the author [6, 8] with the topological Huckel model developed by Mingos [10], one can rapidly compute the characteristic polynomials and eigenvalues of olefin-metal complexes. This leads to a facile noncomputer oriented method for obtaining useful Huckel MO parameters. The ease in which these calculations are performed not only facilitates our chemical thinking processes but also provides us with a unique perspective in the conceptualization of chemical phenomena. The study of different ways of comparing molecules contributes to our better understanding of their chemistry. In this section, we show how to compute the HMO parameters of carbonylmetal η^4-olefin complexes using these methods. A structure-resonance theory study of these metal complexes has been reported by Herndon [11]. Also, the work of King is relevant [12].

The Mingos model assumes the basis-set orbitals for the π-electron calculation as being the hydrocarbon polyene $p\pi$ orbitals (i.e., unhybridized carbon p_z orbitals) and one each of the metal e_{xz} ($d_{xz} + p_x = 2e_{xz}$) and e_{yz} ($d_{yz} + p_y = 2e_{yz}$) hybrid orbitals (Fig. 3.4). The metal and carbon Coulomb integrals ($\alpha_c = \alpha_m = \alpha$) and carbon-carbon $2p\pi$-$2p\pi$ and the metal-carbon e_{xz}-$2p\pi$ and e_{yz}-$2p\pi$ exchange integrals ($\beta_{cc} = \beta_{cm} = \beta$) are taken to be comparable; the effect of electronegativity differences on α_m can be introduced as an additional refinement, later on. The signs of the metal-carbon exchange integrals (β) are chosen to reflect the phase changes in the chosen set of basis orbitals: $-\beta$ is associated with a phase change (Fig. 3.4); a single phase change in a cyclic π-network is a Möbius system [13]. A double phase change acts like a double negative to give a "normal cycle" (Fig. 3.5).

These assumptions describe the metal-polyene fragment as being perturbed to a negligible extent by the carbonyl groups. Justification for this derives from both experimental and theoretical studies [14]. The basis orbitals for tricarbonyl (η^4-butadiene)iron and tricarbonyl(η^4-cyclobutadiene)iron with their corresponding molecular graphs are depicted in Fig. 3.4. The iron $d_{xz} - p_x$ and $d_{yz} - p_y$ hybrid orbitals combine with the organic ligand p_z orbitals to form a three-dimensional delocalized electronic network containing N_c electrons, where N_c is the total number of basis orbitals. The Fe(CO)$_3$ moiety is characterized by the electronic configuration $(e_{xz})^1(e_{yz})^1$ with its remaining six metal electrons
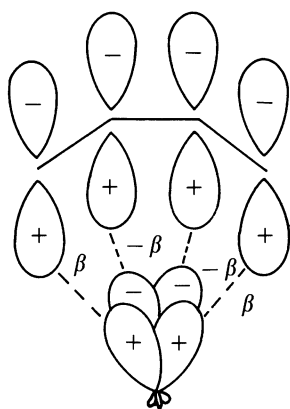
a) basis orbitals for
   $Fe(\eta^4\text{-}C_4H_6)(CO)_3$

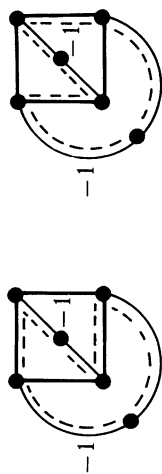b) orbital network graph for $Fe(\eta^4\text{-}C_4H_6)(CO)_3$
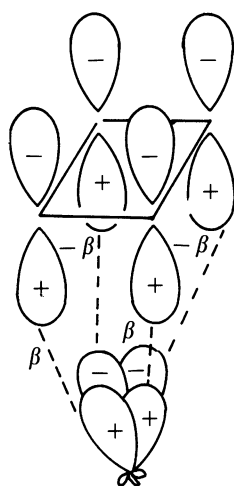
c) basis orbitals for
   $Fe(\eta^4\text{-}C_4H_4)(CO)_3$
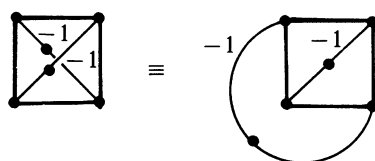
d) orbital network graph for $Fe(\eta^4\text{-}C_4H_4)(CO)_3$

Fig. 3.4. Basis orbitals and corresponding orbital network graphs for $Fe(\eta^4\text{-olefin})(CO)_3$ complexes

occupying the non-bonding d_{z^2}, $d_{x^2-y^2}$, and d_{xy} orbitals. Thus, the $Fe(CO)_3$ group contributes two electrons for metal-butadiene bonding.

In this work and orbital network graph (Fig. 3.4) is a graph where vertices correspond to atomic π-orbitals and edges (lines) connecting the vertices associate the pairs of π-orbital interactions. It should be noted that orbital network graphs and their corresponding computed parameters disregard stereochemistry,

Möbius circuit

Möbius circuit

Möbius circuit

Möbius circuit

Hückel circuit
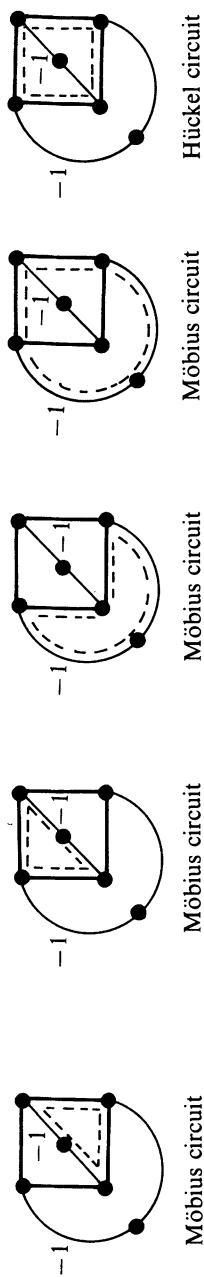
a) All the tetragonal circuits in $Fe(\eta^4\text{-}C_4H_4)(CO)_3$ are shown by the dashed outlines.

b) All the hexagonal circuits in $Fe(\eta^4\text{-}C_4H_4)(CO)_3$ are shown by the dashed outlines.

Fig. 3.5. All the tetragonal and hexagonal circuits (*dashed outlines*) in $Fe(\eta^4\text{-}C_4H_4)(CO)_3$

and the following two orbital network graphs for $Fe(\eta^4\text{-}C_4H_6)(CO)_3$ give identical characteristic polynomials.
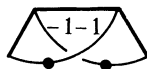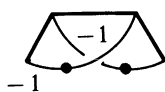

$$X^6 - 7X^4 + 15X^2 - 9$$

3.3.2 Determining Characteristic Polynomials and Eigenvalues

Making use of graph-theoretical methods previously published, one can quickly determine the characteristic polynomials and eigenvalues of the tricarbonyliron complexes presented in Fig. 3.6. Table 1.1 gives a glossary of terms and Table 1.2 gives a summary of the equations that will be used. The tetrahapto-iron complexes of butadiene and cyclobutadiene and compounds **1** to **14** in Fig. 3.6 are alternant π-electronic networks (i.e., contain no odd sized rings) with bonding/antibonding MO energy levels that are paired and have characteristic polynomials with only even terms and a tail coefficient which equals the corrected structure count $(CSC = \mathbf{K})$ to the second power. Herndon's method for determining CSC can be used to obtain the tail coefficient, $a_N = \pm \mathbf{K}^2$, of the characteristic polynomial of alternant π-electronic networks [11]. The second coefficient, $a_2 = -q$, is equal to the negative of the number σ-bonds in the orbital network graph of the metal carbonyl complex molecule. The a_4 and a_6 coefficients are given by Eq. (1) and Eq. (2), respectively, in Table 1.2. In the application of these latter two, it should be noted that r_4 and r_6 give the algebraic sum of the number of tetragonal and hexagonal rings, respectively, where Möbius ring systems are assigned negative values. Also, r_4 and r_6 represent all combinatorial tetragonal and hexagonal circuits, respectively. For example, the octahedron possesses 15 different tetragonal circuits (each of the 12 octahedron edes is central to one tetragonal circuit and each of the three pairs of opposing vertices is central to a tetragonal circuit) and the cube has 16 distinct hexagonal circuits (each of the 12 cube edges is central to one hexagonal circuit and each of four pairs of opposing vertices is central to a hexagonal circuit. It should be noted that Eq. (1) and Eq. (3) are valid for all graphs and Eq. (2) is valid for all graphs having vertices of degree-3 or less.

   Möbius MO circuits arise not only in organometallic molecules (Figs. 3.4 and 3.5) but also occur in transition state complexes in reaction mechanisms involving only organic reactants. Two important generalizations should be noted. First, for alternant conjugated MO systems, the role of $4n + 2$ and $4n$ are reversed in the appraisal of aromatic and antiaromatic character. Second, the pairing theorem is still applicable [16]. Molecular graphs with a single edge having weight $\underline{k} = -1$ will contain Mobius circuits. Application of Eq. (4) and Eq. (5) from Table 1.2 will allow one to handle such molecular graphs or orbital network diagrams in the usual way. Although we use $\mathbf{K}$ for CSC in this
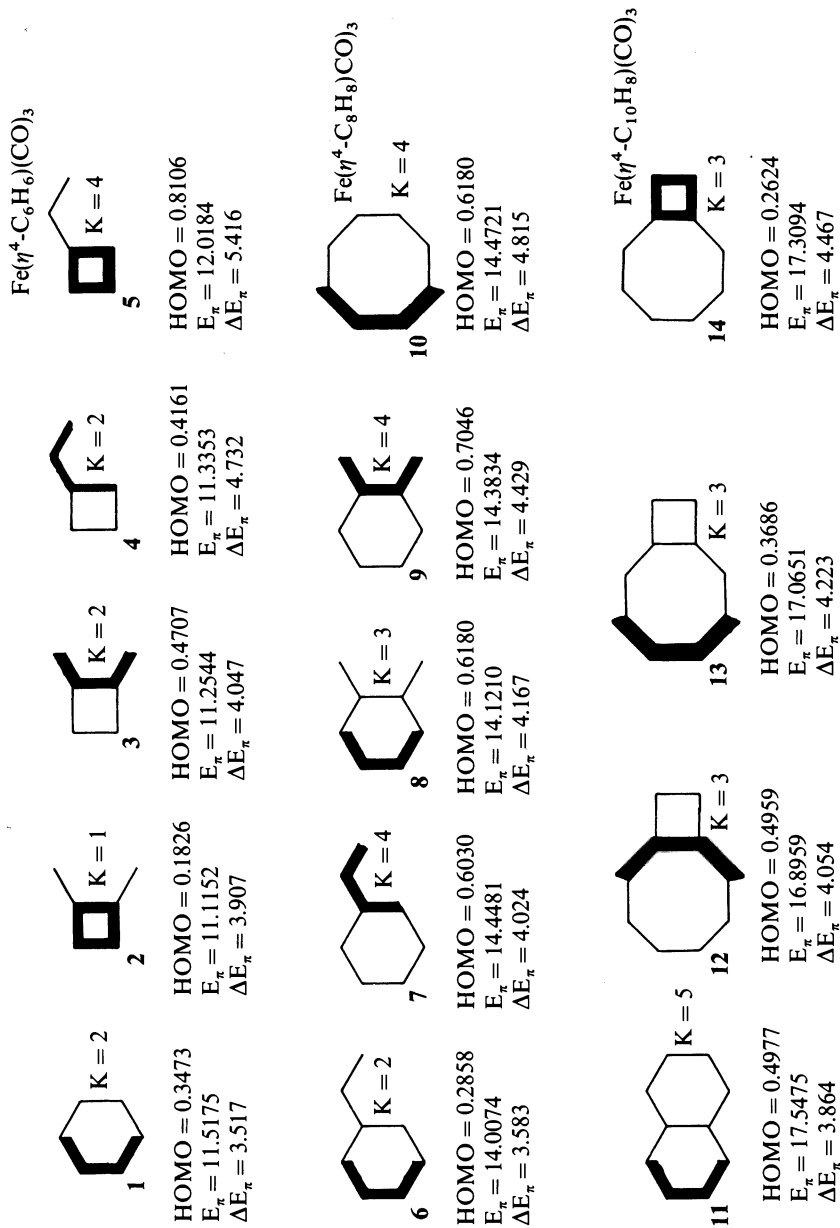
Fig. 3.6. HMO parameters for Fe(η^4-olefin)(CO)$_3$ complexes

section, K is not really the number of Kekule structures but instead the algebraic structure count for systems with $4n$ rings.

To illustrate the use of the equations in Table 1.2 for generating the characteristic polynomials, we will now present the solutions to the graph of the cube and the orbital network graphs of tricarbonyl(η^4-cyclobutadiene)iron and tricarbonyl(η^4-benzene)iron. For the cube graph q = 12, $a_4 = 30$, $a_6 = -28$, and $\mathbf{K} = 3$ which gives $P(\text{cube}; X) = X^8 - 12X^6 + 30X^4 - 28X^2 + 9$. For the tricarbonyl($\eta^4$-cyclobutadiene)iron molecular graph (Fig. 3.4) $N_c = 6$, $q = 8$, and $e(3, 3) = 4$. Figure 3.5 shows all the tetragonal and hexagonal circuits for this molecular graph; there are four Möbius and one regular tetragonal circuits and two hexagonal circuits crossing over two negative unit weighted edges giving $r_4 = -4$ with $\alpha_4 = 4$, $r_4 = 1$ with $\alpha_4 = 4$, and $r_6 = 2$. Inputting these parameters into Eq. (1), Eq. (2), and Eq. (3) gives the characteristic polynomial for tricarbonyl(η^4-cyclobutadiene)iron as $P(\text{TCCBI}; X) = X^6 - 8X^4 + 20X^2 - 16$; the tail coefficient can be verified by using Herndon's CSC method. Finally, for tricarbonyl(η^4 - benzene)iron (1 in Fig. 3.6) $N_c = 8$, $q = 10$, and $e(3, 3) = 3$. Metal complex 1 has two Möbius tetragonal rings ($r_4 = -2$) each having three branches ($\alpha_4 = 3$) and two Möbius and two regular hexagonal circuits ($r_6 = -2 + 2 = 0$) giving $P(1; X) = X^8 - 10X^6 + 33X^4 - 37X^2 + 4$ where the tail coefficient was obtained from the CSC. In this way all alternant molecular graphs up to $N_c = 6$ and all alternant molecular graphs with vertices of degree-3 or less up to $N_c = 8$ can be solved. Solution of larger molecular graphs requires knowledge of some eigenvalues via embedding or by decomposition per Eq. (5) into smaller graphs.

3.3.3 Eigenvalues by Embedding

A molecule possessing a subset of eigenvalues found in another molecule is said to be subspectrally related to it. If a smaller molecule can be embedded onto a larger molecule, then the eigenvalues of the smaller one will be found among the eigenvalues of the larger one (cf. Chapter 1). Common embedding fragments include ethene ($\varepsilon = \pm 1.0\beta$), allyl ($\varepsilon = \pm \sqrt{2}\beta$), 1,3-butadiene [$\varepsilon = \pm 0.5(\sqrt{5} \pm 1)\beta$], and pentadienyl ($\varepsilon = \pm 1.0, \pm \sqrt{3}\beta$). Mixed embedding requires that the different fragments have some common eigenvalues, like ethene and pentadienyl ($\varepsilon = \pm 1.0$). Mixed embedding with the fragments shown in Fig. 3.7 was observed [14]. Tricarbonyl (η^4-butadiene)iron and the metal complexes 3, 9, 10, and 12 (Fig. 3.6) all are embeddable by ethene and, therefore, have eigenvalues of $\varepsilon = \pm 1.0\beta$. Mixed embedding of butadiene and G_1 in Fig. 3.6 occurs in the metal complexes of 8 and 10 which have eigenvalues of $\varepsilon = \pm 0.5(\sqrt{5} \pm 1)\beta$. For allyl, G_2, or mixed allyl and G_2 embedding to be possible, the tail coefficient or $\mathbf{K} = \text{CSC}$ of a test structure must be divisible by 2. Mixed allyl and G_2 embedding of 7 ($\mathbf{K} = 4$) occurs; for pentadienyl, G_2, or mixed pentadienyl and G_2 embedding to occur, the test structure must have a K value divisible by 3. Two distinct mixed embeddings of pentadienyl and G_2 occurs on 14 ($\mathbf{K} = 3$)
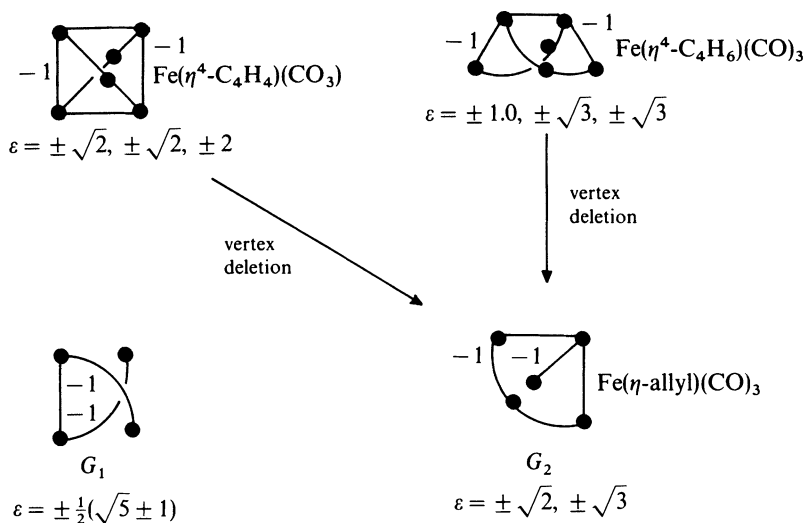
a) Embedding fragments.
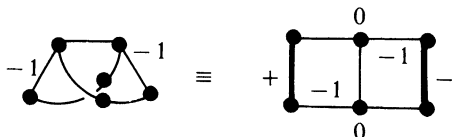

b) Ethene embedding on $Fe(\eta^4\text{-}C_4H_6)(CO)_3$.

Fig. 3.7. Embedding fragments for $Fe(\eta^4\text{-olefin})(CO)_3$ complexes

which is doubly degenerate in eigenvalues of $\varepsilon = \pm\sqrt{3}\beta$. Molecular graphs that have a doubly degenerate eigenvalue subset can have any vertex atom deleted, replaced, or augmented by a polyene substituent giving successor molecular graphs still retaining this eigenvalue subset once. The tricarbonyliron complexes of s-cis-1,3-butadiene and cyclobutadiene are doubly degenerate in eigenvalues of $\varepsilon = \pm\sqrt{3}\beta$ and $\varepsilon = \pm\sqrt{2}\beta$, respectively, and deletion of a carbon vertex from either can generate molecular graph G_2 in Fig. 3.7 which has $\varepsilon = \pm\sqrt{2}$, $\pm\sqrt{3}\beta$. Attachment of a vinyl substituent to tricarbonyl(η^4-cyclobutadiene)-iron gives **5** which has $\varepsilon = \pm\sqrt{2}\beta$. Complexes **8** and **10** which are mixed embeddable by G_1 and L_4 all have the same HOMO $= 0.6180\beta$ value.

3.3.4 ΔE_π as Relative Measure of Reaction Spontaniety

It is assumed in this here that the reaction of a polyene to form a tricarbonyliron complex will have its relative spontaniety governed principally by the change

in π-electronic delocalization energy. Thus, in the following reaction scheme $\Delta E_\pi = E_\pi[\text{polyene-Fe(CO)}_3]-E_\pi[\text{polyene}]$ is a measure of the tendency for the reaction to take place:

$$\text{polyene} + \text{Fe(CO)}_3 \rightarrow \text{polyene-Fe(CO)}_3 \text{ complex}$$
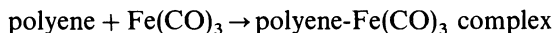
There are two basic kinds of (tetrahapto-polyene)metal complexes. These are typified by the known s-cis-1,3-butadiene and cyclobutadiene complexes of tricarbonyliron (Fig. 3.4). The large difference in the ΔE_π values between tricarbonyl(η^4-butadiene)iron ($\Delta E_\pi = 4.456\beta$) and tricarbonyl($\eta^4$-cyclobutadiene)-iron ($\Delta E_\pi = 5.6578\beta$) is consistent with the three-dimensional aromatic properties exhibited by the latter metal complex. The carbon-carbon bond lengths in tricarbonyl(η^4-cyclobutadiene)iron are all equal, and this complex is known to undergo electrophilic substitution and to resist Diels-Alder reaction. Of all the $\text{Fe}(\eta^4\text{-C}_{10}\text{H}_8)$ $(\text{CO})_3$ isomers (Fig. 3.6), only **14** is known, which is consistent with its larger ΔE_π value [14].

3.3.5 Other Examples of Möbius Circuits

If an ordinary spinning body is rotated in space through 360°, it returns to its original configuration. A particle with spin 1/2, however, will not do this. If such a particle is rotated through 360°, it assumes a quantum state with measurably different physical properties. To return the particle to its initial state, it is necessary to rotate it through 720°. In other words, a spin 1/2 particle requires double rotation relative to "everyday" objects before it comes back to it starting state. This phenomenon is topologically equivalent to drawing a line on a closed Möbius paper strip until it connects. In doing this, the line goes around twice, on both surfaces of the Möbius strip, before it connects. It is worth emphasizing that contrary to one's initial intuition, molecular graphs can have negative weighted edges which correspond to Möbius circuits.

3.4 References

1. Gimarc BM (1983) J Am Chem Soc 105: 1979
2. Dias JR, Liu B (1990) Monatsh Chem 121: 13
3. Herndon WC (1973) Tetrahedron 29: 3 (1974) J Chem Educ 51: 10; (1975) J Org Chem 40: 3583
4. Cooper CF (1979) J Chem Educ 56: 568; Smith WB (1971) J Chem Educ 48: 749
5. Dias JR (1987) Can J Chem 65: 734
6. Dias JR (1988) Handbook of Polycyclic Hydrocarbons, Part B. Elsevier, New York
7. Leupin W, Magde D, Persy G, Wirz J (1986) J Am Chem Soc 1108: 17
8. Dias JR (1988) J Molec Struct (Theochem) 165: 125; (1989) Theor Chim Acta 76: 153
9. D'Amato S (1979) Theor Chim Acta 53: 319; Davidison RA (1981) Theor Chim Acta 58: 193
10. Mingos DMP (1977) J Chem Soc. Dalton Trans 25–37
11. Herndon WC (1980) J Am Chem Soc 102: 1538
12. King RB (1977) Theor Chim Acta 44: 223
13. Randic' M, Zimmerman HE (1986) Int J Quantum Chem 20: 185
14. Dias JR (1990) J Math Chem 4: 127
15. Herndon WC (1972) Prog Phys Org Chem 9: 99; (1979) J Chem Educ 56: 448
16. Randic M; Zimmerman HE (1986) Int J Qunatum Chem: Quantum Chem Symp 20: 185

3.5 Problems

1 Compare the ionic character of the following isoconjugates [(1991) Chem Lett Jpn 2151] assuming $k = h = 1$. Mirror plane fragmentation (Table 2.1) and Eq. (4) (Table 1.2) will be helpful.
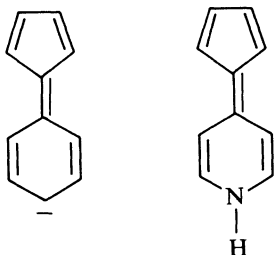
2 Compare the stabilities of the following 3-fold molecular ions [(1991) Tetrahedron Lett 32:601]. See Fig. 2.4 for the appropriate decomposition of this system.
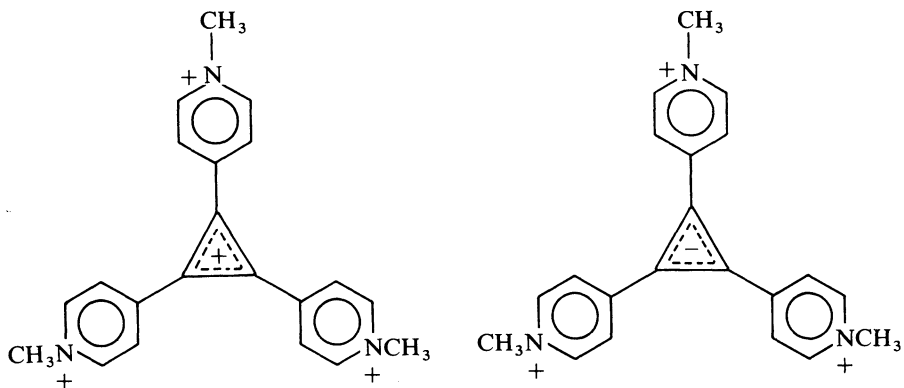
3 The last six irreducible subgraphs in Fig. 3.3 do not have corresponding molecular graphs listed in Fig. 3.2. Draw these missing molecular graphs by reassembling the irreducible subgraph components.

4 The characteristic polynomial of phenalenyl is $X^{13} - 15X^{11} + 84X^9 - 226X^7 + 309X^5 - 207X^3 + 54X$. Using the zero sum rule determine its unnormalized eigenvector for $X = 0$. Show that one can multiply these eigenvector coefficients by the number of Kekule structures associated with the naphthalene substructure to obtain another eigenvector coefficient set whose sum equals the SC of phenalenyl [3] and that the sum of their squares equals the tail coefficient (a_{12}) above. Using pentadienyl embedding determine a_8 and a_{10} from the remaining coefficients that can be determined with the equation in Table 1.2.

5 Given the following cyclopentadienyl anion analogs calculate the ratio of β_{cc} versus β_{pp} [(1988) Angew Chem Int Ed Engl 27:280].
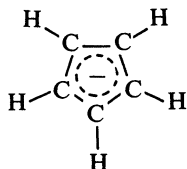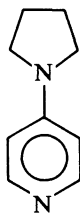

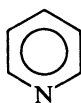$\lambda_{max} = 220\,nm$ $\lambda_{max} = 320\,nm$

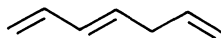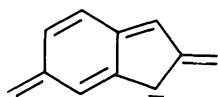6 Rationalize the basicity of the pyridine nitrogens for the following.

pK$_a$ = 9.7   pK$_a$ = 5.3

7 Use resonance theory (SC method from [3]) to determine the charge densities for the following anions and compare these results with HMO calculations. Substitution of which CH by N will give the most stable heterocycle?

8 On pages 79 and 83, the MO solution to the first 3-fold symmetrical $C_{15}H_9N_3$ ring-centric molecular graph in Fig. 3.2 was given. Repeat this calculation for the other isomer, and show that while both isomers are doubly degenerate for $k = 1, 2$ with the same eigenvalues, their $k = 0$ solutions are different.

9 On pages 79 and 83, the solution for both the $k = 1, 2$ irreducible subgraphs for the $C_{10}H_6N_3$ vertex-centric isomers were given. Show that they both give the same equation for $k = 1, 2$ but different equations for $k = 0$.

10 Reproduce the MO calculations in the paper by W. Leupin and J. Wirz in (1980) J Am Chem Soc 102:6068.

11   Determine as many eigenvalues as you can for the following general heterocycles.
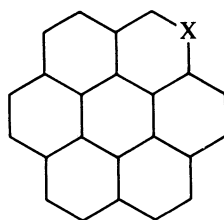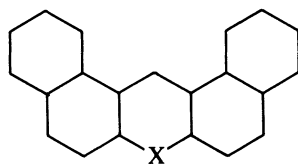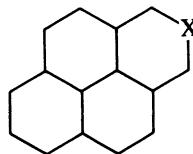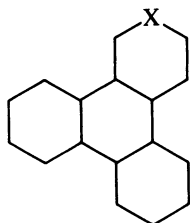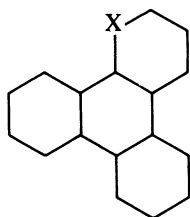
Chapter 4
Large Conjugated Polyenes

4.1 Introduction

In this chapter, we will demonstrate how to extract the maximum amount of data from large molecular graphs with a minimum amount of work. The concept of *similarity*, which is the degree of overlap between two or more structures (molecular graphs), will be exploited. Two or more structures having molecular graphs with a common subset of eigenvalues will exhibit a degree of similarity. This similarity will be strongest when this eigenvalue subset contains the eigenvalues of the HOMO and LUMO of the structures being compared. Other things being equal, the more eigenvalues in common between two structures, the more they are similar [1]. Two or more molecular graphs with a common subset of eigenvalues are said to be subspectral. Two isomeric molecular graphs that have all their eigenvalues in common are said to be isospectral.

From Chapter 2, we saw that symmetry played an important role in subspectrality of molecules. However, the application of butadiene embedding to the following two nonsymmetrical molecules shows that symmetry is not a necessary requirement for the existence of subspectrality.
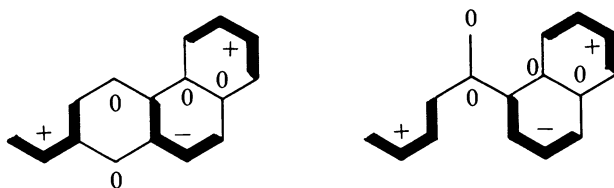
molecules that are subspectral
in the eigenvalues of butadiene

The structures in Fig. 4.1 are illustrative of different degrees of similarity. All three of these structures give the same C_{15} right-hand mirror plane fragment with the listed eigenvalues but are of different sizes. The larger $C_{33}H_{13}$ structure is least similar to the smaller $C_{30}H_{18}$ structure. If a substituent is placed on the mirror plane vertex indicated by a heavy dot on the $C_{33}H_{13}$ structure, the C_{15} right-hand mirror plane fragment will remain unchanged. One does not need to know the eigenvalues of the C_{15} fragment for this set of related structures in order to qualitatively evaluate their relative similarity. Only the $C_{30}H_{18}$ is an AH, and from the pairing theorem one can obtain its paired set of eigenvalues

$C_{33}H_{13}$ $C_{32}H_{14}$

$C_{30}H_{18}$ C_{15}

$K = 29$

$$
\begin{aligned}
&-2.5545\\
&-2.2249\\
&-1.7037\\
&-1.5337\\
&-1.2772\\
&-1.0991\\
&-0.7021\\
&-0.4833\\
&0.4969\\
&0.8295\\
&1.0533\\
&1.3672\\
&1.4722\\
&1.9347\\
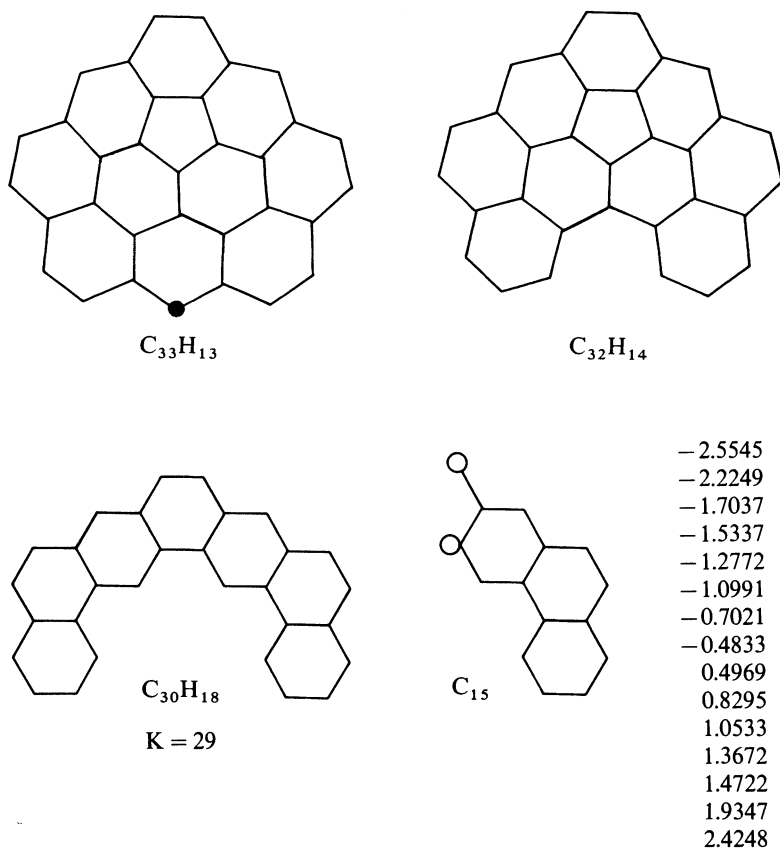&2.4248
\end{aligned}
$$

Fig. 4.1. Subspectral molecular graphs and their common eigenvalues

from the listed ones by changing their signs. The product of all the listed eigenvalues gives the number of Kékulé structures ($K = 29$) for the $C_{30}H_{18}$ AH. Going from the $C_{33}H_{13}$ structure to the $C_{30}H_{18}$ structure is equivalent to simply deleting the three vertices of the former that lie on its nodal mirror plane of symmetry.

As further illustration of partial mirror plane fragmentation, consider the 3-fold molecular graphs and their representative successor molecular graphs shown in Fig. 4.2. The doubly degenerate eigenvalues of the 3-fold molecular graphs are listed below them and can be determined by the methods of Chapter 2. As noted previously, deletion of the central vertex of these 3-fold molecular graphs leads to successor 3-fold molecular graphs still doubly degenerate in these same eigenvalues. Alternatively, we can delete one or two vertices that lie in a mirror plane of symmetry and obtain successor molecular graphs that still retain these eigenvalues once, as do the last two molecular graphs in Fig. 4.2. Additional eigenvalues can be immediately deduced for these last two successor
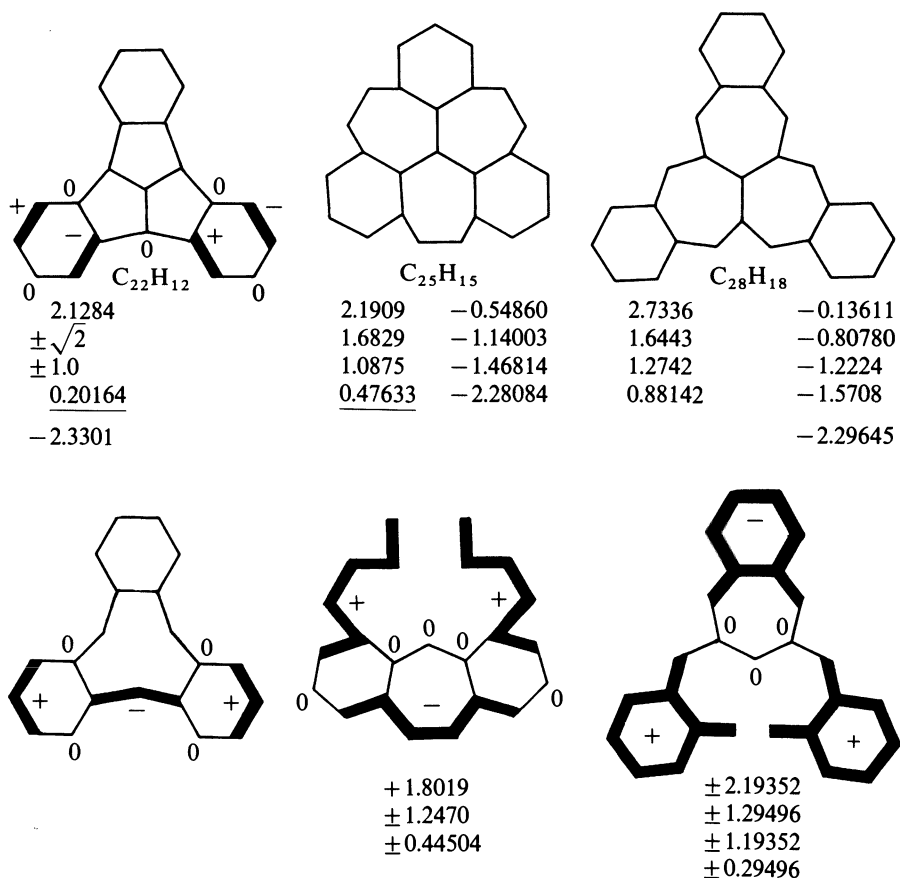
C$_{22}$H$_{12}$		C$_{25}$H$_{15}$		C$_{28}$H$_{18}$	
2.1284		2.1909	−0.54860	2.7336	−0.13611
±√2		1.6829	−1.14003	1.6443	−0.80780
±1.0		1.0875	−1.46814	1.2742	−1.2224
0.20164		0.47633	−2.28084	0.88142	−1.5708
−2.3301					−2.29645

+1.8019	±2.19352
+1.2470	±1.29496
+0.44504	±1.19352
	±0.29496

Fig. 4.2. Example 3-fold vertex-centric molecular graphs and their doubly degenerate eigenvalues with some illustrative successor molecular graphs produced by partial mirror plane fragmentation

molecular graphs by embedding, as shown in bold in Fig. 4.2. It will be further demonstrated in the next section with buckminsterfullerene [2], that mirror plane fragmentation is a powerful diagnostic tool for the study of molecules.

4.2 Molecular Orbital Solution of Buckminsterfullerene

4.2.1 Introduction

Buckminsterfullerene (BMF-C$_{60}$) has sixty carbon vertices with 32 faces ($f = r + 1$ or 31 rings) composed of 20 six-membered rings fused with 12 five membered ring (Fig. 4.3). Using Euler's equation ($f - q + N_c = 2$), one finds that $q = f - 2 + N_c = 90$. No two five-membered rings are together in compliance to the rule for isolated pentagon rings [3]. There are two types of edges –
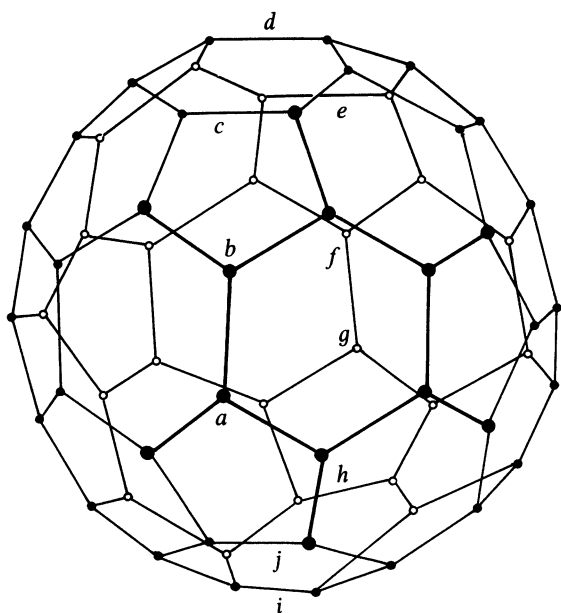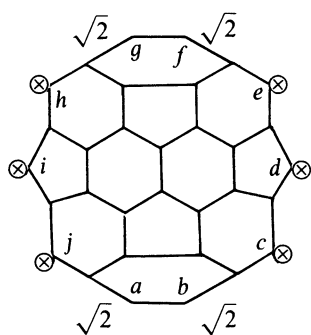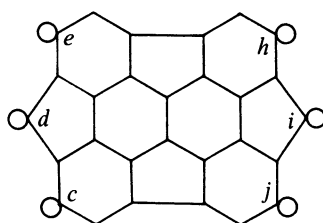
Fig. 4.3. Buckminsterfullerene (BMF-C$_{60}$)

Left mirror plane
C$_{32}$ fragment

Right mirror plane
C$_{28}$ fragment

○   vertex of weight -1
⊗   vertex of weight $+1$

Fig. 4.4. Mirror plane fragments of buckminsterfullerene

there are sixty 5-6 ring fusion edges and thirty 6-6 ring fusion edges. All the 6-6 ring fusion edges all lie on mirror planes of symmetry. Since this 3-dimensional aromatic system has no replaceable hydrogens capable of participating in electrophilic or oxidative substitution type reactions, BMF-C_{60} can only undergo addition reactions. By the principle of minimum electronic reorganization, one would predict that addition reactions of BMF-C_{60} should preferentially take place at the 6-6 ring fusion bonds, though the 5-6 ring ring fusion bonds are statistically favored by 2:1. The chemistry of BMF-C_{60} is consistent with this prediction [4].
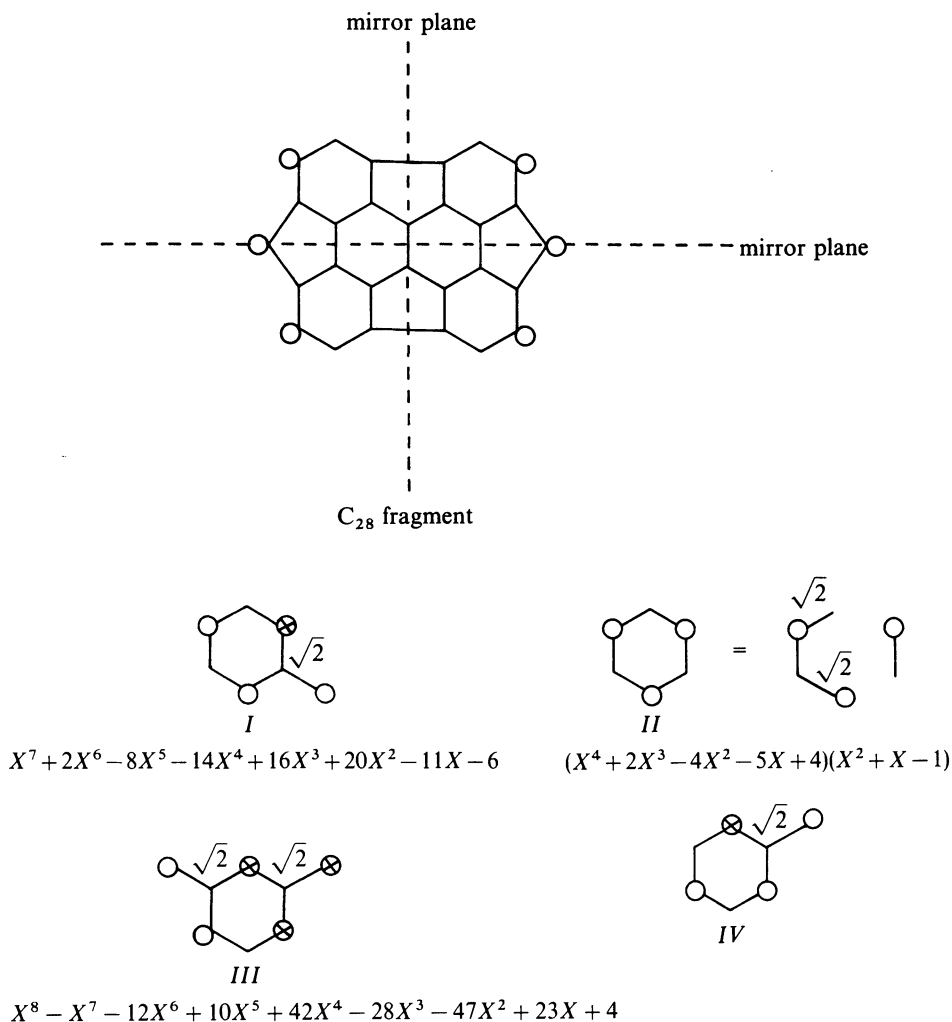

$$X^7 + 2X^6 - 8X^5 - 14X^4 + 16X^3 + 20X^2 - 11X - 6$$

$$(X^4 + 2X^3 - 4X^2 - 5X + 4)(X^2 + X - 1)$$

$$X^8 - X^7 - 12X^6 + 10X^5 + 42X^4 - 28X^3 - 47X^2 + 23X + 4$$

Fig. 4.5. Further mirror plane fragmentation of the right-hand C_{28} fragment of buckminsterfullerene

4.2.2 Eigenvalues of Buckminsterfullerene

Mirror plane fragmentation of BMF-C_{60} through vertices a, b, f, g and edges c, d, e, h, i, j in Fig. 4.3 leads to the C_{28} (right-hand) and C_{32}(left-hand) fragments shows in Fig. 4.4. Because of the high symmetry associated with the truncated icosahedron, these fragments can be submitted to perpendicular mirror plane fragmentation as shown in Figs. 4.5 and 4.6. The size of these eight final frag-
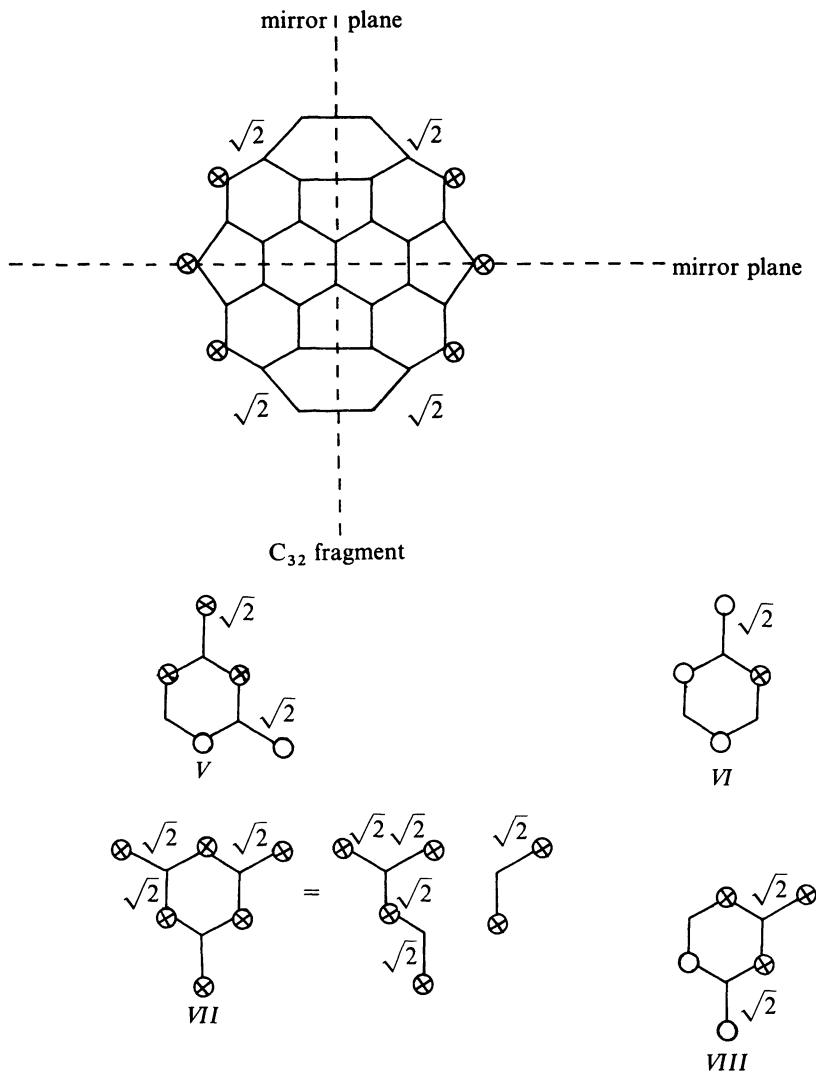
$$(X^6 - 4X^5 - 3X^4 + 23X^3 - 8X^2 - 27X + 18)(X^3 - 2X^2 - 2X + 3)$$

Fig. 4.6. Further mirror plane fragmentation of the left-hand C_{32} fragment of buckminsterfullerene

Table 4.1. The eigenvalues of buckminsterfullerene

| Major Doubly Degenerate Subsets		Unmatched Subset
−2.61803	−2.61803	−2.61803
−2.562	−2.562	−1.61803
−2.562	−2.562	−1.438
−2.0	−2.0	−1.303
−2.0	−2.0	−0.382
−1.61803	−1.61803	−0.139
−1.61803	−1.61803	0.61803
−1.438	−1.438	1.0
−1.303	−1.303	1.820
−1.303	−1.303	2.303
−0.382	−0.382	2.757
−0.139	−0.139	3.0
0.61803	0.61803	
0.61803	0.61803	
1.0	1.0	
1.0	1.0	
1.0	1.0	
1.0	1.0	
1.562	1.562	
1.562	1.562	
1.820	1.820	
2.303	2.303	
2.303	2.303	
2.757	2.757	

Davidson RA (1981) Theor Chim Acta 58:193

ments range from nine to six vertices, which can be easily solved using methods previously published by us [5]. Note that fragments II (Fig. 4.5) and VII (Fig. 4.6) can be mirror-plane-fragmented further, and fragments I, IV, and VI are identical as are III, V, and VIII. The roots to the characteristic polynomials from graph fragments I–VIII in Figs. 4.5 and 4.6 taken together constitute the set of eigenvalues belonging to BMF-C_{60} and are listed in Table 4.1.

We will give a complete solution to I in Fig. 4.5. The following decomposition equation will be employed for the characteristic polynomial of graph G

$$P(G; X) = P(G - e; X) - \underline{k}^2 P(G - (e); X) - 2\underline{k}\Sigma P(G - Z; X) \tag{5}$$

where $G - e$ is graph G with its edge e deleted, $G - (e)$ is graph G with its edge e and associated vertices deleted, $\underline{k}$ is the weight of the edge e, and $G - Z$ is the graph G with the cycle Z containing e deleted. Application of this decomposition to the graph of I gives
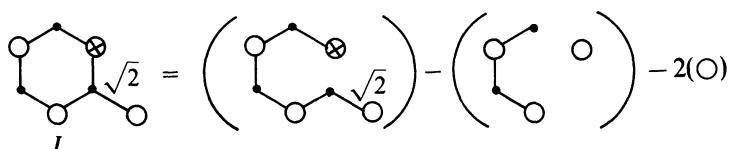
The goal here is to reduce graph I into subgraphs of five or less vertices which give determinants of size 5×5 or less that can be easily solves using Laplace's expansion by minors. The subgraph $G - e$ still possesses seven vertices and can be divided by another successive application of the above equation to give
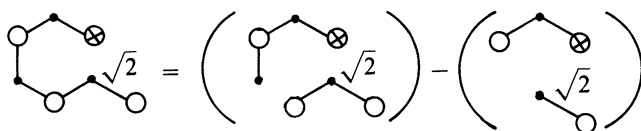
where the absense of cycles in this graph results in the third term being zero. The secular determinant of the 4×4 subgraph is submitted to Laplace's expansion to give

$$P(\quad ;X) =$$

$$
\begin{vmatrix}
X & -1 & 0 & 0 \\
-1 & (X+1) & -1 & 0 \\
0 & -1 & X & -1 \\
0 & 0 & -1 & (X-1)
\end{vmatrix}
=
\begin{vmatrix}
X & -1 \\
-1 & (X+1)
\end{vmatrix}
\begin{vmatrix}
X & -1 \\
-1 & (X-1)
\end{vmatrix}
-
$$

$$
\begin{vmatrix}
X & -1 \\
0 & -1
\end{vmatrix}
\cdot
\begin{vmatrix}
-1 & 0 \\
-1 & (X-1)
\end{vmatrix}
= X^4 - 4X^2 + X + 1
$$

Combining the characteristic polynomials of the subgraphs obtained per the above prescription leads to the characteristic polynomial of fragment I given in Fig. 4.5.

Other 3-connected even carbon (or silicon) clusters that can be solved by the method just illustrated for buckminsterfullerene include the tetrahedron (C_4), trigonal prism (C_6), cube (C_8), pentagonal prism (C_{10}), and regular dodecahedron (C_{20}). However, these clusters are expected to possess strong antiaromatic contributions.

4.3 MO Solution of 3-Fold Coronene Derivatives

4.3.1 Factorization of 3-Fold Coronene Derivatives

In Chapter 2, we demonstrated a factorization scheme developed by D' Amato and presented a procedure for obtaining the characteristic polynomial of the resulting fragments of threefold vertex-centric and ring-centric molecular graphs [6]. By this method the eigenvalues of ring-centric threefold starphenes can be easily determined. Herein, we present a factorization scheme for threefold coronene derivatives and show how to compute the characteristic polynomials of the fragments thus obtained which give the eigenvalues associated with the
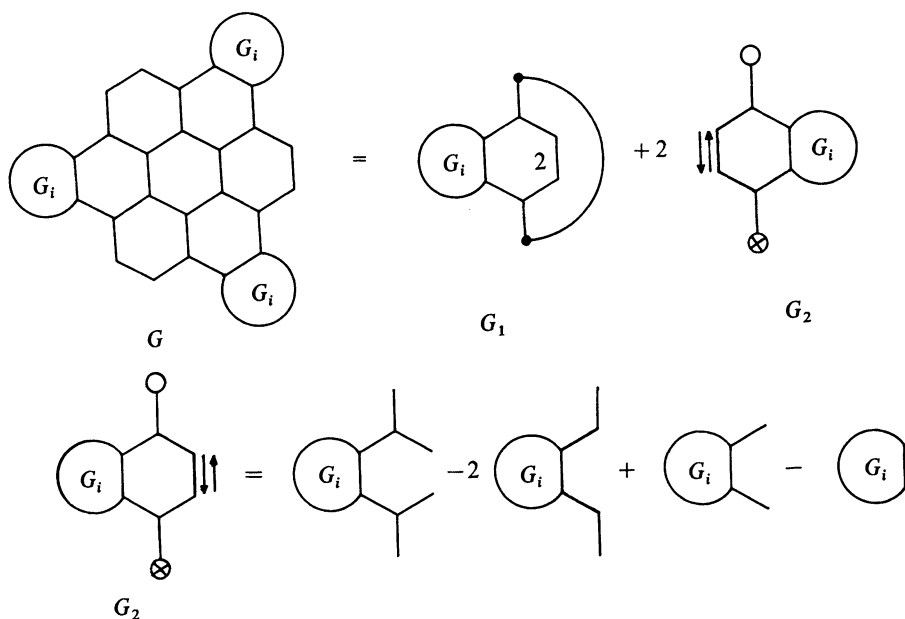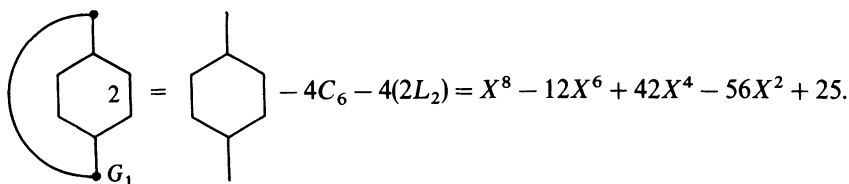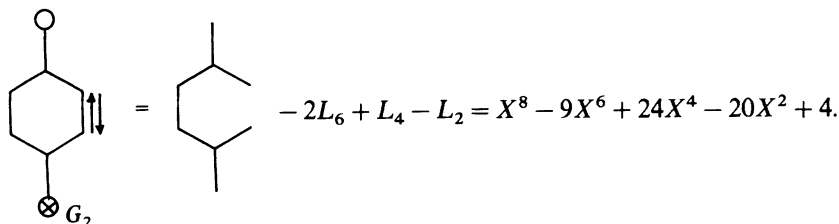
Fig. 4.7. General decomposition scheme for 3-fold coronene derivatives. If G_i is ethene, then the above molecular graph G would be coronene

parent system. Figure 4.7 gives a generalized three-fold symmetrical coronene-related molecular graph with pendant G_i subgraphs which is factored into one subgraph G_1 and two subgraphs G_2. The characteristic polynomial for the subgraph G_1 with its weighted edge of 2 can be determined by using Eq. (5) previously given. For example, consider the G_1 fragment from the decomposition of coronene itself. Application of Eq. (5) with $\underline{k} = 2$ to G_1 gives the following

$$-4C_6 - 4(2L_2) = X^8 - 12X^6 + 42X^4 - 56X^2 + 25.$$

Using the decomposition scheme summarized in Fig. 4.7 for the fragment of coronene gives

$$-2L_6 + L_4 - L_2 = X^8 - 9X^6 + 24X^4 - 20X^2 + 4.$$

$C_{36}H_{18}$

±0.51763
±1.0, ±1.0
±1.50597
±1.93185
±2.39417

$C_{48}H_{24}$

±0.44504
±0.73959
±1.0
±1.24697
±1.36595
±1.80193
±2.12766
±2.46175

$C_{60}H_{30}$

±0.34532   ±1.68179
±0.63327   ±1.95074
±1.0, ±1.0   ±2.26818
±1.22991   ±2.49457
±1.40201

$C_{60}H_{30}$

±0.444245   ±1.320884
±0.759526   ±1.726491
±0.83941   ±1.969095
±1.107925   ±2.147688
±1.230251   ±2.562174

$C_{60}H_{30}$

±0.44902   ±1.426465
±0.67919   ±1.676614
±0.850787   ±1.92611
±1.076088   ±2.26337
±1.216819   ±2.50919

Fig. 4.8. 3-Fold symmetrical coronene derivatives and their doubly degenerate eigenvalues

The eigenvalues of the first polynomials plus those of the last one taken twice given the eigenvalues of coronene. Figure 4.8 presents the doubly degenerate eigenvalues of some chemically relevant 3-fold coronene related derivatives [7].

4.4 Embedding of Benzenoid Hydrocarbons

4.1.1 Examples of Embedding of Allyl, Butadiene, Benzene, Naphthalene, Pentadienyl, and Styrene on Large Benzenoids

A property X of a system G may be categorized in terms of its limiting behavior when the system $G = A \cup B$ is broken into separate noninteracting subsystems A and B. The four different possibilities are additive, constantive, multiplicative, and derivative. Thermodynamic properties are additive quantities. Spectroscopic properties are constantive quantities. Wavefunctions, statistical mechanical partition functions, and probabilities are multiplicative quantities. Multiplicative properties can be transformed to additive ones by the logarithmic operation and derivative properties are similar to multiplicative ones. The functional group is an example of a constantive property. Additive and constantive properties form the basis for the major strategy in molecular modelling.

An embeddable graph G can be broken into fragments collectively called a spanning subgraph G' where $V(G') = V(G)$. The fragments will be K_1 and F_i components where the latter will possess common eigenvalues. If a bipartite subgraph G^* of a graph G can be embedded (covered) by alternating K_1 fragments with m identical F fragments with alternating signs, then $F_+ \cup K_1 \cup F_- \cup K_1 \cup \cdots \subset G^* \subseteq G$ and $F_+ \cap K_1 \cap F_- \cap K_1 \cap \cdots = 0$. K_1 represents a node position (vertex) which has zero coefficients in the corresponding eigenvector. Also, the sum of the associated coefficients of vertices attached to each K_1 node vertex must equal zero which is fulfilled if the fragment signs alternate. A functional group is defined as a group of interconnected atoms having a specific set of chemical and physical properties; it is the site where a chemical reaction can occur in an organic molecule. Within the context of set algebra, a functional group is defined as a disjoint subsystem F of system G such that $G = F \cup G'$ where $F \cap G' = 0$. Similarly, for more than one functional group F_i, $G = F_1 \cup F_2 \cup \cdots G'$ where $F_1 \cap F_2 \cap \cdots G' = 0$. Specific eigenvalue subsets associated with specific embedding fragments and mirror plane fragments are the constantive properties examined in this section. A primary thesis here is that embedding fragments and mirror plane fragments are types of functional groups.

In general, if a large molecule can be partitioned into recognizable elementary substructures, then one should be able to deduce much of the properties of this molecule from the sum of the properties of the elementary substructures. Additional properties which arise from special interactions between the elementary substructures can then be included. Studying the
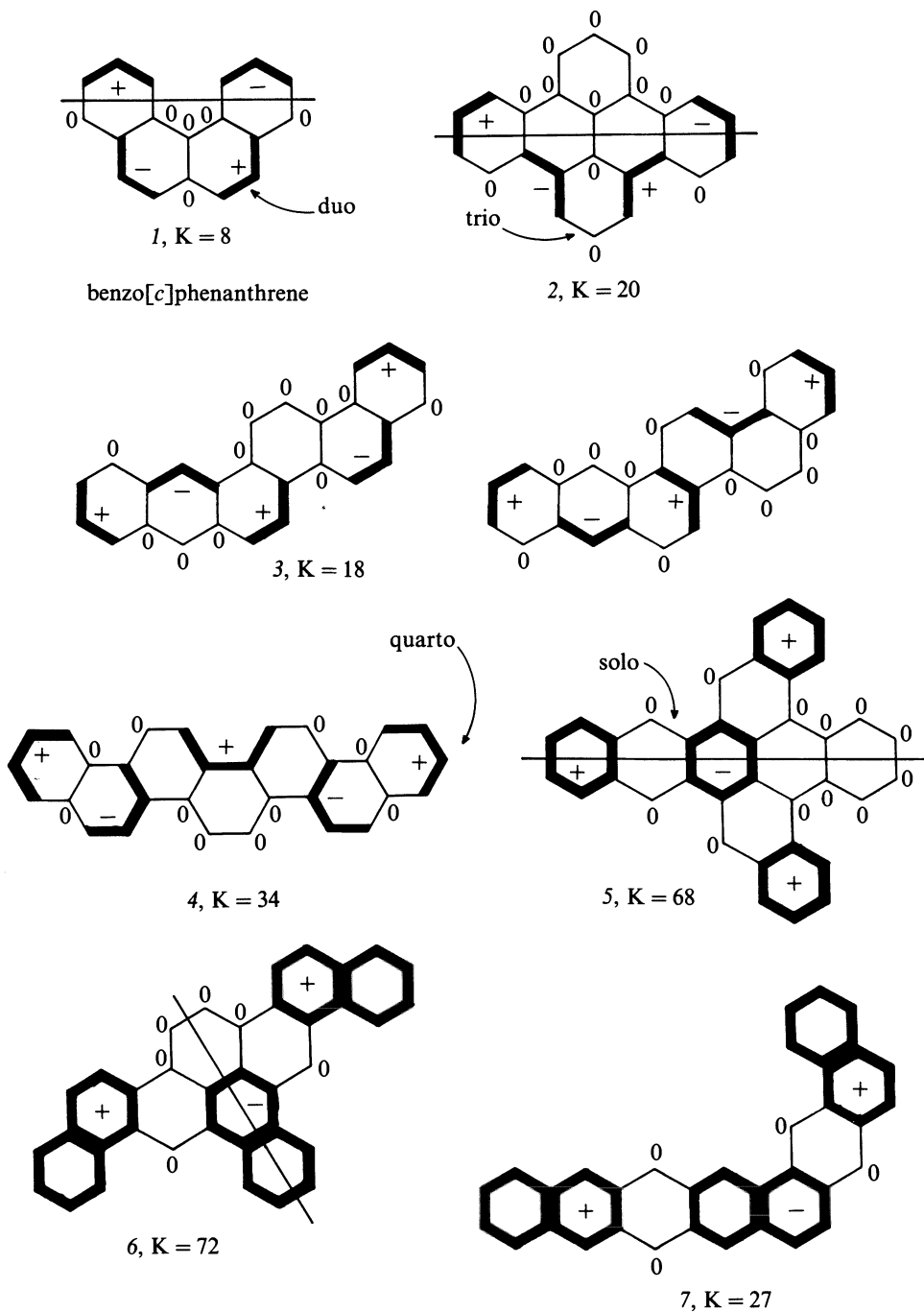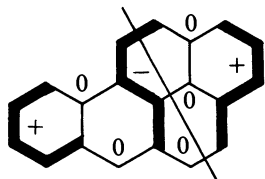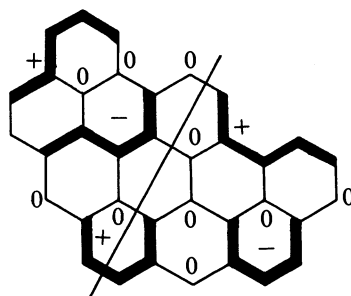
Fig. 4.9. Illustrative embeddings of allyl, butadiene, benzene, naphthalene, pentadienyl, and styrene on large benzenoid hydrocarbons

K = 9
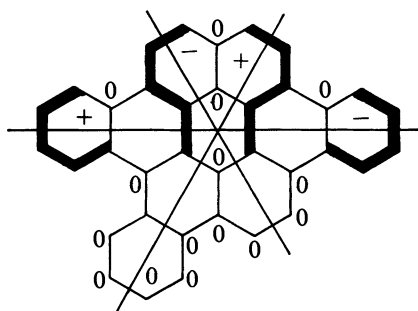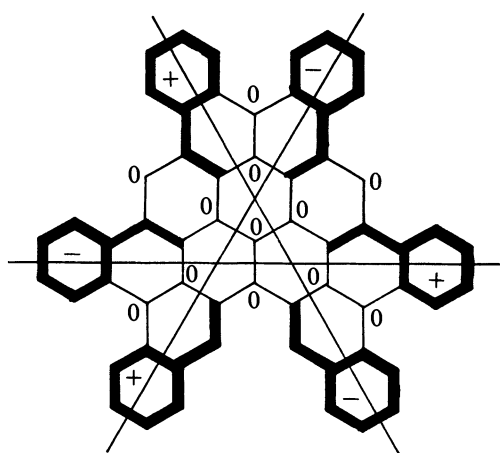$\varepsilon = \pm 1.0, \pm \sqrt{3}\,\beta$
benzo[a]pyrene

K = 84
$\varepsilon = \pm 1.0, \pm 1.0, \pm \sqrt{3}, \pm \sqrt{3}\,\beta$

K = 96
$\varepsilon = \pm 1.0, \pm 1.0, \pm 1.0, \pm \sqrt{3}\,\beta$
tribenzo[a, g, j]coronene

$\varepsilon = \pm \left[\tfrac{1}{2}(5 \pm \sqrt{17})\right]^{1/2}, \pm 1.0,$
$\pm 1.0, \pm 1.0, \pm \sqrt{2}\,\beta$

Fig. 4.9. (contd)

similarity between molecules provides insight concerning both elementary substructures and their interaction terms and enhances our understanding of their properties. The concepts of molecular symmetry and functional groups are important components of our appraisal of similarity between molecules. Functional groups, embedding fragments, and mirror plane fragments are elementary substructures, the latter of which is derived from symmetry. The embedding examples in Fig. 4.9 are illustrative of various aspects of this approach. The number of Kékulé structures (K) is a measure of the relative stability of isomeric benzenoids, and numerous methods for quickly determining this parameter are known [8]. Allyl and benzene embedding requires that K be divisible by 2, and pentadienyl and naphthalene embedding requires K to be divisible by 3 [9]. For each selective lineation (a line perpendicular to a succession of bonds drawn from one side of the benzenoid molecule to the other with its end points relatively convex) there exists a ± 1.0 eigenvalue pair

[10]. Solo perimeter C-H units are most reactive to electrophilic and oxidative reactions and central trio C-H units are least reactive [11].

The benzenoid structures in Fig. 4.9 are illustrative of these ideas. Both *1* and *2* are subspectral in the eigenvalues of ± 1 and $\pm\sqrt{2}$ with their **K** values divisible by 2. Both *2* and *3* have two distinct allyl embeddings and are doubly degenerate in the eigenvalues of $\pm\sqrt{2}$. Benzo[*c*]phenanthrene is subspectral in the eigenvalues of styrene, can be embedded by styrene, and has styrene as a mirror plane fragment. Both *6* and *7* have **K** values divisible by 3 and are subspectral in the eigenvalues of naphthalene. Since *7* has eight solo positions, one should expect it to be relatively reactive.

The concept of elementary substructure subsumes the functional group concept. The excised internal structure is another elementary substructure of considerable importance to polycyclic hydrocarbons [12]. The concepts of elementary substructures, similarity, and symmetry have been important to the enhancement of our chemical understanding, and the study of different ways of comparing molecules will continue to contribute to our better understanding of their chemistry.

4.5 References

1   Dias JR (1989) Theor Chim Acta 73: 153
2   Kroto HW; Heath JR; O'Brien SC; Curl RF; Smalley RE (1985) Nature 318: 162
3   Kroto HW (1987) Nature 329: 529
4   Hawkins JM (1992) Acc Chem Res 25: 150
5   Dias JR (1989) J Chem Educ 66: 1012
6   Dias JR (1989) J Molec Struct (Theochem) 185: 57
7   Dias JR (1988) Handbook of Polycyclic Hydrocarbons, Part B. Elsevier, New York
8   Cyvin SJ; Gutman I (1988) Kekulé Structures in Benzenoid Hydrocarbons. Springer, Berlin Heidelberg, New York
9   Dias JR (1987) Handbook of Polycyclic Hydrocarbons, Part A. Elsevier, New York
10 Dias JR (1987) J Molec Struct (Theochem) 149: 213
11 Dias JR (1991) J Molec Struct (Theochem) 230: 155
12 Dias JR (1991) Theor Chim Acta 81: 125; (1990) Theor Chim Acta 77: 143

4.6 Problems

1   Show that the following can be embedded by pentadienyl in exactly the same way that benzo[*a*]pyrene in Fig. 4.9 is embedded by pentadienyl [7].
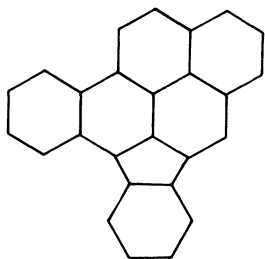
2   Show that all benzenoid D_{6h} derivatives of coronene (cf. with Fig. 2.10), circumcoronene, and kekulene can be embedded by the repeating unit on their perimeters as shown by the following representative example which shows the embedding of naphthalene units in bold. Removal of the six nodes on the perimeter will give hexanaphtho[2, 3-a, d, g, j, m, p]coronene which is still embedded by naphthalene in exactly the same way. Show that the structure below has three selective lineations and, therefore, has three eigenvalue pairs of ± 1.0. Thus, we know that the following structure has the eigenvalues of naphthalene plus two additional ± 1.0 eigenvalues. In all, we have deduced 14 of the 78 eigenvalues of this structure by simple inspection.
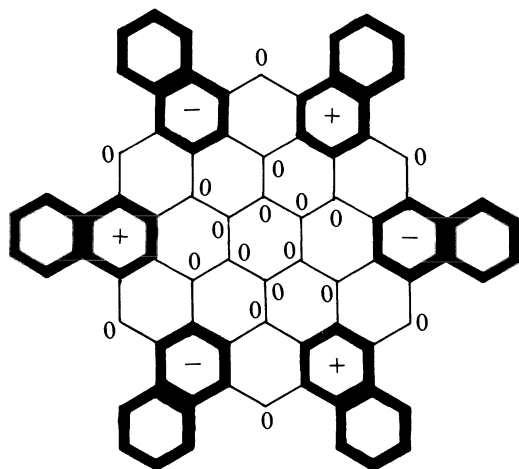
$$C_{78}H_{30}$$

3   Kekulene ($C_{48}H_{24}$) is a 6-fold symmetrical benzenoid-like structure with a coronene hole. Show that both kekulene and hexaaza-kekulene [(1985) Tetrahedron Lett 26:6179] can be embedded by benzene. Pentaphene is subspectral to kekulene. Using perpendicular mirror plane fragmentation determine the eigenvalues for kekulene. Equation (4) in Table 1.2 will be required to remove the weighted vertices associated with the right-hand fragments.

4   The following two odd carbon benzenoids are isospectral (Babic D; Gutman I (1992) J Math Chem 9:261]. Show that they both give the same right-hand mirror plane fragment.
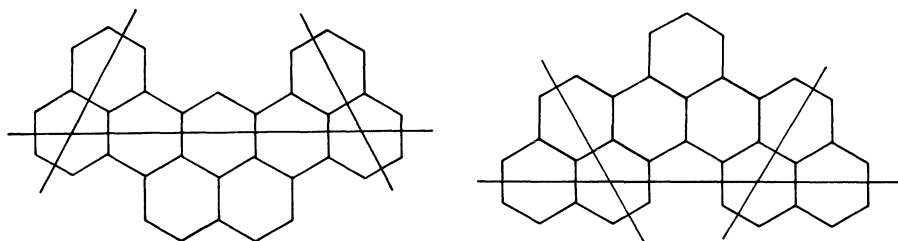

$$C_{33}H_{17}$$

Both these isomers have three selective lineations and, therefore, are at least triply degenerate in the eigenvalues of ± 1.0. Confirm that there is a distinct embedding of ethene along each of these lines. Both these structures have four bay regions and are monoradicals. Show that the characteristic polynomial coefficients of a_2, a_4, and a_6 are identical for these isomers.

5 Show that dibenzo[a, j]coronene can be embedded by pentadienyl in two distinct ways (cf. with tribenzocoronene in Fig. 4.9) and has three selective lineations. Mirror plane fragmentation of this dibenzocoronene gives 1,4-divinylnaphthalene. Determine the characteristic polynomial and eigenvalues of 1,4-divinylnaphthalene.

6 Structure 2 in Fig. 4.9 is a total resonant sextet benzenoid of considerable stability [Dias JR (1991) J Chem Inf Comput Sci 31:89]. Determine the characteristic polynomial and eigenvalues of its mirror plane fragment, 1,2-divinylbenzene.

7 Show that the following are doubly degenerate in the eigenvalues given.
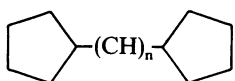
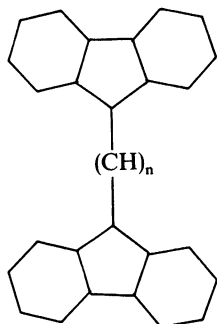
$\frac{1}{2}(\sqrt{5} - 1)$
$-\frac{1}{2}(\sqrt{5} + 1)$
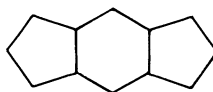

1.2470
-0.4450
-1.8019

(CH)$_n$
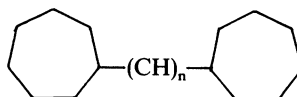
1.8912
1.0
0.7046
-1.0
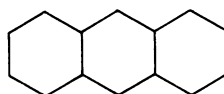-1.3174
-2.2784

$\frac{1}{2}(\sqrt{5} - 1)$
$-\frac{1}{2}(\sqrt{5} + 1)$

$\pm \sqrt{2}, \pm 1$
anthracene

Appendix A

BASIC program for finding real roots of the characteristic polynomial that uses the Bairstow's method which incorporates a simple Newton iteration subroutine for finding the odd root. The number of carbon vertices (N) is inputted at 121 and the coefficients are inputted at lines 114 to 120 where $a_1 = COF(0)$, $a_2 = COF(1)$, $a_3 = COF(2), \ldots, a_N = COF(N-1)$. The example given below is for naphthalene.

```
109:DIM COF(21),
    A(21), B(21)
110:DIM PP(11),
    QQ(11)
111:DIM RR(21)
112:DIM C(21), D(21)
114:COF(0) = 0.0:COF
    (1) = -0 11:COF(2)
    = 00.:COF(3) = 41.0:
    COF(4) = 0000
115:COF(5) = -65.0:
    COF(6) =
      0.0:COF(7) =
      43:COF(8)
    = 0
116:COF(9) = -9
121:N = 10
126:GOSUB 268
130:FOR I = 0 to N - 1
131:USING "##.####
    ##"
132:PRINT RR(I)
133:NEXT I
134:PRINT"

    "
135:END
268:M = N:P = 0:Q = 0
```

```
269:L = INT((N + 1)/2)
271:FOR I = 0 to N - 1
272:A(I) = COF(I)
273:NEXT I
280:FOR J = 0 to L - 2
281:GOSUB 360
282:PP(J) = P
283:QQ(J) = Q
284:M = M - 2
285:IF M = 2 THEN
    GOTO 310
286:FOR K = 0 TO
    M - 1
287:A(K) = B(K)
288:NEXT K
289:IF M = 3 THEN
    GOTO 298
290:NEXT J
298:X = - B(0)
299:GOSUB 404
300:PP(L - 2) = A(0) +
    X
301:QQ(L - 2) = -
    A(2)/X
302:GOTO 323
310:PP(L - 1) = B(0)
311:QQ(L - 1) = B(1)
312:L = L + 1
```

323:For K = 0 TO N − 1
324:A(K) = COF(K)
325:NEXT K
326:IF   M = 4   THEN
    GOTO 331
327:M = N
328:GOSUB 404
329:RR(N − 1) = X
331:M = N
332:FOR J = 0 to L − 2
333:P = PP(J)
334:Q = QQ(J)
335:GOSUB 360
336:D = P*P − 4*Q
338:RR(2*J) = (− P +
    SQR(D))/2.
339:RR(2*J + 1) =
    (− P − SQR(D))/2.
347:NEXT J
349:RETURN
360:B(0) = A(0) − P
361:B(1) = A(1) − P*B
    (0) − Q
362:C(0) = − 1.
363:C(1) = − B(0) + P
364:D(0) = 0.
365:D(1) = − 1.
366:FOR I = 2 to M − 3
367:B(I) = A(I) − P*B
    (I − 1) − Q*B(I − 2)
368:C(I) = − B(I − 1) −
    P*C(I − 1) − Q*C
    (I − 2)
369:D(I) = C(I − 1)
370:NEXT I
371:R = A(M − 2) − P
    *B(M − 3) − Q*B
    (M − 4)
372:S = + A(M − 1) −
    Q*B(M − 3)
373:RQ = − B(M − 3)
    − P*C(M − 3) −
    Q*C(M − 4)
374:RP = − B(M − 3)
    − P*C(M − 3) −

Q*C(M − 4)
375:RQ = − B(M − 4)
    − P*D(M − 3) −
    Q*D(M − 4)
376:SP = − Q*C
    (M − 3)
377:SQ = − B(M − 3)
    − Q*D(M − 3)
378:DE = RP*SQ −
    SP*RQ
379:DP = (S*RQ −
    R*SQ)/DE
380:DQ = (R*SP −
    S*RP)/DE
381:IF ABS (DP) >
    0.001*ABS(P)GOTO
    386
382:IF ABS (DQ) >
    0.001*ABS(Q)GOTO
    386
383:P = P + DP
384:Q = Q + DQ
385:RETURN
386:ICT = ICT + 1
387:IF ICT >
    100THEN
    GOTO 391
388:P = P + DP
389:Q = Q + DQ
390:GOTO 360
391:PRINT "NO
    SOLN"
392:RETURN
404:ICT = 0
406:F = X ∧ M + A
    (M − 1)
407:DF = M*X ∧
    (M − 1)
408:FOR I = 0 to M − 2
409:F = F + A(I)*X ∧
    (M − 1 − I)
410:DF = DF + A(I)*
    (M − 1 − I)*X ∧
    (M − 2 − I)
411:NEXT I

413:DX = − F/DF
414:IF ABS(DX) >
   .0001∗ABS(X) THEN
   GOTO 417
415:X = X + DX
416:RETURN
417:ICT = ICT + 1

418:IF ICT > 100
   GOTO 421
419:X = X + DX
420:GOTO 406
421:PRINT "100
   ITERATION S"
422:RETURN

The above BASIC program has been routinely used for solution of characteristic polynomials up to degree 14 with a SHARP EL-5500 II programmable hand calculator. Some polynomials caused various execution problems which can usually be remedied. Several examples below are illustrative. The polynomial $X^5 - 4X^3 + 3X$ gave an error message (Calc Error in 379) which was rectified by factoring out the $X = 0$ root. In some cases, factoring out the roots $X = \pm 1$ was necessary for proper execution. If the messages of lines 391 (No Soln) or 421 (100 Iterations) appear, force the program to continue to execute by depressing ENTER. This will give some, if not all, the remaining roots; to obtain up to four missing roots use the method of Sect. 1.5.4. The polynomial $X^5 - 5X^3 + 5X - 2$ gave an error message (Calc Error in 379) which was resolved by temporarily adding 0.1 to line 378 in the program.

Compound Index

Many general molecules given in Table 2.1 and Figures 2.3, 2.4, 2.5, 2.7, 2.11, 3.2, 3.6, 4.2, 4.8, and 4.9 are not listed below.

General Index

adjacency matrix   5, 7
alternant hydrocarbon   6, 8, 11, 16

basis orbitals   4, 84–85
benzenoids   56, 104
bond order   24

characteristic polynomial   4, 7, 10, 23, 74, 76, 84, 87
charge density   72, 77
complex edge   47, 61
Coulomb integral   5, 8, 29, 84

decomposition   29, 103
degenerate   47, 64, 69, 79, 97, 101, 104

edge   7–9, 45, 69
eigenvalue   2, 8, 13, 24, 87, 100
eigenvector   2, 5, 8, 14, 18–24, 42, 61, 72, 77
electron density   23–24, 72, 77
embedding   13–17, 46, 89, 105, 108
energy level   2, 5, 8, 25
elementary substructures   3, 64, 105, 108

1-factor   7
2-factor   7
factorization   44, 45, 49, 50, 52
fragment   14, 29, 31, 105
fragmentation   3, 29
frontier orbitals   2, 8, 24, 62
functional group   3, 105, 107

graph   6

HOMO   2, 8, 16, 64

invariant   8
ionization potential   1, 6, 64
irreducible subgraph   47–49, 55–62, 65, 73, 83
isoconjugate   8, 26, 41, 69, 70
isospectral   28, 95, 109

Kékulé structures   7, 13, 17

linear polyenes   7, 8, 41
LUMO   2, 16

mirror plane fragmentation   29–44, 96–100
Möbius circuits   69, 84–87, 91
molecular graph   6–8, 69
moments   67

NBMO   12, 16, 72
normalization   19, 22, 43, 72

orbital network diagram   69, 85

pairing theorem   16, 46

radical   6, 15–16, 28, 72–74
ring-centric   45, 51

Sachs graphs   3, 7–13
secular determinant   4–5, 7, 18, 29
similarity   8, 95, 105
starring   6, 15, 16, 24, 72, 74
subspectral   8, 63, 95, 96
subgraph   7, 8, 29–40, 105
symmetry   29, 41, 47, 49, 50, 107
   2-fold   29, 45, 96
   3-fold   49, 52, 75–83, 97, 102
   4-fold   50, 54
   n-fold   30, 43, 44
   local   30, 43–44

terminology   6–8

Ulam subgraphs   3, 8, 22, 70

vertex-centric   50, 63, 97

wavefunction   3, 5, 8, 16, 19

zero node   14–16, 24, 46, 69, 71
zero sum rule   24, 46–47, 72–74

Springer-Verlag
and the Environment

We at Springer-Verlag firmly believe that an international science publisher has a special obligation to the environment, and our corporate policies consistently reflect this conviction.

We also expect our business partners – paper mills, printers, packaging manufacturers, etc. – to commit themselves to using environmentally friendly materials and production processes.

The paper in this book is made from low- or no-chlorine pulp and is acid free, in conformance with international standards for paper permanency.